



Technische Universität München
Fakultät Wissenschaftszentrum Weihenstephan für Ernährung,
Landnutzung und Umwelt
Lehrstuhl für Chemie der Biopolymere

The development of activity-based probes for serine proteases

Sevnur Serim

Vollständiger Abdruck der von der Fakultät Wissenschaftszentrum Weihenstephan für Ernährung, Landnutzung und Umwelt der Technischen Universität München zur Erlangung des akademischen Grades eines

Doktors der Naturwissenschaften

genehmigten Dissertation.

Vorsitzender: Univ.-Prof. Dr. D. Langosch

Prüfer der Dissertation:

1. TUM Junior Fellow Dr. S. Verhelst
2. Univ.-Prof. Dr. A. Kapurniotu

Die Dissertation wurde am __23.10.2013__ bei der Technischen Universität München eingereicht und durch die Fakultät Wissenschaftszentrum Weihenstephan für Ernährung, Landnutzung und Umwelt am __17.02.2014__ angenommen.

Acknowledgements

First and foremost, I owe my sincere gratitude to my supervisor Dr. Steven Verhelst for his guidance, giving me the opportunity to step into biochemistry, always having his door open for questions, applying his good aura to my mutants and for being the friend who is always right.

I am deeply grateful to Prof. Dr. Dieter Langosch, my committee chair, for the support especially during the submission process and the opportunity to work in the chair.

This work would have not been possible or at least not as fun without my beloved colleagues of the Verhelst Lab, who not only patiently taught biochemistry to a chemist but also created many memories that I'll remember for a life time. Many thanks to Olli for being his awesome-self, a constant source of fun (and drumming!) in the lab, along with his all-round scientific creativity and not to forget many beers shared together. Thank you Ute, for all the discussions about life and science, inspiring future plans, starting the chain reaction of running, for the non-judgmental listening ear which I know I can (and I will!) always turn to and making the Zusammenfassung of this thesis actually German. Many thanks to Eliane for making paper writing less frustrating, patiently being the molecular biotechnology supervisor of my students and me, and for being the chatterbox we like. I am thankful to dear Annett, Ute and Eliane for careful proofreading of the thesis. I also would like to thank Christian for many delightful scientific and unscientific conversations and all the movie sessions at his place.

Throughout my PhD I was very lucky to supervise many students who made my work easier. I am grateful to Jonas Lohse, Mathias Leidl, Peter Graf, Melanie Honz, Bettina Prieler and especially Susanne Mayer and Philipp Baer for their contributions.

I owe thanks to Dr. Oliver Frank from Lehrstuhl für Lebensmittelchemie und molekulare Sensorik for NMR measurements.

I would like to acknowledge the members of the chair; Markus, Walter, Yang, Oxana, Jan, Christoph, Chris, Martin, Ellen, Martina, Mark and Ayse for the nice working atmosphere and many shared lunches.

Special thanks are extended to my Munich Turkish friend Sezgin for being the best travel buddy and for the “harmonized” runs; as well as to outside of Munich: my “life coach” Balca for being everything I wanted in a friend, my dearest Banu for best online support, Ayça for being my roomie in the most stressful times, and to my “civilian” friends; Shaughn for endless online encouragement and Christian for many shared rides to the most beautiful places and the language sessions.

And my family... Son ve sonsuz teşekkürler en güzel aileye. Sizin bitmeyen desteğiniz olmadan burada, bu tez ve doktora mümkün olamazdı. Benimle beraber enzimler moleküller öğrendiniz, makaleler yazdınız, laboratuvara gelip deneyler yaptınız, tez yazdınız benimle. Nerde olursam olayım hepinizi hep çok seviyorum. Son olarak, olur da bir daha birilerine ithaf edilebilecek bir iş yapmazsam endişesiyle, bu tez anneannem ve dedeme adanmıştır.

Contents

Acknowledgements	iv
Abstract	1
Zusammenfassung	3
1 Introduction	5
1.1 Proteases	6
1.1.1 Serine proteases	6
1.1.1.1 Catalytic mechanism	7
1.1.1.2 Regulation of proteolytic activity	8
1.1.1.3 Substrate recognition sites	9
1.1.1.4 Lon protease	9
1.2 Activity-based probes	12
1.2.1 Fluorescently quenched ABPs	13
1.2.2 Activity-based protein profiling	15
1.2.2.1 Phosphonates in ABPP	15
1.2.2.2 Applications of ABPP	18
2 Scope of this work	19
3 Results and discussion	21
3.1 On-resin strategies for synthesis of diphenyl phosphonate ABPs	22
3.1.1 General remarks	22
3.1.2 Synthetic strategy	22
3.1.3 Labeling experiments	26
3.1.3.1 Labeling of purified serine proteases	26
3.1.3.2 Labeling of purified proteases in a proteome background	28
3.1.3.3 Labeling in enterokinase-activated rat pancreas lysate	29
3.1.4 Molecular docking of probe 10 bound to trypsin	30

3.2 Quenched phosphonate ABPs for imaging protease activity	32
3.2.1 General remarks	32
3.2.2 Synthetic strategy	33
3.2.2.1 Synthesis of a basic P1 probe	33
3.2.2.2 Synthesis of a P1 Valine probe	36
3.2.3 Labeling of purified serine proteases with qABPs	37
3.2.4 Quenching efficiency	37
3.3 FRET-based assay for inhibitor screening of Lon protease	39
3.3.1 General remarks	39
3.3.2 Synthetic strategy	39
3.3.3 Expression and purification of <i>E. coli</i> Lon	43
3.3.4 Activity Assay of the <i>E. coli</i> Lon Protease	44
3.3.5 Assay development	45
3.3.6 Hit characterization	48
4 Conclusions and Outlook	55
4.1 On-resin strategies for synthesis of diphenyl phosphonate ABPs	56
4.2 Quenched phosphonate ABPs for imaging protease activity	59
4.3 FRET-based assay for inhibitor screening of Lon protease	62
5 Experimental	65
Organic chemistry	66
General	66
TLC stains	66
Cbz deprotection	67
General SPPS procedures	67
Amino acid coupling and Fmoc deprotection	68
Biochemistry	68
General procedure for labeling of purified enzymes	68
Preparation of competent <i>E. coli</i> cells	69
Buffers and solutions	69

5.1 On-resin strategies for synthesis of diphenyl phosphonate ABPs	71
5.1.1 Synthesis	71
5.1.1.1 General methods for the synthesis of propynoylated diphenyl α -aminoalkylphosphonate building blocks	71
5.1.1.2 General methods for solid phase peptide synthesis of peptide diphenyl α -aminoalkylphosphonates	76
5.1.2 Docking experiments	79
5.1.3 Labeling experiments	79
5.1.3.1 Labeling of purified enzymes	79
5.1.3.2 Labeling of purified proteases in a proteome background	79
5.1.3.3 Labeling in enterokinase-activated rat pancreas lysate	80
5.2 Quenched phosphonate ABPs for imaging protease activity	81
5.2.1 Synthesis	81
5.2.1.1 General procedure for dealkylation with LiBr	81
5.2.1.2 General procedure for coupling of 5-hexynoic acid	81
5.2.1.3 General procedure for coupling of QSY-7	81
5.2.3 Labeling experiments	87
5.2.3.1 Labeling of purified enzymes	87
5.3 FRET-based assay for inhibitor screening of Lon protease	88
5.3.1 Synthesis	88
Boc-Lys(DABCYL)-COOH (24)	88
K(DABCYL)RGITCSGRK(FITC) (27)	88
5.3.2 Buffers	89
Mary buffer	89
Lon reaction buffer	89
ATP stock solution	89
5.3.3 Protein expression and purification	90
5.3.4 Gel-based activity assay of Lon	91
5.3.5 FRET assay	91
5.3.6 Reversibility check	92
5.3.7 Labeling of <i>E. coli</i> Lon	92
5.3.8 Site-directed mutagenesis	93

List of Abbreviations	95
List of figures	99
List of schemes	101
References	103
Supplementary	119
Publications	139
Curriculum Vitae	141

Abstract

Serine proteases play crucial roles in physiological and pathological processes ranging from non-specific digestion to highly regulated functions like cell death, immune response and blood clotting. Like all other proteases, they are synthesized in the cell as inactive zymogens, and are activated often by proteolytic processing. Once active, their activity is tightly regulated mostly by endogenous protease inhibitors. Therefore, the abundance of a protease does not correspond to its activity. For a better understanding of enzyme function there has been considerable interest in the design and development of activity-based probes (ABPs).

ABPs are small molecules that covalently bind to the enzymes in an activity-dependent manner, distinguishing between active proteases and inactive zymogens or inhibitor bound forms. This allows studying the active fraction of a particular enzyme rather than its overall abundance.

Diphenyl esters of α -aminophosphonates (DPPs) are low molecular weight, irreversible serine protease inhibitors and represent useful reactive head groups for ABPs. While synthetic strategies to generate DPPs in solution have been reported, a major challenge remains to achieve an efficient and rapid way of synthesis. We therefore developed a new synthetic route combining solution and solid phase peptide synthesis, which allows rapid diversification of the recognition moiety and convenient synthesis of DPP ABPs. Using this approach, we generated a small library of diphenyl phosphonate probes. We showed the ability to modulate the reactivity and selectivity of these probes' and demonstrated activity-dependent labeling of endogenous proteases within a tissue proteome.

In many studies fluorescent reporters have been incorporated into ABPs for target visualization. However, these probes also show fluorescence when free in solution, thus creating high background. To overcome this, quenched activity-based probes have been designed that become fluorescent only after covalent modification of a specific protease target. Here we describe the synthesis and evaluation of the first fluorescently quenched ABPs for serine proteases. Our ABPs carry a fluorophore and

a quencher pair, a phosphonate warhead and a guanidinophenyl or a valine recognition element. The probes show a high quenching efficiency, a strong activity-dependent reactivity and the expected protease specificity. Real-time imaging experiments of atherosclerosis tissue sections and of neutrophil elastase secreted from primary neutrophils are ongoing.

Apart from ABPs, inhibitors are important tools for assessing protease function in normal and disease states. The ATP-dependent Lon protease lacks specific inhibitors to enable a clear understanding of its mechanism. Lon is a homo-oligomeric heat shock protein which selectively degrades abnormal and damaged proteins, as well as short-lived regulatory proteins and is therefore essential for cellular homeostasis. As bacterial Lon has been shown to be involved in pathogenicity, it has become an important target in the development of novel therapeutic agents. To date, even though few inhibitors of Lon are reported, none of them are highly potent or specific. We established an *in vitro* assay to monitor its enzymatic activity and screened for new inhibitors. A peptide substrate of Lon with a fluorophore and a quencher pair was synthesized. The intact peptide is only weakly fluorescent as a result of Förster resonance energy transfer (FRET), whereas an increase in fluorescence can be detected after cleavage by Lon, making it possible to measure and quantify the enzymatic activity. This FRET assay was then used to screen a total of 123 compounds, of which four were found out to have an inhibitory effect against Lon. Among them we identified thiiranes as a new class of inhibitors of *E. coli* Lon.

Zusammenfassung

Serinproteasen spielen entscheidende Rollen in physiologischen und pathologischen Prozessen, angefangen von unspezifischer Degradierung von Proteinen bis hin zu stark regulierten Prozessen wie Zelltod, Immunantwort und Blutgerinnung. Wie alle anderen Proteasen werden sie in der Zelle als inaktive Zymogene synthetisiert. Häufig werden sie ihrerseits durch Proteolyse aktiviert und kurz darauf wieder durch endogene Proteaseinhibitoren gehemmt, wodurch eine strenge Regulation gewährleistet wird. Daher lässt sich von der Menge einer Protease nicht auf ihre Aktivität schließen. Um die Funktionen dieser Enzyme besser untersuchen zu können, besteht ein großes Interesse an der Entwicklung von aktivitätsbasierten Sonden (engl.: activity-based probes, ABPs).

ABPs sind kleine Moleküle, die auf eine aktivitätsbasierte Weise kovalent an Enzyme binden. Sie unterscheiden damit zwischen aktiven und inaktiven Proteasen oder inhibitorgebundenen Formen. Dies ermöglicht die gezielte Untersuchung des aktiven Anteils einer Gruppe eines bestimmten Enzyms anstelle der Gesamtheit.

Diphenylester von α -Aminophosphonaten (DPPs) sind niedermolekulare irreversible Inhibitoren für Serinproteasen, die sich gut als reaktive Kopfgruppen für ABPs eignen. Obwohl bereits Strategien zur DPP-Synthese in Lösung beschrieben wurden, bleibt die schnelle und effiziente Synthese eine Herausforderung. Wir haben einen neuen schnelleren Syntheseweg erschlossen, indem wir synthetische Schritte in Lösung und an der Festphase kombiniert haben. So wird eine schnelle Diversifizierung des Erkennungselements und insgesamt eine einfache Synthese von DPP ABPs ermöglicht. Mit diesem Ansatz wurde eine kleine Bibliothek von DPP-Sonden hergestellt. Wir konnten zeigen, dass sowohl die Reaktivität als auch die Selektivität der DPP ABPs modulierbar sind. Desweiteren demonstrieren wir die aktivitätsabhängige Markierung von endogenen Proteasen im komplexen Gewebelysat.

Fluoreszente Substituenten dienen der Visualisierung von Targets und werden deshalb oft in ABPs integriert. Allerdings fluoreszieren diese Sonden auch dann,

wenn sie frei in Lösung vorhanden sind, und erzeugen so unerwünschte Hintergrundsignale. Um dieses Problem zu überwinden, wurden gequenchte ABPs entworfen, die erst nach kovalenter Bindung an eine spezifische Protease fluoreszieren. Hier beschreiben wir die Synthese und Evaluierung der ersten fluoreszenzgequenchten ABPs für Serinproteasen. Unsere ABPs haben ein Fluorophor und Quencher Paar, ein Phosphonat als reaktive Kopfgruppe und Guanidinophenyl oder Valin als Erkennungselement. Diese Sonden zeigen eine hohe Quencheffizienz, eine starke aktivitätsabhängige Reaktivität und die erwartete Proteasespezifität. Echtzeit-Bildgebung Experimente von atherosclerotischen Gewebe sowie von primären Neutrophilen sekretierter neutrophiler Elastase dauern an.

Neben ABPs sind auch Inhibitoren wichtige Werkzeuge zur Erforschung der Funktionen von Proteasen im normalem und Krankheitszustand. Für die ATP-abhängige Lon Protease fehlen spezifische Inhibitoren, die ein klares Verständnis ihres Wirkmechanismus ermöglichen könnten. Lon ist ein homooligomeres Hitzeschockprotein, das selektiv beschädigte sowie kurzlebige regulatorische Proteine abbaut. Daher ist sie von wesentlicher Bedeutung für die zelluläre Homöostase. Seitdem gezeigt wurde, dass bakterielle Lon an der Pathogenität beteiligt ist, gilt sie als ein wichtiges Ziel für die Entwicklung neuer Medikamente. Bis heute gibt es nur wenige Lon-Inhibitoren, von denen keine hochpotent oder spezifisch sind. Wir haben einen *in vitro* Assay etabliert um die enzymatische Aktivität der Lon zu messen und nach neuen Inhibitoren zu suchen. Dafür wurde ein Peptidsubstrat für Lon mit einem Fluorophor-Quencher-Paar synthetisiert. Das intakte Peptid fluoresziert nur schwach, da die Energie auf den nichtfluoreszierenden Quencher übertragen wird (Förster-Resonanz- Energie-Transfer, FRET). Nach der Peptidspaltung durch Lon wird dieser Effekt aufgehoben, so dass verstärkte Fluoreszenz gemessen werden kann. Dieses Signal kann als enzymatische Aktivität detektiert und quantifiziert werden. Dieser FRET-Assay wurde verwendet um vier Inhibitoren aus einer Bibliothek von insgesamt 123 Verbindungen zu identifizieren. Dabei werden Thiirane als eine neue Klasse von Inhibitoren der *E. coli* Lon identifiziert.

1 Introduction

"Chemists are a strange class of mortals, impelled by an almost maniacal impulse to seek their pleasures amongst smoke and vapor, soot and flames, poisons and poverty, yet amongst all these evils I seem to live so sweetly that I would rather die than change places with the King of Persia." Johann Joachim Becher, 1667

1.1 Proteases

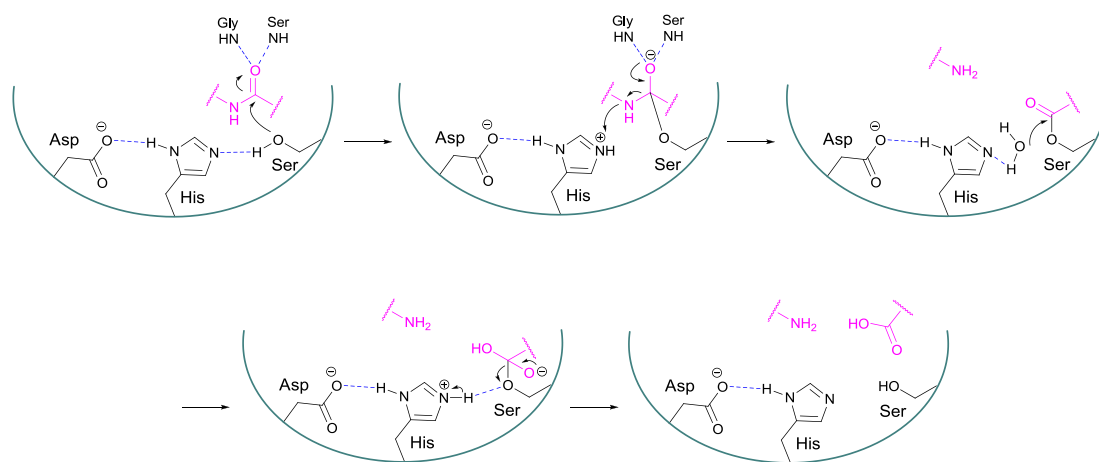
Proteases, also known as proteolytic enzymes, form one of the largest groups of enzymes with approximately 2% of the total number of proteins present in all types of organisms. They catalyze the irreversible hydrolysis of peptide bonds resulting in the breakdown of proteins into smaller peptides. Proteases are classified according to their mechanism of action:² Serine, threonine and cysteine proteases take part in covalent catalysis, in which the nucleophile that attacks the peptide bond carbonyl is the hydroxyl of the active site serine/threonine or the thiol of the active site cysteine. Usually histidine functions as a base. Aspartic, glutamic and metalloproteases, however, function via noncovalent catalysis, where an activated water molecule acts as a nucleophile. Aspartic acid/Glutamic acid residues or metal ions (usually zinc, but also cobalt, manganese, nickel, copper, and iron) serve as acids and bases. The debatable class of asparagine lyases cleave themselves with asparagine as the nucleophile, and this self-cleavage does not involve hydrolysis.³

1.1.1 Serine proteases

Serine proteases are found in all kingdoms of life and constitute the largest group of proteases. They are involved in tightly regulated cascades and signaling events, such as blood coagulation, fibrinolysis, apoptosis, and immune response. Dysregulation of proteolytic activity can lead to pathological conditions like inflammatory diseases, cancer, neurodegenerative and cardiovascular disorders.⁴ Therefore, the study of both inhibition and activity detection of this group of proteases is of great importance for target identification and drug discovery.

1.1.1.1 Catalytic mechanism

Most serine proteases have the Ser/His/Asp catalytic triad.⁵ Stabilized by the proton-withdrawing aspartate, the imidazole of the histidine acts as a base and deprotonates the hydroxyl of the serine. The nucleophilic hydroxyl then attacks on the carbonyl of the substrate. This results in the formation of a tetrahedral intermediate and an imidazolium ion. The oxyanion of the tetrahedral intermediate is stabilized by several hydrogen bonds, formed with the protease backbone in the so-called oxyanion hole. The tetrahedral intermediate breaks down to the acyl-enzyme and the amine product is eliminated. The acyl-enzyme is then attacked by a water molecule, forming a second tetrahedral intermediate, followed by deacylation of the acyl-enzyme and the release of the carboxylic acid product (**Scheme 1**).



Scheme 1 Ser/His/Asp catalytic triad mechanism. Aspartate stabilizes histidine, which deprotonates the hydroxyl of the active site serine. The nucleophilic hydroxyl attacks the carbonyl of the substrate, forming a tetrahedral intermediate. The oxyanion hole is stabilized by several hydrogen bonds. After the elimination of the amine product the acyl-enzyme is attacked by a water molecule, forming a second tetrahedral intermediate, followed by deacylation of the acyl-enzyme and the release of the carboxylic acid product.

1.1.1.2 Regulation of proteolytic activity

Like many proteolytic enzymes serine proteases are in most cases expressed as inactive enzyme precursors called zymogens or proenzymes. This prevents uncontrolled proteolytic degradation of cellular proteins and regulates when and where the enzyme is active. The enzymatic activity is usually switched on by the cleavage of a propeptide. The switch off of serine proteases on the other hand is done by specific protease inhibitors such as serpins.⁶ Due to inactive zymogens and inhibitor-bound enzymes the expression level of a protease does not necessarily reflect its activity.

In the same manner, pancreatic enzymes are expressed as zymogens and activated by a protease activation cascade initiated by enteropeptidase.⁷ Enteropeptidase activates trypsinogen into trypsin, which in turn activates more trypsinogen as well as all pancreatic zymogens, namely trypsinogen, chymotrypsinogen, proelastase, procarboxypeptidase, and prolipase (**Figure 1**).

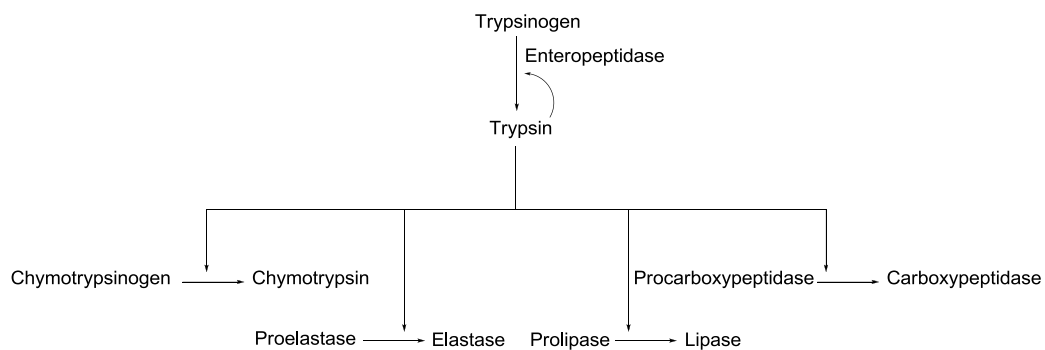


Figure 1 Activation of pancreatic enzymes. Enteropeptidase initiates the protease activation cascade in the pancreas. It activates trypsinogen into trypsin, which in turn activates more trypsinogen and other zymogens.

1.1.1.3 Substrate recognition sites

The active site of a protease is fundamental to its function as it binds to the protein substrate and catalyzes the cleavage of the peptide bond. The residues around the cleavage site allow the enzyme to discriminate between substrates. According to the nomenclature described by Schechter and Berger⁸ the active site of the enzyme is composed of subsites each accommodating a single side chain of the substrate (**Figure 2**). N-terminal to the scissile bond the substrate residues are numbered P1-Pn, and P1'-Pn' towards the C terminus. The subsites are referred to as S1-Sn and S1'-Sn' in the same manner. The nature of the subsites determines the substrate specificity of the enzyme. The mapping of the subsites is therefore of great importance when selective inhibitors and probes are required.

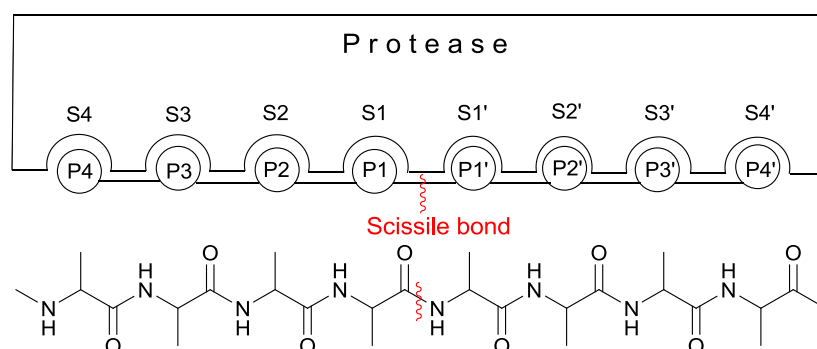


Figure 2 Nomenclature of protease specificities. The active site of the enzyme is composed of subsites each accommodating a single side chain of the substrate. N-terminal to the scissile bond the substrate residues are numbered P1-Pn, and P1'-Pn' towards the C terminus. The subsites are referred to as S1-Sn and S1'-Sn' in the same manner.

1.1.1.4 Lon protease

One example of an unconventional serine protease is the Lon protease. Lon is a homo-hexamer ATP-dependent serine protease which is highly conserved in all kingdoms of life. It is found in the cytosol of prokaryotes as well as in mitochondria

and peroxisomes of eukaryotes.⁹ As a heat shock protein it mainly functions in protein quality control by selectively degrading abnormal and damaged proteins, as well as short-lived regulatory proteins and is therefore essential for cellular homeostasis.

In *E. coli* Lon is involved in the regulation of the SOS response by degrading the cell division inhibitor Su1A.¹⁰ This allows cells to resume division after the physiological response to DNA damage. Lon also degrades the positive regulator of bacterial capsule synthesis RcsA,¹¹ as well as the bacteriophage λ N protein.¹² In the pathogenic bacteria *Salmonella enterica* Serovar Typhimurium (*S. Typhimurium*) the expression of host invasion genes is negatively regulated by Lon.¹³ In *Pseudomonas aeruginosa* infections in cystic fibrosis (CF) patients it has been proposed that the induction of Lon by antibiotic treatment is involved in adaptive resistance.¹⁴ PIM1, the Lon-like enzyme in mitochondria of *Saccharomyces cerevisiae* directly affects the biogenesis of respiratory chain complexes and thus the respiratory competence of yeast cells while its absence results in extensive mitochondrial DNA deletions.¹⁵ Mammalian Lon also exhibits a chaperone-like function, and it promotes the assembly of cytochrome c oxidase (COX) subunits independent of its proteolytic activity.¹⁶ Downregulation of Lon in human lung fibroblasts leads to massive apoptosis due to accumulation of aggregated proteins inside mitochondria caused by the proteolytic defect. Loss of chaperone function severely affects mitochondrial respiration and membrane potential, making cells highly susceptible to apoptotic stimuli.¹⁷

Lon belongs to the AAA⁺ family of proteins¹⁸ (ATPases Associated with various cellular Activities) and each subunit of Lon contains the N-terminal domain, the ATPase domain (AAA⁺ module) and the protease domain. The crystal structure of the protease domain of *E. coli* Lon protease disclosed that unlike most other serine proteases Lon employs a Ser-Lys dyad for catalysis.¹⁹

The first step in the degradation of substrates is their recognition and binding. This is followed by the AAA⁺ module unfolding the folded protein substrates but not the less structured or denatured proteins. This step requires ATP-binding and -hydrolysis. Unfolded substrates are then translocated into the proteolytic chamber

where they are degraded.²⁰ It has been demonstrated that only ATP binding is required for the degradation of short unstructured peptides.²¹ However, the degradation of larger folded protein substrates by Lon requires ATP hydrolysis as well.²²

Lon does not cleave proteins at a specific peptide sequence; however, it recognizes hydrophobic sequences that are exposed in unfolded proteins but hidden in most native structures.²³

As a serine protease Lon is inhibited nonspecifically by general serine protease inhibitors such as diisopropyl fluorophosphate (DFP) and phenylmethanesulfonyl fluoride (PMSF), however, only in high inhibitor concentrations and after long exposures. On the other hand peptidyl chloromethyl ketones with hydrophobic residues inactivate the enzyme more efficiently in lower inhibitor concentrations.²⁴ Using *S. Typhimurium* Lon as a model, the screening of commercially available peptide-based proteasome inhibitors identified the boronate MG262 as a potent inhibitor of Lon.²⁵ However, it is about 2000-fold more potent against the proteasome. Furthermore, screening of compounds against the human Lon protease in a FITC-casein cleavage assay revealed coumarins as inhibitors of Lon.²⁶ These small, nonpeptidic molecules inhibit only the Lon but not the 20S proteasome. Another attempt of reaching specific Lon inhibitors resulted in the design of the inhibitor DBN93, which was based on a hydrolysis product of the synthetic FRETN 89-98 substrate²⁷ (residues 89-98 of λ N protein with a fluorophore and quencher pair). This boronic acid distinguishes the activities of human Lon and human ClpXP, inactivating only human Lon.²⁸

1.2 Activity-based probes

An activity-based probe (ABP) is a small molecule, designed to covalently bind to active enzymes but not their inactive or inhibited forms. It consists of three main parts: a reactive group - also referred to as the warhead, a spacer and a reporter tag (**Figure 3**).

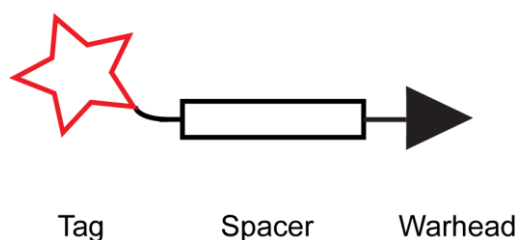


Figure 3 General design of an activity-based probe. A detection tag for visualization and/or purification; a spacer, which can include recognition elements; and a reactive warhead that binds covalently to the target enzyme.

The majority of ABPs contain an electrophilic warhead that covalently links the probe to its target. The reactivity and the potential targets of the probe are determined by the nature of this electrophile. A soft electrophile like a Michael acceptor reacts with soft nucleophiles such as sulfur, making the probe selective for cysteine proteases. On the contrary, harder electrophiles prefer to react with harder nucleophiles such as the hydroxyl of the active site residue of serine proteases. By this means the warhead provides a first degree of probe selectivity.

The spacer mainly links the warhead and the tag together while preventing sterical hindrance that can be caused by the bulky tags. It may also include recognition elements that modulates the affinity of the probe and directs the warhead to a subset of enzymes within the targeted class.²⁹

The reporter tag of an ABP enables the detection and if desired the enrichment of the covalent enzyme-probe complex.³⁰ Most commonly used tags are fluorophores

and biotin. Fluorescently tagged enzymes can be easily visualized on gel by scanning with a fluorescent scanner. Biotinylated ABPs are detected by Western-blot and can also be used for further protein purification and enrichment by the use of streptavidin-coated beads.

Instead of a bulky tag a small bioorthogonal reaction handle can be incorporated in the ABP structure. This allows the introduction of the reporter tag of choice as a second step after the reaction with the enzyme. This tandem labeling strategy not only gives the flexibility to choose between tags for different applications, it also prevents the sterical hindrance that results from the use of bulky fluorophores. Several methods for specific bioorthogonal ligation of the two reaction partners have been reported:³¹ Staudinger ligation,³² Cu(I) catalyzed 1,3-dipolar cycloaddition,³³ commonly known as the “click chemistry³⁴”, copper-free strain-promoted click chemistry,³⁵ and the Diels-Alder ligation.³⁶

1.2.1 Fluorescently quenched ABPs

Proteases are synthesized as inactive zymogens and activated mostly by proteolytic processing. Once active, they are tightly regulated often by endogenous protease inhibitors. Changes in protease expression levels and activities are the basis of many human diseases.³⁷ Thus, traditional methods that report the total protein levels are not always suitable for protease research as they fail to provide information about the active fraction of these enzymes. As determination of not only the activity but also the localization of proteases is crucial for a better understanding of their role in the promotion of diseases, imaging of protease activity in complex cellular environments has become an interesting field of research.

Several classes of fluorescent small molecules can be used to image protease activity.³⁸ These include fluorescently quenched substrates, fluorescent ABPs and fluorescently quenched ABPs (qABPs). Unlike substrates, the covalent binding of fluorescent ABPs precludes diffusion from the reaction site and enables direct biochemical analysis of the targets. Besides, it is possible to design highly selective

probes by adjustment of the recognition elements and the type of reactive functional group. A number of ABPs carrying assorted fluorescent reporter tags have facilitated fluorescent imaging studies and subsequent analysis of the active protease targets. However, the intrinsic fluorescence of the probes requires extensive washings of cells in culture or long clearance times *in vivo* in order to remove unreacted probe and obtain a sufficient contrast.

qABPs combine the covalent nature of ABPs with the fluorescently quenched properties of substrate probes. These ‘smart’ probes carry a warhead with a leaving group that is expelled upon reaction with the target protease. A fluorescent quencher that is attached to the leaving group will therefore result in a dark probe that emits a fluorescent signal only after activity-dependent covalent modification of the specific protease target (**Figure 4**). Hence, qABPs allow monitoring of real-time protease activity in live cells.

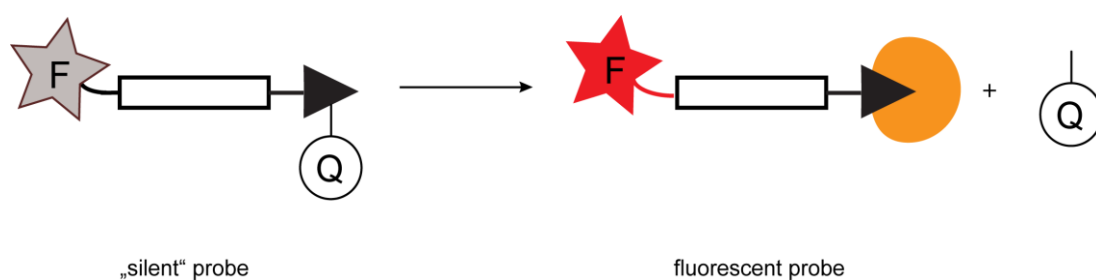


Figure 4 Design of a quenched activity-based probe. F: Fluorophore, Q: Quencher. The probe covalently binds to its target and forms a fluorescently labeled enzyme due to the loss of the quencher.

While substrates are turned over and can theoretically generate multiple fluorescent molecules per protease, qABPs react 1:1 with their targets, preventing signal amplification. However, in a comparative study, it was suggested that ABPs offer a more rapid and selective uptake into tumors and a higher overall signal strength compared to commercially available polymer-based quenched substrates. This is presumably due to the small size of ABPs and the overall rapid clearance *in vivo*.³⁹

Peptidic⁴⁰ and nonpeptidic⁴¹ qABPs have been designed and used in noninvasive optical imaging of cysteine protease activity in tumor-bearing mice. As an alternative application an acyloxymethyl ketone (AOMK) -based qABP was used topically to identify tumor tissues and aid resection.⁴² To the best of our knowledge a qABP for the real time monitoring of active serine proteases has yet not been reported.

1.2.2 Activity-based protein profiling

Activity-based protein profiling (ABPP) has played an increasing role in the functional analysis of enzymes within complex biological systems.⁴³ It combines proteomics techniques with small synthetic probes that covalently bind to active enzymes but not their inactive or inhibited forms.⁴⁴ The small molecules, called ABPs, thus provide a functional readout of the proteome. They have proven particularly useful for the study of proteases. ABPP has rapidly expanded its applications due to advancements in chemical probe synthesis, proteomics techniques and screening methods. Over the years, it has revealed several proteases as potential new drug targets.

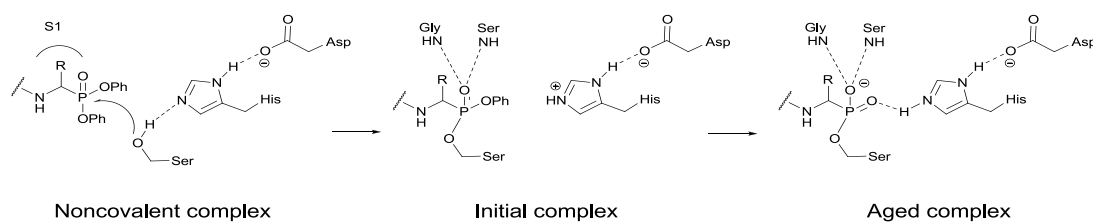
1.2.2.1 Phosphonates in ABPP

ABPP has been especially important for the study of proteases⁴⁴ since their activities are tightly regulated by several post-translational mechanisms. For cysteine cathepsin proteases, general⁴⁵ and selective ABPs⁴⁶ have been designed based on the epoxysuccinate and vinyl sulfone electrophile. Both general⁴⁷ and selective⁴⁸ AOMK-based probes have been reported for caspases. For serine proteases, general fluorophosphonate⁴⁹ and sulfonyl fluoride probes⁵⁰ and more selective isocoumarins⁵¹ and peptidyl diphenyl phosphonates⁵² (DPPs) are available.

α -Aminophosphonates are defined as amino acid analogues in which the carboxylic acid is replaced by a phosphonic acid, resulting in an N-C-P scaffold. Their activities ranging from antibacterial, herbicidal and physiological are long

known.⁵³ Peptide phosphonates represent a class of potent, irreversible and selective active site-directed inhibitors of serine proteases.⁵⁴ The tetrahedral geometry of the phosphonate group resembles the transition state during peptide bond hydrolysis, making them transition state analogues.

The reactivity of phosphonate inhibitors come from the electrophilic nature of the phosphorous atom. DFP is the first phosphonate discovered with an inhibitory activity against serine proteases.⁵⁵ In case of such phosphonyl fluorides, the high electronegativity of the fluorine atom causes the phosphorous atom to have strong electrophilic properties. This results in high reactivity but low chemical stability.⁵⁶ In addition, DFP is a very potent neurotoxin due to its irreversible binding to acetylcholinesterase.⁵⁷ The ensuing design of α -aminoalkylphosphonates is a compromise between reactivity and stability.⁵⁸ These compounds have two phenoxy groups instead of a fluorine atom, making the phosphorous atom electrophilic enough to undergo nucleophilic substitution. The nucleophilic attack of the hydroxyl group of the active site serine on the phosphorous atom, followed by the loss of a phenoxy group, leads to the formation of a covalent enzyme-inhibitor complex (**Scheme 2**). This initial complex then ages to a monoester.⁵⁹



Scheme 2 Mechanism of serine protease inhibition by α -aminophosphonate diphenyl esters. First a reversible enzyme-inhibitor complex is formed. This is followed by the phosphorylation of the active site serine residue. The irreversible complex then undergoes hydrolysis in a process called “aging”.

Diphenyl phosphonates are chemically stable in acidic and neutral conditions, but hydrolyze at pH values over 8. They show no reactivity towards cysteine, threonine,

aspartyl and metalloproteases and display no toxicity.⁶⁰ These features of the aromatic ester derivatives of aminophosphonates led to their utility as activity-based probes as chemical tools to study function and activity of serine proteases.⁶¹ Furthermore, the selectivity of phosphonate inhibitors as well as ABPs is easily adjusted by incorporation of a peptide chain (**Figure 5**).

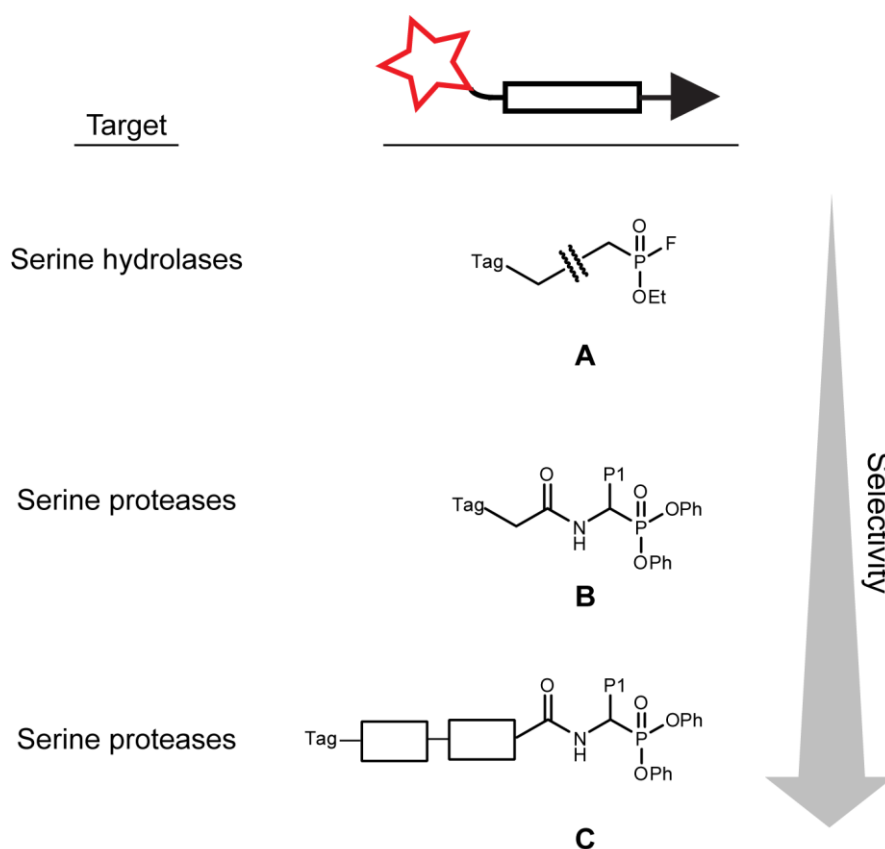


Figure 5 Influencing the selectivity of phosphonate ABPs. The warhead (triangle) and spacer or recognition element (black box) determine the selectivity of the probe. Fluorophosphonates (A) are general probes that label most serine hydrolases. Peptide diphenyl phosphonates (B and C) label serine proteases. The selectivity is steered by the side chain in the P1 position and optional additional elements at distal sites.

1.2.2.2 Applications of ABPP

The first applications of ABPs involved the gel-based profiling of serine hydrolases^{49b} and cysteine proteases.⁴⁵ These simple, well-established gel-based assays were then applied to the comparative analysis of active proteases in invasive cancer cells,⁶² in various life stages of parasites,⁶³ during viral infections,⁶⁴ and in pathogenic bacteria.⁶⁵ This method was used not only in identification of new drug targets but also in inhibitor screenings.⁶⁶ Furthermore, enrichment and purification of the targets with biotinylated ABPs, followed by peptide fingerprinting facilitated target identification. In this concept, the incorporation of cleavable linkers decreases the false-positive identifications.⁶⁷

High-throughput inhibitor screenings were accomplished by combining ABPP with fluorescence polarization – FluoPol-ABPP.⁶⁸ This technique makes use of the increase in fluorescence polarization signal of a fluorescent ABP when bound to its target. FluoPol-ABPP has been employed for the discovery of inhibitors for various serine hydrolases⁶⁹ as well as the intramembrane serine protease rhomboids.⁷⁰

Isotope-coded affinity tagging⁷¹ (ICAT), isobaric tags for relative and absolute quantification⁷² (iTRAQ) and stable isotope labeling of amino acids in cell culture⁷³ (SILAC) make use of general ABPs that target the proteome globally and have provided the means to analyze and quantify the cysteine, lysine and serine residues, respectively. ABPP combined with multidimensional protein identification⁷⁴ (MudPIT) bypasses the use of isotopes and allows the quantification of levels of specific enzyme activities by spectral counting.

Moreover, ABPP has also been combined with microarrays via immobilization of either the enzymes⁷⁵ or the ABPs⁷⁶ on a chip surface for protease fingerprinting⁷⁷ and the determination of inhibitor potency and selectivity⁷⁷⁻⁷⁸.

Imaging of enzymatic activities have been achieved in tissue sections with ABPs employed in imaging mass spectrometry,⁷⁹ and *in vivo* with fluorescently quenched ABPs (p. 13).

2 Scope of this work

With the ever-growing applicability of activity-based protein profiling (ABPP) there is a constant interest in designing new activity-based probes (ABPs). The ability to modulate probe selectivity is crucial for their applicability. Diphenyl esters of α -aminophosphonates (DPPs) bind selectively, covalently and irreversibly to the active site serine residue of serine proteases. These features qualify them as attractive warheads for ABPs. The selectivity of DPPs can be modulated via the adjustment of the group at the P1 position and other non-primed site residues. While synthetic strategies to generate DPPs in solution have been reported, an easy and rapid way to synthesize DPP ABPs remains a challenge. In chapter 1 of this thesis a new synthetic route is described that enables an overall convenient construction of DPP ABPs and simple modification of the extended peptide sequence to tune their activity as well as selectivity.

Fluorescent ABPs have the disadvantage of showing fluorescence when free in solution, thus creating background. The need to wash excess probe or long clearance times makes them not suitable for real time imaging applications. Therefore we aimed to synthesize quenched versions of phosphonate ABPs (qABPs). The probes carry a fluorophore and a quencher pair. The quencher is introduced to the only leaving group on the phosphonate warhead. In this form the probe is “silent” and only upon reaction with the enzyme fluorescence signal is generated. The synthesized qABPs are aimed to be used in imaging of atherosclerosis tissue sections and of neutrophil elastase secreted from primary neutrophils.

The ABPs mentioned above target conventional serine proteases. In order to also develop ABPs for a nonconventional protease, we set up a method for the Lon protease to screen for covalent inhibitors that can be used as warheads for ABPs. Lon protease is an ATP-dependent serine protease which is mainly involved in protein quality control and degradation of some regulatory proteins. It is inhibited by general serine protease inhibitors in high inhibitor concentrations and after long exposures. Coumarins and boronates have been reported as well, however, they are not specific for Lon. To the best of our knowledge no potent specific inhibitors and ABPs for

Lon protease exist. To address this problem we synthesized a FRET peptide and developed an assay to screen a library of small molecules for their ability to inhibit *E. coli* Lon to cleave this peptide. We further evaluated the hit compounds for their potential use in activity-dependent labeling of the enzyme.

3 Results and discussion

“Synthesis is an academically sanctioned opportunity to live on the edge. Handling dangerous materials can be thrilling, like skydiving in a lab coat.”
Dylan Stiles

3.1 On-resin strategies for synthesis of diphenyl phosphonate ABPs

The work in the following chapter has been in parts published in *Org. Biomol. Chem.* 2013⁸⁰ and is described here in detail.

3.1.1 General remarks

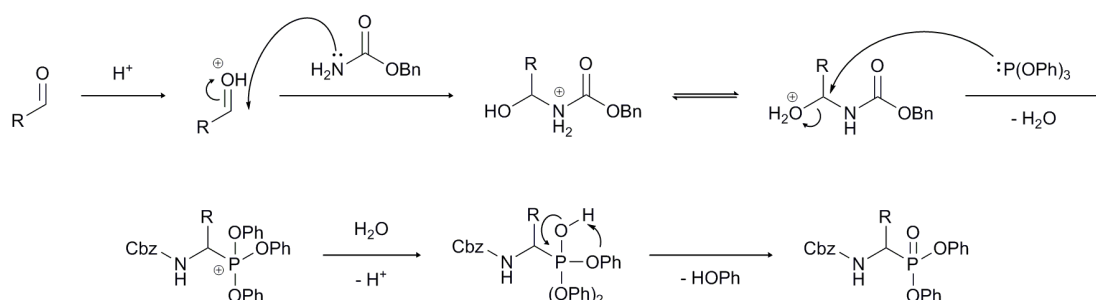
We implemented a solid phase strategy for the synthesis and selectivity modulation of serine protease ABPs. We chose diphenyl esters of α -aminophosphonates (DPPs) because they are low molecular weight, irreversible inhibitors exhibiting explicit selectivity⁸¹ for serine proteases and therefore represent useful warheads for ABPs. DPPs have been validated as covalent irreversible inhibitors of serine proteases and they can be fine-tuned both via modification of the group in the P1 position, which interacts with the enzyme S1 pocket and via introduction of additional recognition sites that interact with more distal non-primed site pockets. The here reported approach allows rapid diversification of the recognition moiety and convenient synthesis of DPP ABPs. In addition, their applicability for selective labeling of endogenous proteases within complex proteomes is demonstrated.

3.1.2 Synthetic strategy

Our initial synthetic strategy towards phosphonate ABPs with extended peptide recognition elements comprised the connection of a DPP to a solid support followed by peptide elongation using solid phase peptide synthesis conditions. However, linking the DPP via either its amino group or its side chain led to the destruction of the electrophilic phosphonate during elongation or cleavage from the resin. Furthermore, the lability of diphenyl phosphonates under basic conditions limits the reaction conditions that can be used during the synthesis. Our synthetic approach therefore comprised the connection of a DPP warhead to a solid support during the

last step using mild and chemoselective click chemistry. In this route, the peptidic portions of the probes are generated by solid phase peptide synthesis and the amino group of the last amino acid is converted to an azide by on-resin diazo transfer.⁸² The azide allows for the introduction of the DPP building blocks via on-resin click reaction⁸³ forming a 1,4-substituted 1,2,3-triazole. Triazoles have been used in selective probe design for cathepsin S.⁴¹ Moreover, they are proteolytically and metabolically stable and provide good analogues of peptide bonds due to their strong dipole and H-bond accepting and donating properties.⁸⁴ We anticipated that the interactions at the P3 and P4 positions would provide desired modulation of selectivity.

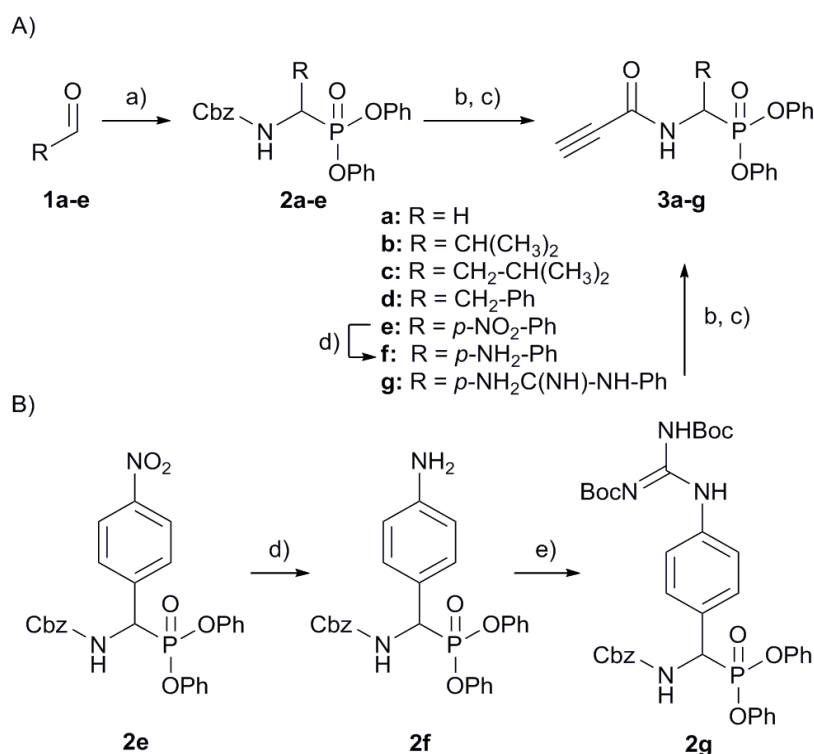
We synthesized alkynylated versions of diphenyl α -aminoalkylphosphonates in three easy steps. Cbz protected derivatives with hydrophobic side chains or a hydrogen in the P1 position, such as glycine (**2a**), valine (**2b**), leucine (**2c**), phenylalanine (**2d**) and *p*-nitrophenylglycine (**2e**) were prepared from commercially available aldehydes (**1**) as described by Oleksyszyn *et al.*^{59, 85} The mechanism of this Mannich-type reaction is the same as first described for α -ureidophosphonates⁸⁶ (**Scheme 3**). The aldehyde is activated via acid catalysis and subsequently attacked by benzyl carbamate resulting in an α -hydroxycarbamate. Water is liberated upon attack of triphenylphosphite on the α -carbon. Diphenyl phosphonate is formed after the attack of water on the phosphorus, releasing phenol. The condensation products were obtained as pure solids after crystallization with yields ranging from 26 to 86%.



Scheme 3 Mechanism of the Birum-Oleksyszyn reaction. Acid catalyzed activation of the aldehyde, followed by the attack of benzyl carbamate results in an α -hydroxycarbamate. Water is liberated upon attack of triphenylphosphite on the α -carbon. Diphenyl phosphonate is formed after the attack of water on the phosphorus, releasing phenol.

One drawback of this reaction is the lack of a chiral selector, resulting in the products as a racemic mixture of both enantiomers. It has been reported that the (*R*)-enantiomer of the phosphonate diphenyl esters are about 22-fold more preferred by serine proteases over the (*S*)-enantiomer.⁸⁷ This *R*-configuration corresponds to the L-amino acids. A recent study showed that the influence of such asymmetric preference is more pronounced (over 1:1500) when longer phosphonic peptides with an optimal structure towards the target enzyme is tested.⁸⁸ To overcome this problem some methods for stereoselective synthesis of α -aminophosphonic acids have been developed.⁸⁹ For simplicity, we here used the nonchiral phosphonate building blocks.

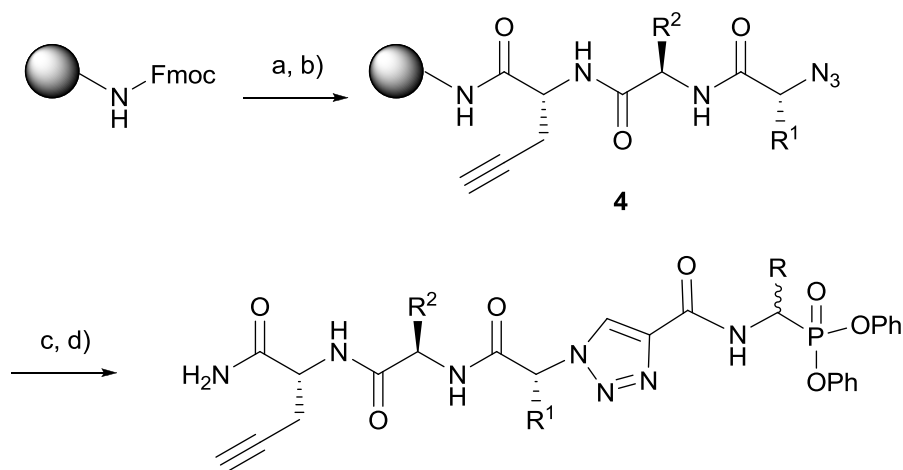
Cbz deprotection of the phosphonates was carried out with HBr/AcOH in a nucleophilic substitution reaction. Subsequent introduction of an alkyne handle to form the building blocks **3a-e** was achieved by coupling of propiolic acid through preactivation with DIC (**Scheme 4A**). As a basic P1 residue we chose a diphenyl phosphonate with a *p*-guanidinophenyl side chain, which was made by using two additional reaction steps.⁹⁰ The *p*-nitrophenyl moiety of **2e** was reduced to an aniline (**2f**) using iron powder in acetic acid in quantitative yield. The aniline was then transformed into a Boc-protected guanidine in a HgCl₂-catalyzed reaction with 1,3-di-Boc-2-methylisothiourea giving compound **2g** in a yield of 57% (**Scheme 4B**). The introduction of the propiolic acid to both **2f** and **2g** was then performed as for the other building blocks.



Scheme 4 A) Synthesis of building blocks with hydrophobic side chains. a) CbzNH₂, P(OPh)₃, AcOH, 80 °C. b) 33% HBr/AcOH. c) propiolic acid, DIC (preactivation in THF 0 °C), TEA, DMF. B) Synthesis of building blocks with basic side chains. d) Fe powder, AcOH, 70 °C. e) 1,3-Di-Boc-2-methylisothiourea, HgCl₂, TEA, DCM.

The extended recognition elements of the probes were generated by solid phase peptide synthesis on a Rink amide resin (**Scheme 5**). All probes contain an L-propargylglycine to enable visualization of target proteases after labeling using click chemistry. This gives the flexibility to choose between different reporter tags such as biotin for further enrichment or different fluorophores. Further elongation took place by coupling of two amino acids which form the P4 and P3 positions. We chose either two alanine residues or two residues according to the substrate specificities of different serine proteases.⁹¹ The N-terminal amine was then transformed into an azide (**4**) via on-resin diazo transfer. Subsequently, the alkyne DPP building blocks were reacted with the azide via on-resin Cu(I)-catalyzed 1,3-dipolar cycloaddition. At this point we did not observe any intramolecular cycloaddition product. Final

cleavage from the resin resulted in eight different DPP ABPs (**5-11**) with yields varying from 3 to 40% after purification.



5 (AE-V):	R = CH(CH ₃) ₂	R ¹ = CH ₂ -CH ₂ -COOH	R ² = Me
6 (AA-L):	R = CH ₂ -CH(CH ₃) ₂	R ¹ = R ² = Me	
7 (AA-F):	R = CH ₂ -Ph	R ¹ = R ² = Me	R ² = CH ₂ -CH ₂ -S-CH ₃
8 (MF-F):	R = CH ₂ -Ph	R ¹ = CH ₂ -Ph	
9 (AA-Gua):	R = <i>p</i> -NH ₂ C(NH)-NH-Ph	R ¹ = R ² = Me	
10 (AS-Gua):	R = <i>p</i> -NH ₂ C(NH)-NH-Ph	R ¹ = CH ₂ -OH	R ² = Me
11 (nT-Gua):	R = <i>p</i> -NH ₂ C(NH)-NH-Ph	R ¹ = CH(CH ₃)-OH	R ² = CH ₂ -CH ₂ -CH ₂ -CH ₃
12 (LF-Gua):	R = <i>p</i> -NH ₂ C(NH)-NH-Ph	R ¹ = CH ₂ -Ph	R ² = CH ₂ -CH(CH ₃) ₂

Scheme 5 Solid phase peptide synthesis of DPP ABPs. a) piperidine/DMF (1/4, v/v); then, Fmoc-AA-OH, HOBT, DIC, DMF. b) piperidine/DMF (1/4, v/v); then, TfN₃, CuSO₄, DCM/MeOH (9/1, v/v). c) Building blocks **3**, CuSO₄, sodium ascorbate, TBTA, DMF/H₂O (10/1, v/v). d) 95% TFA, 2.5% TIS, 2.5% H₂O. The abbreviations indicated behind each compound number correspond to the residues in the P4, P3 and P1 positions.

3.1.3 Labeling experiments

3.1.3.1 Labeling of purified serine proteases

With both the P1 probes and the extended probes in hand we set out to test their labeling capability using commercially available, purified serine proteases of

different specificities: bovine chymotrypsin, known for its P1 specificity for large hydrophobic residues; human cathepsin G with tryptic-chymotryptic “dual specificity”⁹²; human neutrophil elastase, known for its P1 specificity for small hydrophobic residues; bovine trypsin and human urokinase-type plasminogen activator (uPA) known for their basic P1 specificity. For comparison we included a nonselective fluorophosphonate ABP, FP-rhodamine⁹³ (FP-R). Proteases tagged by DPP ABPs **3a-g** and **5-12** were visualized by clicking a tetramethylrhodamine (TAMRA) derivative carrying an azide function.

Both the P1 probes **3a-g** and the extended probes **5-12** resulted in labeling of proteases (**Figure 6**). The reactions between the probes and proteases occur in an activity-dependent manner, since pretreatment with an active site-directed inhibitor competes away the labeling. The influence of the extended peptide recognition element on the probes’ affinity towards their target proteases can be clearly observed from the overall increase of the labeling intensities in comparison to the P1 probes.

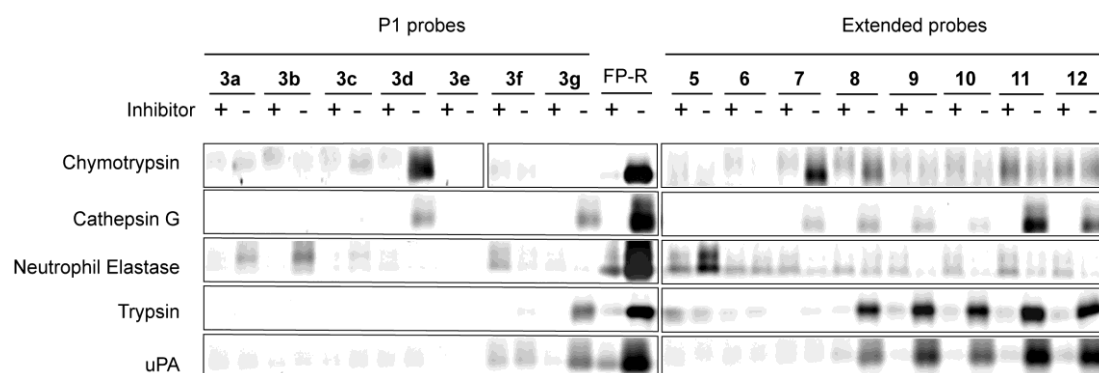


Figure 6 Labeling of purified proteases with FP-rhodamine, P1 and extended DPP probes. Probe concentrations: 5 μ M for DPPs, 1 μ M for FP-R.

The general serine hydrolase ABP FP-R labeled all proteases regardless of their P1 preferences while a change in the extended recognition elements resulted in different selectivities of the different probes. Probe **7**, with a Phe in the P1 position, mainly labels chymotrypsin. Unexpectedly, a change in the P3 and P4 position in probe **8**, led to labeling of trypsin and uPA as well. Another example of the modulation of the selectivity was observed for probes with a basic P1 side chain. Trypsin, uPA and

human cathepsin G were all equally labeled with the Gua P1 probe (**3g**) and the extended probe nT-Gua (**11**). This result is in line with previously reported phosphonate inhibitors of these enzymes.^{1, 94} In contrast, AS-Gua (**10**) displayed a high intensity band for trypsin and only a weaker band for uPA.

3.1.3.2 Labeling of purified proteases in a proteome background

We next investigated whether the extended probes can be applied within the context of a complex proteome. To demonstrate that the presence of other proteins does not interfere with the labeling of the target proteases, we spiked selected proteases into a cell lysate and incubated with probes that displayed the most selective activity-based labeling of the purified proteases. In-gel fluorescence showed intense activity-dependent bands for each enzyme without much cross-reactivity with other proteins (**Figure 7**). Only nT-Gua (**11**) when reacted with cathepsin G displayed some background bands which were not competed away by pretreatment with PMSF.

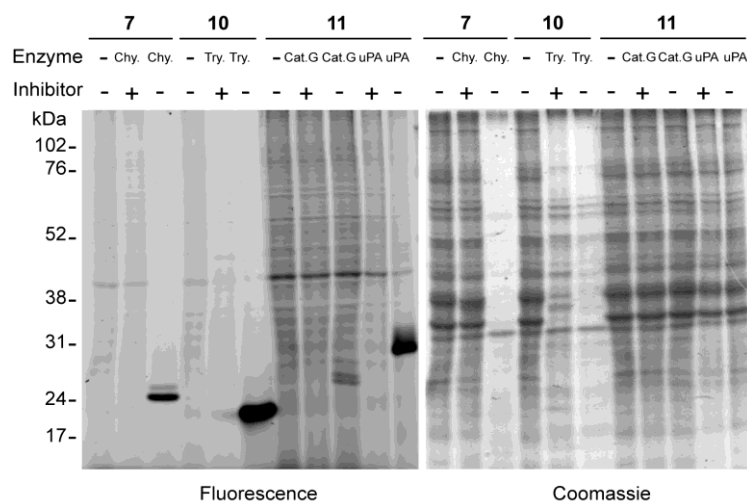


Figure 7 In-gel fluorescence (left) of proteases labeled in the context of a proteome (a cell lysate of the human colon adenocarcinoma cell line HT-29). The Coomassie stain (right) shows protein loading. The apparent lower amount of protein in the uninhibited lanes for chymotrypsin and trypsin are likely due to the high digestive properties of these proteases. Chy.: Chymotrypsin; Try.: Trypsin; Cat. G: Cathepsin G; uPA: urokinase-type plasminogen activator.

3.1.3.3 Labeling in enterokinase-activated rat pancreas lysate

Finally, to illustrate the applicability of DPP ABPs in the labeling of endogenous serine proteases within a complex proteome, we used a rat pancreas lysate that was activated by treatment with enterokinase. Enterokinase activates trypsinogen into trypsin, the common activator of all pancreatic zymogens. Both activated and unactivated proteomes were used in labeling experiments with decreasing concentrations of probes that displayed strong activity towards chymotrypsin and trypsin in the previous experiments. A selective labeling of chymotryptic and tryptic enzymes was detectable (as confirmed by pretreatment with chymotryptic inhibitor DAP22c and tryptic inhibitor TLCK) with probe concentrations down to 0.1 and 1 μ M, respectively (**Figure 8**). No labeling was observed in case of unactivated or preinhibited lysates, as well as buffer containing only enterokinase.

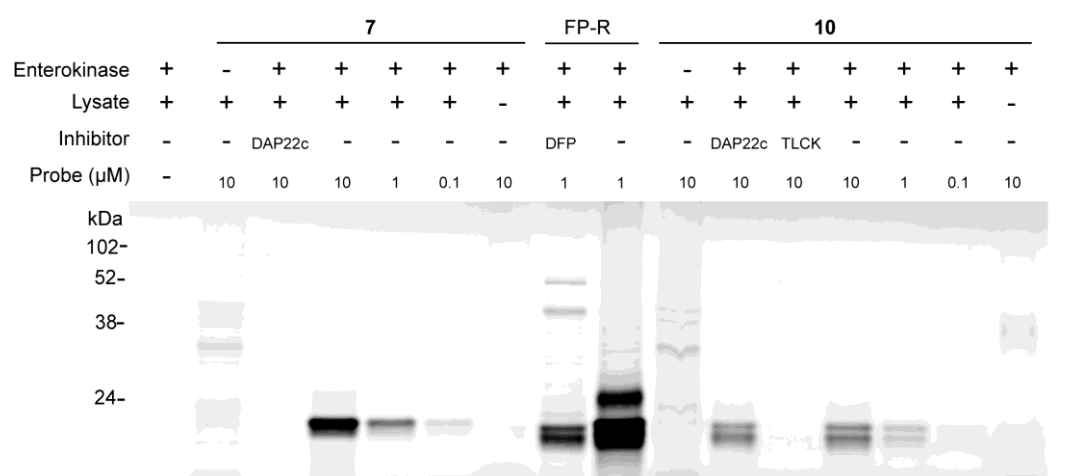


Figure 8 Fluorescent labeling of endogenous proteases in enterokinase-activated rat pancreas lysate by DPP ABPs with extended recognition elements and FP-R. The relatively unstable inhibitor DFP did not completely inhibit all labeling by FP-R.

3.1.4 Molecular docking of probe **10** bound to trypsin

To gain insight in the binding mode of the extended probes that carry a triazole in their backbone, we performed molecular docking of a covalently bound probe **10** inside a bovine trypsin crystal structure. As expected, the *p*-guanidino-phenyl ring in the P1 position of the probe occupies the S1 pocket, where it forms a salt bridge with Asp189 (**Figure 9**, lower panel). The triazole occupies the S2 site and has a similar position as a proline in the P2 position of a non-covalent trypsin inhibitor. The alanine and propargylglycine interact with the more distal S3/S4 sites (**Figure 9**, upper panel). Overall, this structure suggests that the probes – despite the non-natural triazole and the reversed polarity of the P3-P5 backbone, interact with the non-primed site to give increased potency compared to the P1 only probes.

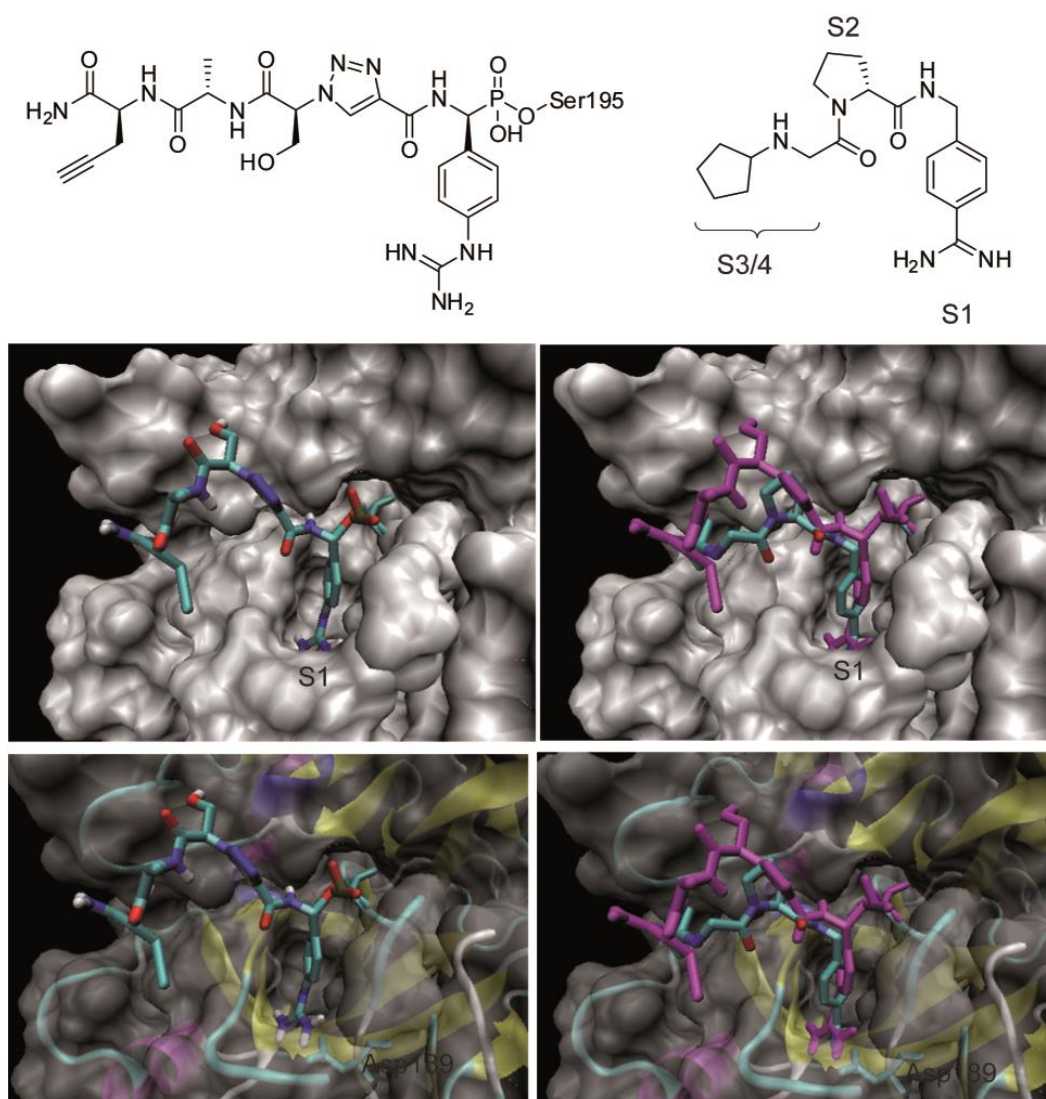


Figure 9 Docking of probe **10** bound to Ser195 in bovine beta-trypsin. Upper panel: The enzyme surface is represented in white, except for the S195 residue, which is shown as a stick model as are the small molecules. Left: probe **10** (colored by element: red = oxygen, blue = nitrogen, cyan = carbon, brown = phosphorous) docks with its *p*-guanidino-phenyl group into the S1 pocket. Right: probe **10** is colored in magenta and overlaid with a non-covalent inhibitor.¹ The triazole of probe **10** takes a similar position as the proline in the other inhibitor, while the other residues interact with various sites on the non-primed site. Lower panel: Beta-trypsin is displayed with a transparent surface and a cartoon representation of the backbone. Probe **10** (left: colored by element; right: colored in magenta) and the indicated inhibitor (overlaid with probe **10** in the right panel) are shown as stick models. Asp189, at the bottom of the S1 pocket, also in stick model, forms a salt bridge with the guanidine and amidine, respectively.

3.2 Quenched phosphonate ABPs for imaging protease activity

3.2.1 General remarks

Fluorescent reporters have been incorporated into ABPs for target visualization in-gel as well as imaging by fluorescence microscopy. However, these probes also show fluorescence when free in solution, thus creating background and making them unsuitable for real-time imaging. To overcome this, quenched activity-based probes (qABPs) have been designed that become fluorescent only after covalent modification of a specific protease target. A number of qABPs have been described for cysteine proteases of clan CA and CD and been successfully used in the imaging of cathepsins in live cells⁹⁵ and xenografted tumors⁴⁰, and of legumain⁹⁶ in primary macrophages and in mouse cancer models.

Here we describe the first fluorescently quenched ABP for serine proteases. Our qABP carries a fluorophore and a quencher pair, a phosphonate warhead and either a valine or an arginine-like recognition element (**Figure 10**). It shows a high quenching efficiency, a strong activity-dependent reactivity and specificity towards trypsin-like proteases and neutrophil elastase, respectively. The probes are aimed to be used in imaging of atherosclerosis tissue sections and of neutrophil elastase secreted from primary neutrophils.

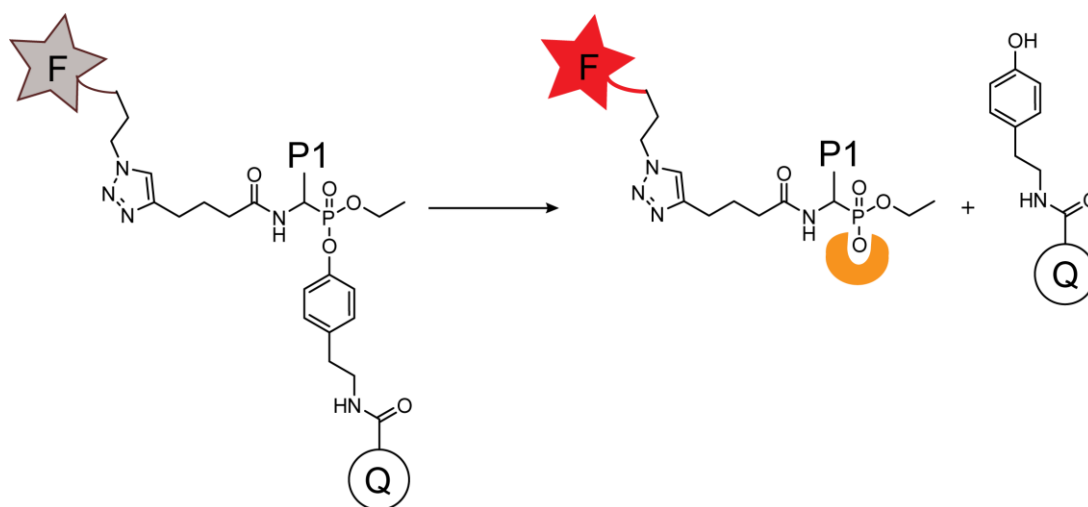


Figure 10 Schematic illustration of a phosphonate qABP, binding to a serine protease. The reaction results in the loss of the quencher, leading to an increase in fluorescence emission. F: fluorophore, Q: quencher, orange circle: probe bound enzyme.

3.2.2 Synthetic strategy

Diaryl α -aminophosphonates have been reported as ABPs and irreversible inhibitors of serine proteases.⁸¹ However, in our design it is crucial to have only one leaving group. Therefore, we started with making a diethyl phosphonate carrying the P1 recognition element, and selectively removed one of the ethyl groups to introduce a leaving group. We then attached an alkyne handle on the amino group of the phosphonate to enable chemoselective introduction of a fluorophore under mild conditions and coupled the quencher to the leaving group, obtaining the qABP. We synthesized two qABPs either with a valine or *p*-guanidinophenyl side chain as a recognition element.

3.2.2.1 Synthesis of a basic P1 probe

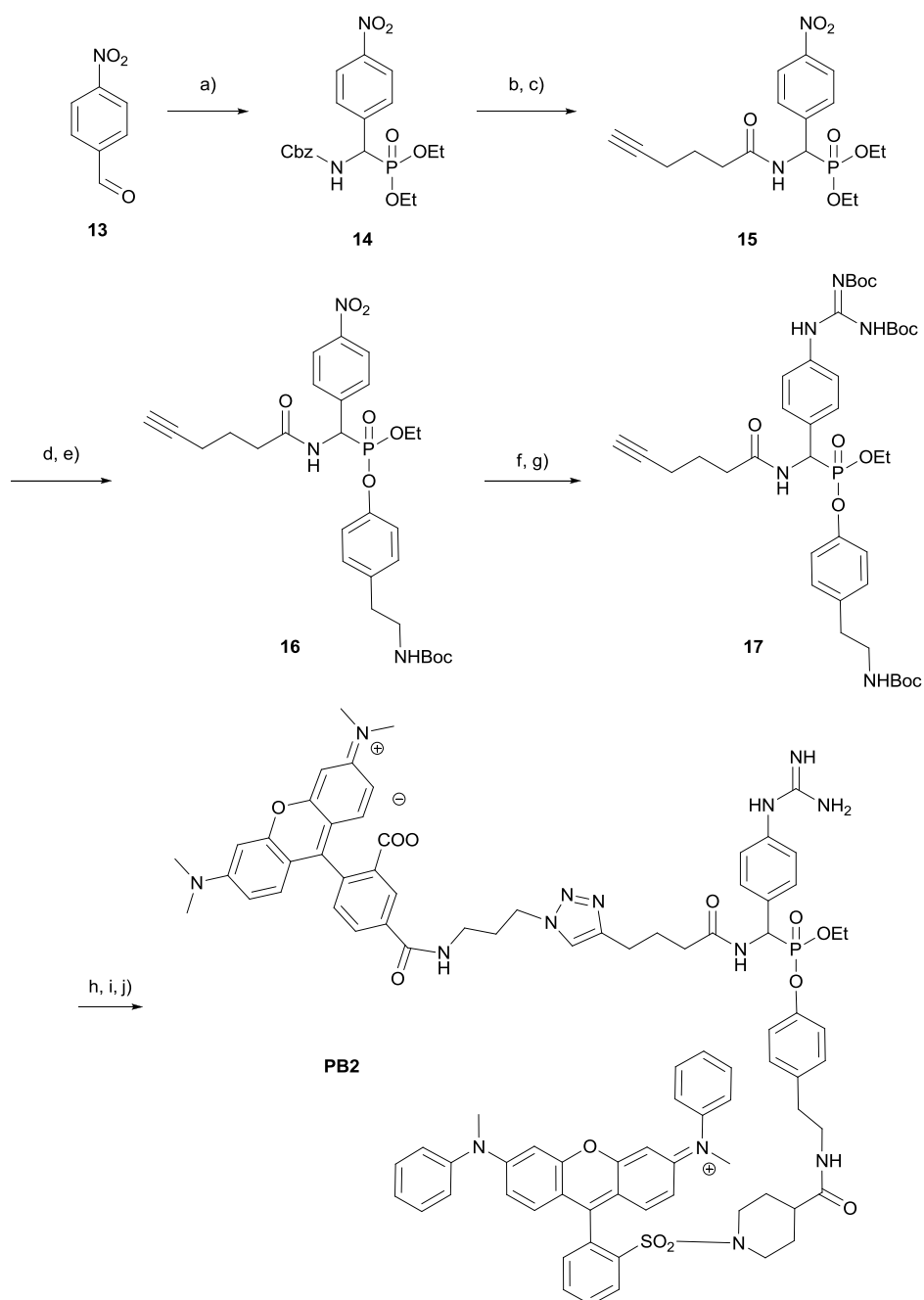
Synthesis of an ABP with a basic P1 side chain was difficult due to the complicated protecting group strategy. The base labile nature of the phosphonate warhead and the acidic conditions of the Mannich-type reaction leave not many options for the

protection of the amino groups of a lysine or an arginine side chain. We therefore chose to use a NO₂-mask and synthesize a *p*-guanidinophenyl mimicking an arginine residue.

The synthesis started with 4-nitrophenylbenzaldehyde (**13**) reacting with diethyl phosphite and benzyl carbamate in AcOH/SOCl₂ through a Mannich-type reaction to yield the Cbz protected diethyl phosphonate (**Scheme 6**). The condensation product (**14**) was obtained as pure solid after crystallization. The Cbz group was removed with HBr/AcOH, which involves protonation of the carbamate and nucleophilic addition of bromine to give benzyl bromide and the corresponding carbamic acid. The carbamic acid is unstable and breaks down to the amine and CO₂. The alkyne handle to later enable clicking of a fluorophore was introduced by coupling of hexynoic acid to the primary amine with HATU.

For the subsequent selective hydrolysis of one ethyl group we initially used saponification with NaOH. However this reaction always resulted in mostly dihydrolysis of both ethyl groups even when only 1.2 eq. was used. We therefore moved on to a non-hydrolytic monodealkylation by means of LiBr, and did not observe any didealkylation. A Boc-protected tyramine was then introduced as a leaving group to this lithium salt through esterification.

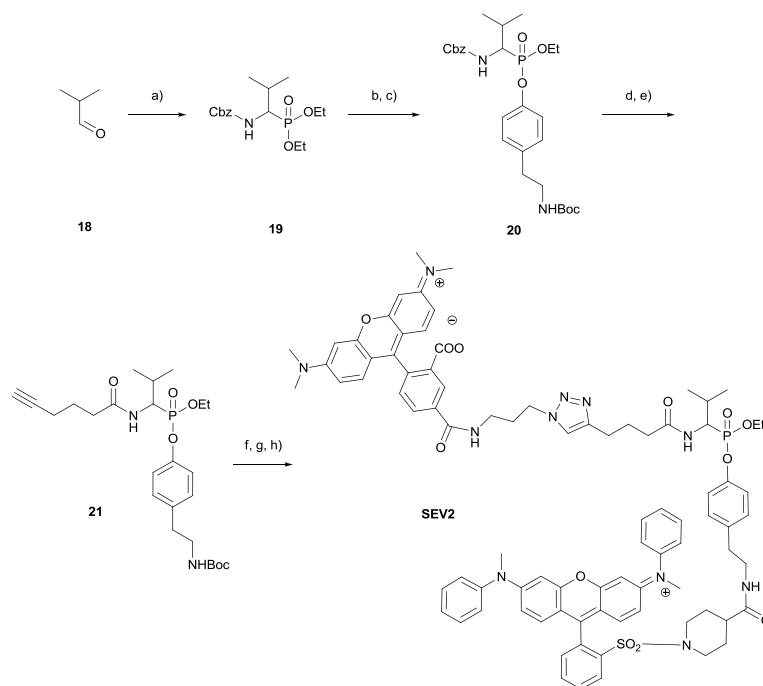
The basic recognition element was constructed by first the transformation of the nitrophenyl group to an aniline by SnCl₂ catalyzed reduction, and consecutive guanidinylation by using di-Boc-protected triflylguanidine. To finalize the probe structure all the Boc protecting groups were removed with TFA, and afterwards the fluorophore and the quencher were incorporated. TAMRA-N₃ was attached via Cu(I)-catalyzed 1,3-dipolar cycloaddition whereas the quencher QSY-7 was linked via an amine reactive succinimidyl ester.



Scheme 6 Synthesis of a basic P1 probe. a) CbzNH₂, HPO(OEt)₂, AcOH/SOCl₂ (93%) b) 33% HBr/AcOH (64%) c) Hexynoic acid, HATU, DIEA, DMF (74%) d) LiBr, MEK, 80 °C (65%) e) *N*-Boc-Tyramine, DIC, DMAP, DMF, 70 °C (90%) f) SnCl₂, EtOH, 70 °C g) 1,3-Di-Boc-2-(trifluoromethylsulfonyl)guanidine, TEA, DCM, 40 °C (19% over 2 steps) h) TFA, TIS, DCM (37%) i) TAMRA-N₃, CuSO₄, Na ascorbate, TBTA, CuBr, ACN/H₂O (16%) j) QSY-7 OSu, DIEA, DMSO (18%)

3.2.2.2 Synthesis of a P1 Valine probe

The three-component reaction took place in AcOH with isobutyraldehyde (**18**), diethyl phosphite and benzyl carbamate (**Scheme 7**). According to the procedure for **PB2** the phosphonate was then dealkylated with LiBr via an S_N2 reaction, followed by esterification to introduce the Boc-protected tyramine as a leaving group. For the removal of the Cbz group Pd catalyzed hydrogenation was preferred over HBr/AcOH to remove only the Cbz, but not the Boc group. Hexynoic acid was then attached to the primary amine by standard peptide coupling with HATU to allow clicking of the fluorophore TAMRA carrying an azide to the alkyne group in the next step. Based on the previous experience the deprotection of the Boc group was done after the introduction of the fluorophore to overcome solubility problems. The final product (**SEV2**) was obtained after the subsequent coupling of the quencher QSY-7 to the tyramine.



Scheme 7 Synthesis of a P1 Valine probe. a) CbzNH₂, HPO(OEt)₂, AcCl (78%) b) LiBr, MEK, 80 °C c) *N*-Boc-Tyramine, DIC, DMAP, DMF, 70 °C d) H₂, Pd/C, AcOH, EtOH e) Hexynoic acid, HATU, DIEA, DMF (26% over 4 steps) f) TAMRA-N₃, CuBr, Na ascorbate, TBTA, *t*BuOH/H₂O (1/1) g) TFA, DCM h) QSY-7 OSu, DIEA, DMSO (16% over 3 steps)

3.2.3 Labeling of purified serine proteases with qABPs

Labeling experiments using commercially available, purified serine proteases of different specificities were carried out to test the capability of the qABPs. **PB2** was tested with bovine chymotrypsin, human cathepsin G, pancreatic elastase, bovine trypsin and human uPA, while **SEV2** was tested additionally with human neutrophil elastase.

The binding of all probes takes place in an activity-dependent manner since preblocking of the enzyme with an active site-directed inhibitor competes away the labeling (**Figure 11**). The binding behavior matches the natural substrate selectivity of the proteases. qABP with a basic P1 residue shows high reactivity towards trypsin-like proteases; trypsin and uPA, whereas the P1 valine probe displayed a high intensity band for neutrophil elastase, and a rather weak band for pancreatic elastase.

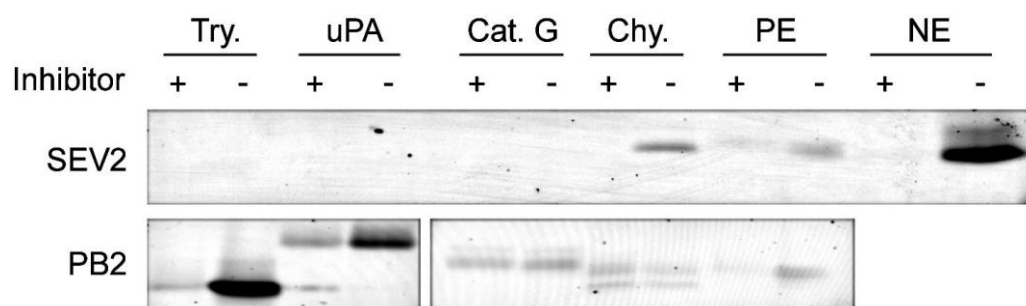


Figure 11 Labeling of purified serine proteases with qABPs. Try.: trypsin, uPA: urokinase-type plasminogen activator, Cat. G: cathepsin G, PE: pancreatic elastase, NE: neutrophil elastase. Probe concentrations: **SEV2**: 5 μ M, **PB2**: 2 μ M.

3.2.4 Quenching efficiency

For imaging applications it is of fundamental importance that there is a clear difference between the probe's fluorescence intensity in the unbound/quenched state and the bound/unquenched state. This was tested by measuring the fluorescence intensity of the fluorophore only, the probe only and the probe together with the

enzyme. We showed this for **PB2** (**Figure 12**). As expected the fluorophore showed the highest fluorescence intensity. **PB2** showed no fluorescence signal, similar to PBS buffer. **PB2** and trypsin together showed an increase of the fluorescence intensity over time.

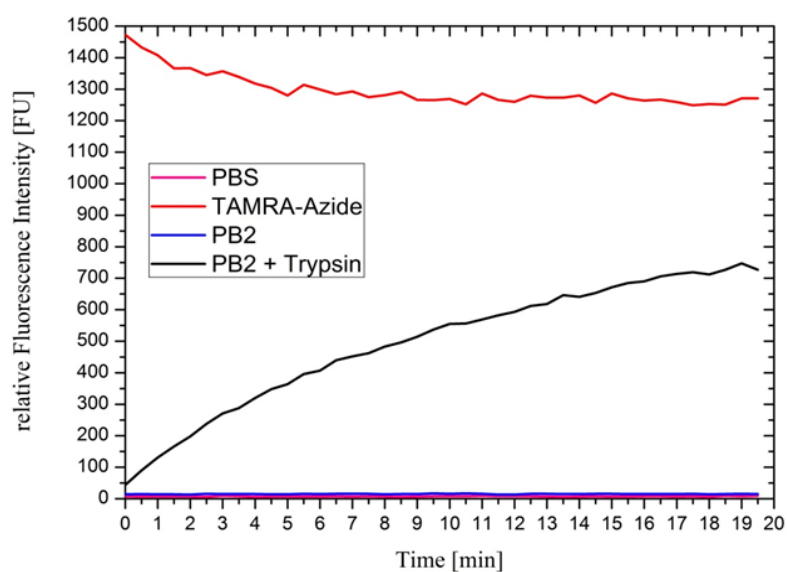


Figure 12 Quenching efficiency of **PB2**. In the “silent” state, the qABP does not show any fluorescence whereas it is quenched and an increase in fluorescence intensity over time is observed when it reacts with the active enzyme.

3.3 FRET-based assay for inhibitor screening of Lon protease

3.3.1 General remarks

Lon is an ATP-dependent homo-oligomeric serine protease, which can be found in all kingdoms of life. It is mainly involved in protein quality control and it selectively degrades some regulatory proteins. Its involvement in bacterial pathogenicity made it an important target in the development of novel therapeutic agents. However, the lack of inhibitors and ABPs for Lon hinders a clear understanding of its function in normal and disease states. To date, even though few inhibitors of Lon are reported, none of them are highly potent or specific. There are also no ABPs for visualization of Lon activity available.

We aimed to establish an *in vitro* assay to monitor the enzymatic activity of Lon and screen for inhibitors with this assay. Lon protease from *E. coli* was expressed, purified and the optimal reaction conditions were determined. In parallel, a peptide substrate of Lon with a fluorophore and a quencher pair was synthesized. The intact FRET peptide is only weakly fluorescent, whereas an increase in fluorescence can be detected after cleavage, making it possible to measure and quantify the enzymatic activity of Lon. This FRET assay was then used to screen a total of 123 compounds for new inhibitors of Lon, of which four hit compounds with an inhibitory effect against Lon were identified. The best two hits are boronates, which was to be expected as boronic acids have been reported as inhibitors of the proteasome with a known potency against Lon,⁹⁷ confirming the reliability of the assay. The other hits are thiiranes, representing a new class of irreversible inhibitors of *E. coli* Lon.

3.3.2 Synthetic strategy

In an effort to study the *in vitro* activity of Lon on a physiological substrate, Maurizi reported the degradation of λ N protein by Lon.⁹⁸ The N protein of λ was selected since it is a rapidly degraded native protein found in *E. coli* whose degradation is

controlled by Lon. In a following study a 10-amino-acid FRET peptide was generated to investigate the kinetics of its degradation by Lon.²⁷ The sequence of this peptide corresponds to the 89-98 residues of the N protein.

Based on the reported sequence we synthesized a FRET peptide with a C-terminal fluorophore and an N-terminal quencher. The choice of fluorophore and quencher was fluorescein isothiocyanate (FITC) and 4-(dimethylamino)azobenzene-4-carboxylic acid (DABCYL), respectively (**Figure 13**).

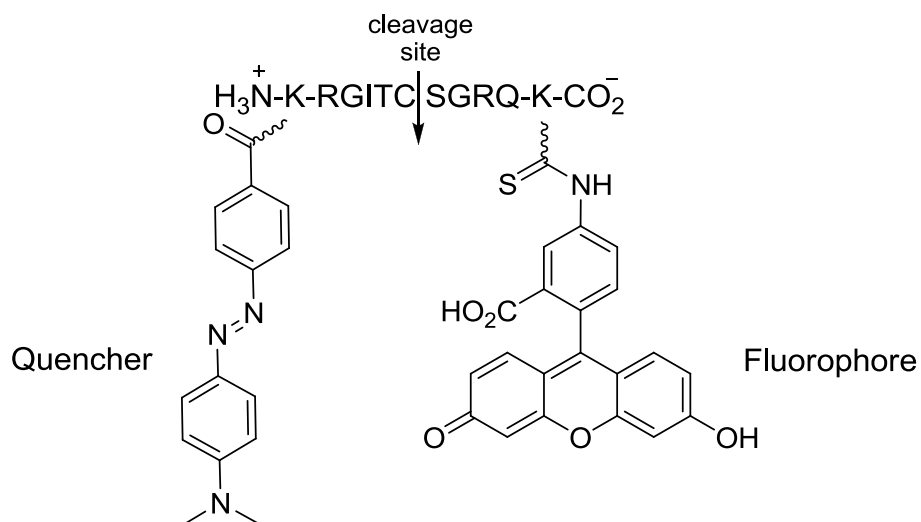
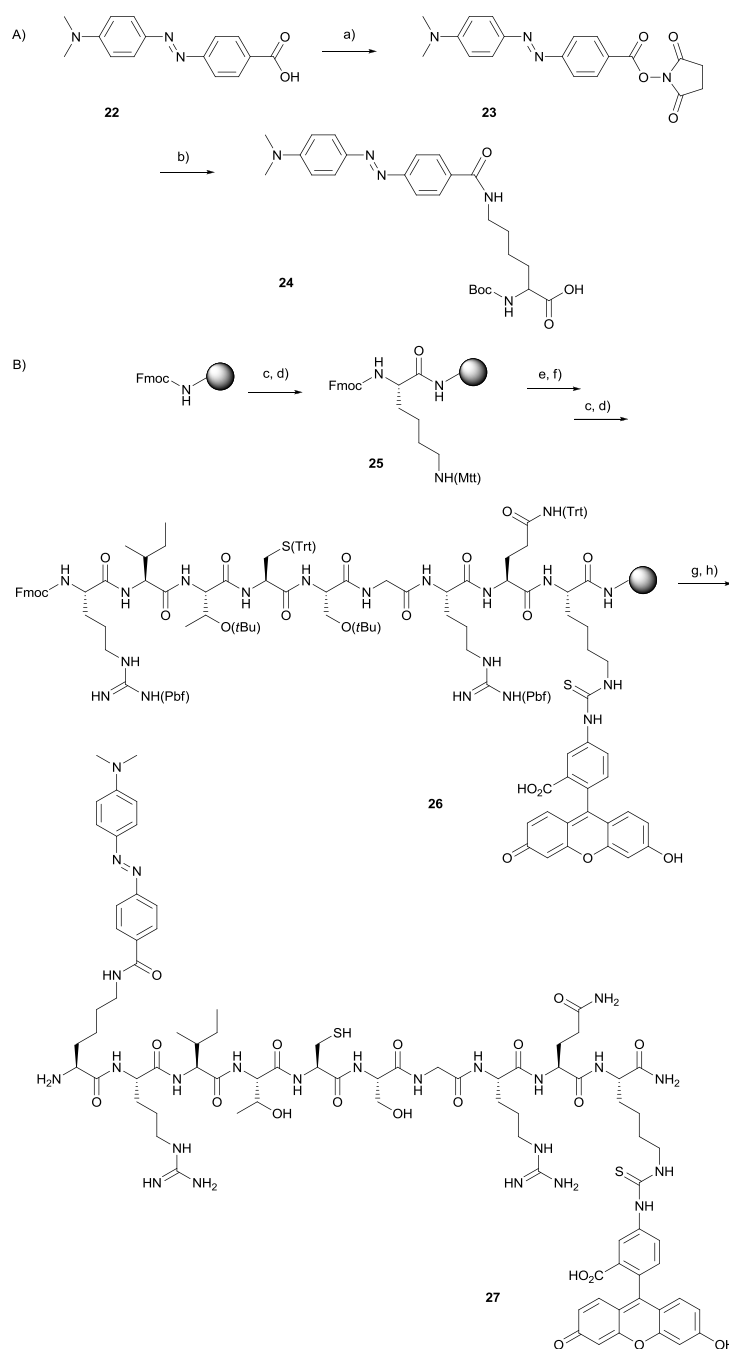


Figure 13 FRET peptide with the N-terminal quencher DABCYL and the C-terminal fluorophore FITC.

The initial attempt of endcapping the N-terminus by acetylation to prevent reaction of the N-terminus resulted in one time, two times and even a small fraction of three times acetylated peptides. Since the functional groups of all amino acids were protected at the time of acetylation, it is likely that the hydroxyl groups of the FITC were acetylated. As this ester bond would be less stable than an amide bond, deacetylation of undesired product with NaOH was tried. However, it was not possible to achieve this without degrading the peptide.

In a second approach the complete sequence was synthesized on solid support without acetylation as described in the original procedure, followed by the removal of the methyltrityl (Mtt) protecting group of the N-terminal lysine under mild acidic conditions. However, the final reaction to introduce the quencher resulted in double dabcylation even when only one equivalent of NHS-DABCYL was used. It is very likely that the trityl (Trt) protection of the cysteine was removed together with the Mtt as both groups are highly acid-labile. Hydroxyl groups⁹⁹ as well as sulfhydryl¹⁰⁰ have been reported to react with NHS esters. Therefore, the additional dabcylation might have occurred on the hydroxyl of the fluorescein and the cysteine side chain. The ester and thioester bonds are base-labile and it was indeed possible to cleave the additional DABCYL from the peptide with NaOH after the addition of 10 eq. ethanolamine to react with all NHS-DABCYL still in solution. Under these basic conditions the Fmoc protecting group was also removed as revealed by LC-MS. Finally it was possible to obtain the final compound with a yield of 10%. However, this strategy is inefficient and expensive due to the need for an extra step to cleave half of the coupled DABCYL from the peptide. These results finally led to the development of a new synthesis strategy.

The optimized synthetic strategy to obtain the FRET peptide comprised the separate synthesis of two building blocks. The first building block (**24**) was synthesized in solution and coupled to the second building block (**26**) which was produced using solid phase peptide synthesis procedures (**Scheme 8**). The dabcylic acid (**22**) was reacted with *N*-hydroxysuccinimide (NHS) and DIC to give the activated ester (**23**), which was then reacted with a Boc-protected lysine to form Boc-Lys(DABCYL)-OH (**24**) (**Scheme 8A**). The peptide synthesis was done by general Fmoc solid phase synthesis procedures. Fmoc protection was removed by 20% piperidine in DMF, and amino acid couplings were done by HOBt/DIC, except for Ile, which was coupled by HATU/DIEA. Directly after coupling of the first amino acid to the resin, the fluorophore was introduced to the ϵ -amino group of this C-terminal lysine. The last step of the SPPS was the on-resin coupling of **24** to **26**. The final cleavage of the product from the resin and simultaneous removal of all protecting groups with TFA gave the desired FRET peptide (**27**) with a yield of 27% (**Scheme 8B**).



Scheme 8 Synthesis of the FRET peptide **27**. **A)** Solution phase synthesis of Boc-Lys(DABCYL)-OH. a) NHS, DIC, DMF b) Boc-Lys-OH, DIEA, DMF. **B)** Solid phase peptide synthesis. c) piperidine/DMF (1/4, v/v). d) Fmoc-AA-OH, HOBT, DIC, DMF. (For Ile: HATU, DIEA, NMP) e) 1% TFA in DCM. f) FITC, DIEA, DMF. g) Boc-Lys(DABCYL)-OH, HBTU, DIEA, DMF/DCM (1:1). h) 88% TFA, 5% DTT, 5% H₂O, 2.5% TIS.

3.3.3 Expression and purification of *E. coli* Lon

Lon protease, the main component of the assay, was overexpressed in *E. coli* BL21 (DE3) cells for 2 h. An N-terminal His₆-tag allows the detection of the expressed protein through Western blot using His₆-antibodies. When Lon was expressed the first time inoculation of a starter culture was done from a glycerol stock. After expression, cells were lysed by sonication, and the target protein was purified by using Ni-NTA beads. The activity of the enzyme was determined with a gel-based β -casein digestion assay. β -casein is an artificial substrate of Lon. In case of an active enzyme the β -casein is digested and the β -casein band is weaker or disappears completely. With this assay the Lon seemed to be inactive and the expression was repeated with a fresh transformation of electrocompetent *E. coli* BL21 (DE3) cells. In addition, the method of lysis was switched to the milder French press instead of sonication. The protein was then purified using Ni-NTA beads (**Figure 14**), and its concentration was determined.

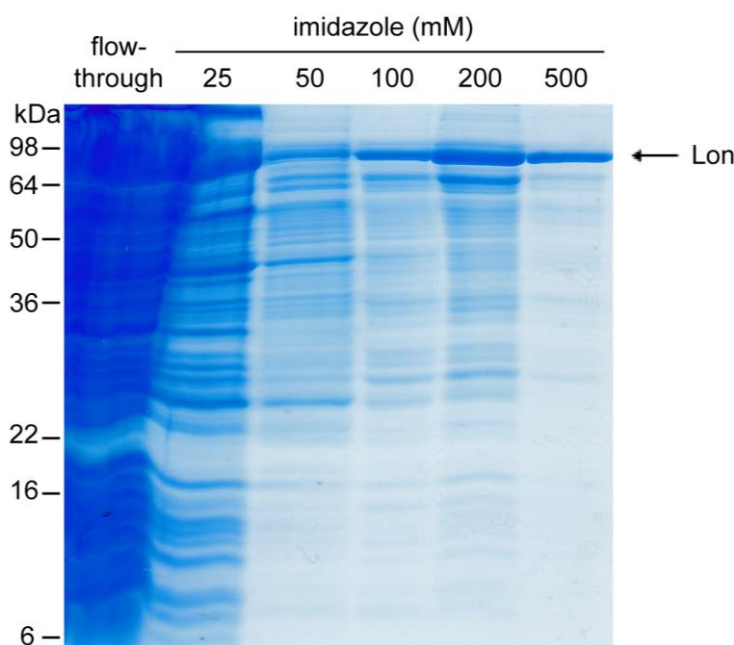


Figure 14 Purification of *E. coli* Lon via the His₆-tag using Ni-NTA beads. Beads were washed with increasing imidazole concentrations (25 – 100 mM). The proteins were eluted with 200 and 500 mM imidazole.

3.3.4 Activity Assay of the *E. coli* Lon Protease

The activity of the expressed and purified Lon was determined by β -casein digestion. Four different reactions were prepared for the pure 500 mM elution fraction and samples were taken after 1 h, 2 h and o/n (**Figure 15**). The first reaction consisted only of β -casein and served as negative control. Lon and β -casein were contained in the second reaction and the third reaction additionally included ATP as cofactor. The fourth reaction was a negative control where Lon was preincubated with the serine protease inhibitor PMSF to block the active site and thus inhibit the digestion of β -casein. The gel showed only a slight digestion after 1 h in the second and third reactions. After 2 h, more digestion was clearly observed in the sample containing ATP. Almost complete digestion of β -casein was seen after overnight regardless of the presence of ATP. Moreover, PMSF was not successful in inhibiting Lon as could be seen in the o/n sample being mostly digested as well. This is not surprising since it is reported that PMSF inhibits Lon only at relatively high concentrations and after prolonged exposures, leaving around 50% activity at 5 mM concentration.²⁴

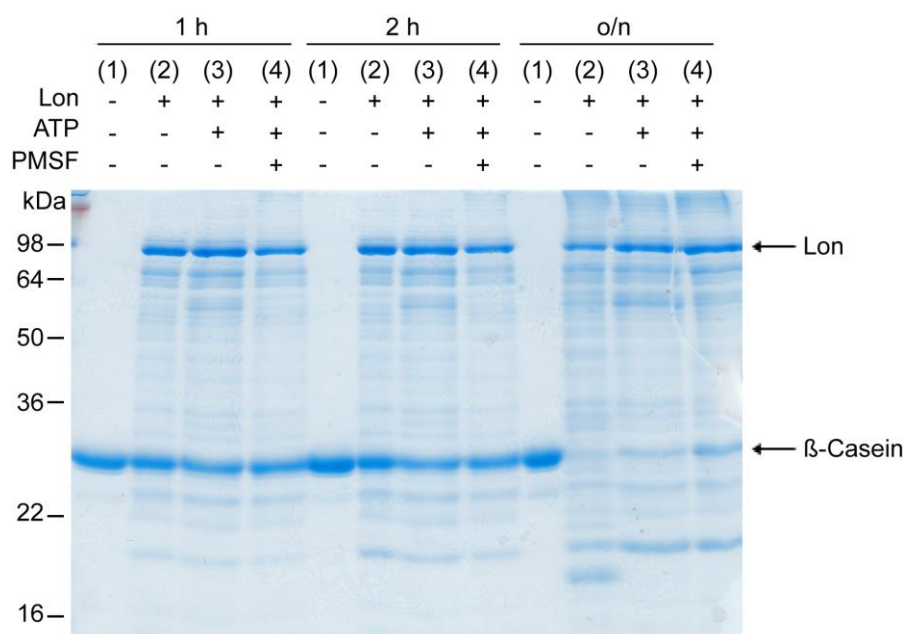


Figure 15 Lon activity assay. Time course of β -casein digestion in four different reactions: 1) Only casein 2) Casein and Lon without the cofactor ATP 3) Casein, Lon and ATP 4) Casein, Lon and ATP including preinhibition with PMSF

3.3.5 Assay development

The FRET assay was developed as a 96-well plate reader assay to measure the enzymatic activity of the *E. coli* Lon protease. The FRET peptide **27** was used as a substrate for Lon. When this peptide is intact it emits faintly at 520 nm upon excitation at 485 nm. After cleavage of the peptide, the FITC fluorophore on the C-terminal end is not quenched anymore and there is a significant increase in fluorescence intensity (**Figure 16**). This increase over time can then be used as a direct measure of the enzymatic activity.

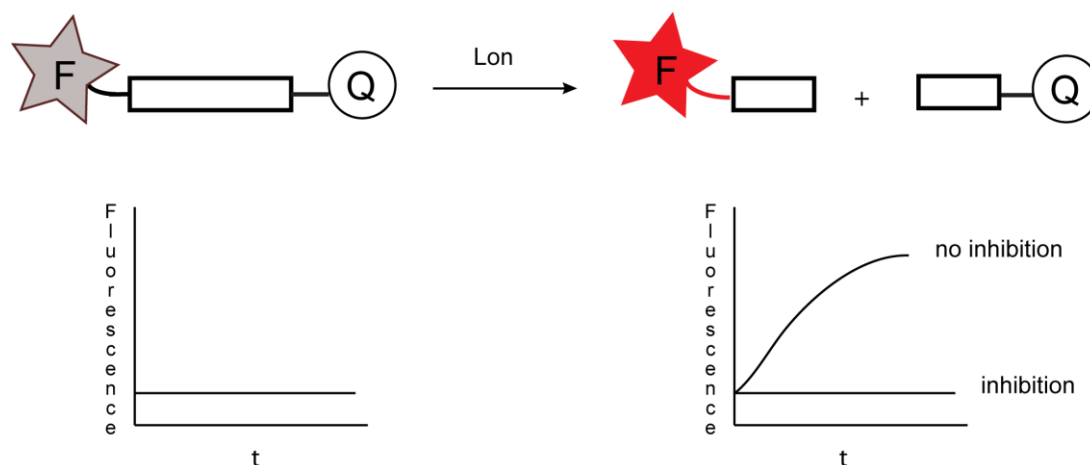


Figure 16 FRET assay for the inhibitor screening of *E. coli* Lon. The peptide in the quenched state emits only faintly. Lon is pretreated with a library compound and added to this peptide. When Lon is not inhibited a significant increase in fluorescence is observed.

A small molecule library (**Table 3**), consisting of isocoumarins, phosphonates, sulfonyl fluorides, chloromethyl ketones, phosphoramidates, beta-lactones, beta-lactams, boronates and thiiranes was screened for inhibition of Lon. After preincubating the Lon either with DMSO or with a library compound for 30 min, the FRET peptide was added and the fluorescence intensity of all reactions was measured simultaneously in a photometer. The slope of the linear part of the fluorescence signal curve was used as a measure of enzymatic activity. 100% was

defined with the slope of the DMSO control, whereas 0% was that of Lon-free negative control. The slopes of all other samples were normalized according to these two values. The known inhibitor of Lon, PMSF, was included in the measurements in order to compare the potency of potential inhibitors. The results were then displayed as a bar graph (**Figure 17**).

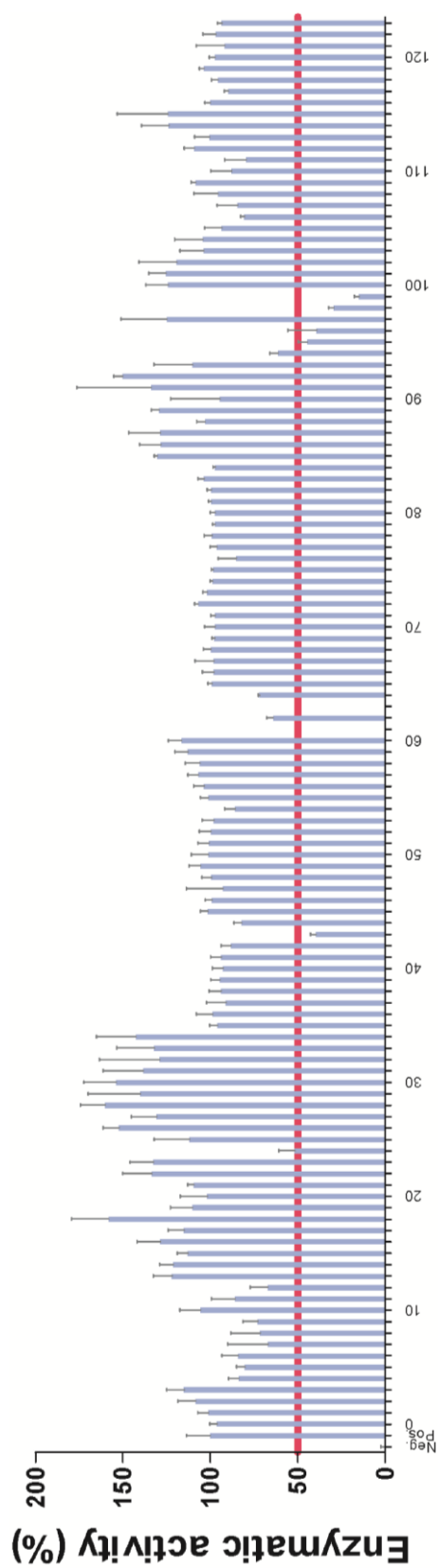


Figure 17 Inhibitor screening of *E. coli* Lon. Neg.: Negative control without Lon; Pos.: Positive control without inhibitor; 0: PMSF; 1-123: Library compounds. Lon was preincubated with a library compound (100 μ M) for 30 min, the FRET peptide was added and the fluorescence intensity was measured in a photometer (Excitation: 485 nm, Emission: 520 nm). The slope of the linear part of the fluorescence signal curve was used as a measure of enzymatic activity. 100% was defined with the slope of the DMSO control, whereas 0% was that of Lon-free negative control. The slopes of all other samples were normalized according to these two values.

3.3.6 Hit characterization

Seven (**43**, **61**, **63**, **95**, **96**, **98**, **99**) of the 123 compounds showed an inhibitory effect towards Lon leaving the enzyme with lower than 50% activity. These hit compounds were taken for further evaluation to discover their potencies, binding modes and potential use as ABPs. Compound **24**, namely TPCK that left Lon with 51% enzymatic activity was not included as it is already a reported inhibitor of Lon.¹⁰¹

The first confirmation was done by a gel-based assay to test the potential inhibitors in their ability to inhibit Lon from digesting β -casein. Lon was pretreated either with DMSO or a hit compound for 30 min and allowed to digest casein overnight. The sample without Lon served as a negative control while the DMSO pretreated sample served as the positive. Samples were then analyzed by SDS-PAGE and stained with Coomassie (**Figure 18**). The inhibitory effect of compound **43** could not be confirmed with this assay. Thus, it was considered to be a false positive. The complete inhibition of enzymatic activity by compounds **61** and **63** observed with the FRET assay was confirmed by the inhibition of casein digestion as well. Of compounds **95** and **96**, only **95** was tested in this assay. Compounds **95**, as well as **98** and **99** showed a moderate inhibition.

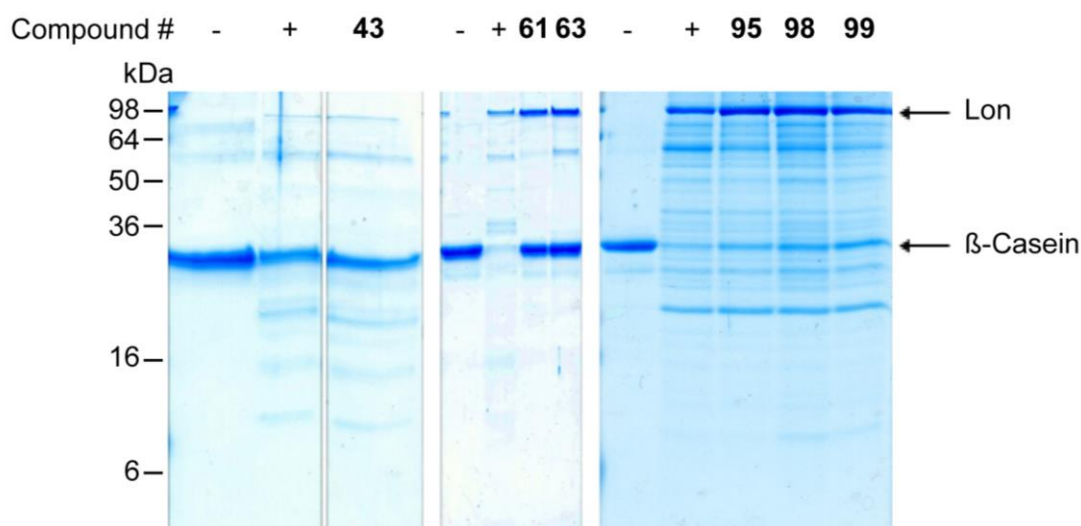


Figure 18 Inhibition of β -casein digestion by *E. coli* Lon with potential inhibitors discovered by the FRET assay. -: Negative control without Lon; +: Positive control without inhibitor.

In order to determine whether the new potential inhibitors **95**, **96**, **98** and **99** bind irreversibly, we preincubated Lon with the compounds, performed a gel filtration to remove noncovalently bound molecules. The flow-through was then used in the FRET assay. The results identified the peptidyl phosphonates as false positives since they did not show any inhibitory effect after the removal of unbound molecules. The thiiranes, on the other hand, was confirmed as irreversible inhibitors (**Figure 19**).

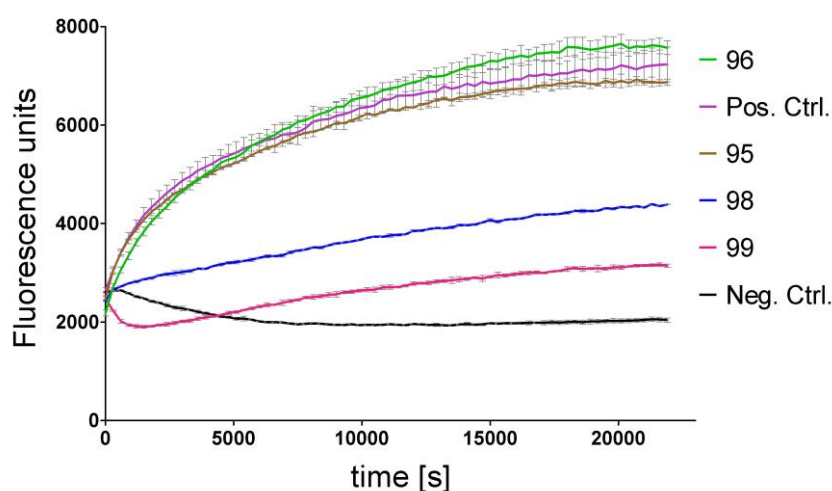


Figure 19 Reversibility check of the hit compounds **95**, **96**, **98** and **99**. Lon was pretreated with the compounds, followed by gel filtration and subsequent analysis with the FRET assay. Pos. Ctrl.: Positive control with *E. coli* Lon. Neg. Ctrl.: Negative control without Lon.

Out of the seven compounds identified by the FRET assay, the boronates **61** and **63** were confirmed by the gel-based digestion assay. The thiiranes **98** and **99** were confirmed after the reversibility check. These four compounds make up the final hits of the screening (**Figure 20**).

Boronic acids are known serine protease inhibitors.¹⁰² The empty *p*-orbital of boron is available to accept the oxygen lone pair of the active site serine residue. According to the crystal structure of subtilisin, the tetrahedral geometry of boronic acids makes for good transition state analogs.¹⁰³ The boronates **61** and **63** have been described as potent new proteasome inhibitors, obtained by mixing of structural elements of known proteasome inhibitors.¹⁰⁴ In 2006 the boronic acid MG262 was

reported as a reversible inhibitor of *S. Typhimurium* Lon protease with an IC_{50} of 122 nM.²⁵ Even though it is one of the best inhibitors of Lon to date, it has approximately 2000-fold higher potency against the proteasome.¹⁰⁵

Thiiranes have diverse activities as antitumor drugs to immunosuppressants, respiratory stimulants, and antibacterial, blood pressure increasing as well as hypoglycemic agents.¹⁰⁶ Recently they were reported to label essential enzymes in *S. aureus* and *L. monocytogenes* and to have an antibiotic effect in these clinically relevant pathogens.¹⁰⁷

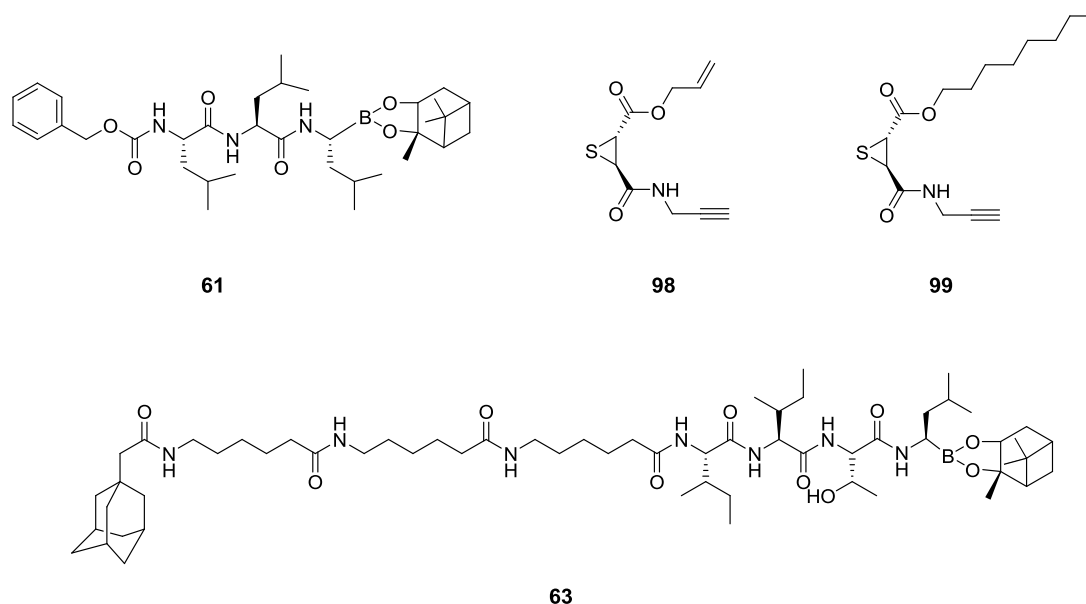


Figure 20 Inhibitors of *E. coli* Lon identified with the FRET assay library screening. Compounds **61** and **63** are boronates, whereas **98** and **99** are thiiranes.

To compare the potencies of the two types of inhibitors we have identified, we tested them at different concentrations with the FRET assay. The compounds in the inhibitor screening were used at 100 μ M concentrations. The boronates were titrated down to concentrations from 20 μ M to 20 nM since they completely inhibited the Lon at 100 μ M. The thiiranes, on the other hand, were titrated both up and down from 500 μ M to 20 μ M. Boronates **61** and **63** completely inhibited Lon with as little as 2 and 20 μ M, respectively. At 0.2 μ M Lon was still inhibited by 72% with **61**.

Thiiranes **98** and **99** at 100 μM almost completely inhibited Lon with a remaining enzymatic activity of 5 and 11%, respectively (**Figure 21**).

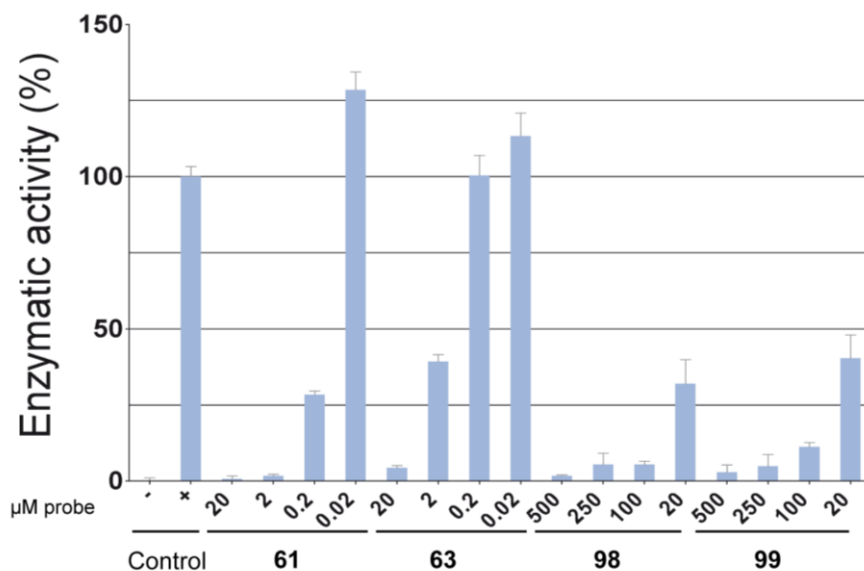


Figure 21 Titration of the boronates **61** and **63** and the thiiranes **98** and **99** in inhibiting *E. coli* Lon. -: Negative control without Lon; +: Positive control without inhibitor. Lon was preincubated with the compounds for 30 min, the FRET peptide was added and the fluorescence intensity was measured in a photometer (Excitation: 485 nm, Emission: 520 nm). The slope of the linear part of the fluorescence signal curve was used as a measure of enzymatic activity. 100% was defined with the slope of the DMSO control, whereas 0% was that of Lon-free negative control. The slopes of all other samples were normalized according to these two values.

Encouraged by the irreversible binding of the thiiranes we set out to make use of their alkyne groups and test their applicability as ABPs. To discover the binding mode of the inhibitors we introduced several pretreatments as controls, then labeled the enzyme with the potential ABPs and clicked a TAMRA fluorophore on the probe to enable visualization with a fluorescent scanner. The first control was treatment with the general serine protease inhibitor to preblock the active site of Lon. This was tested both with and without ATP as it was done for the DMSO control. Second control was preheating of the enzyme for 25 min at 72 °C to see if the native folded

structure is required for binding. Last control was pretreatment with iodoacetamide (IAM) to block the free cysteine residues.

The following conclusions could be drawn from this experiment (**Figure 22**): The positive control with DMSO showed that *E. coli* Lon could be labeled with both probes regardless of the presence of ATP. Labeling with **98** was weaker with ATP. This was assumed to be due to a loss of enzyme, probe or click reagents during sample preparation. Furthermore, PMSF could not inhibit labeling with thiiranes when ATP was present. The reason for labeling despite PMSF could be the binding of the probes to other residues than the active site serine, which are likely to be cysteine residues as it was mentioned that all modifications took place at a cysteine residue when living *S. aureus* cells were labeled with the thiiranes.¹⁰⁷ However, preblocking of the free cysteine residues with IAM could also not inhibit labeling. Heat denaturation prior to labeling showed that the native folded structure was required for the interaction of compound **98**, but not **99**.

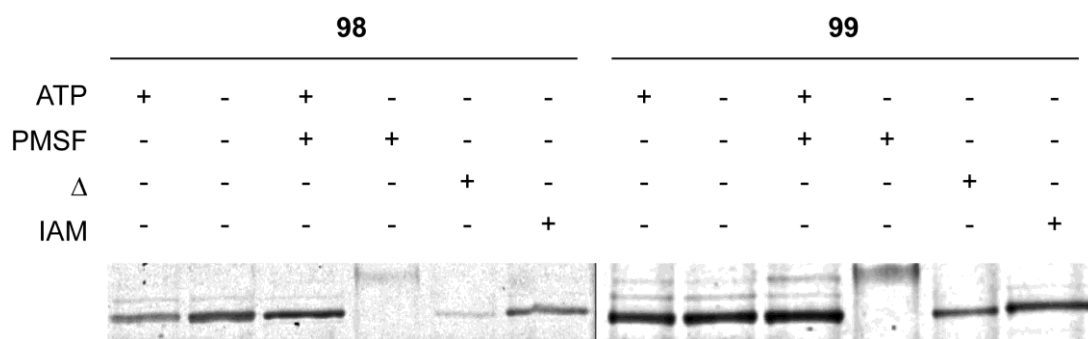


Figure 22 Labeling of *E. coli* Lon with thiiranes. PMSF: Phenylmethanesulfonyl fluoride (5 mM) to preblock of the active site, Δ: heat denaturation prior to labeling, IAM: Iodoacetamide (100 mM) pretreatment to block the free cysteine residues. Probe concentration: 20 μM.

In order to elucidate which residue or residues of Lon the thiiranes bind to we mutated the active site serine Ser679, and the three cysteines in the catalytic domain, namely Cys617, Cys685 and Cys691 to alanines. The mutants' enzymatic activities were then tested with the FRET assay (**Figure 23**). As expected out of the four

mutants only the active site mutant S679A did not show any activity. C617A appeared less active in comparison to the wild type and the two other cysteine mutants.

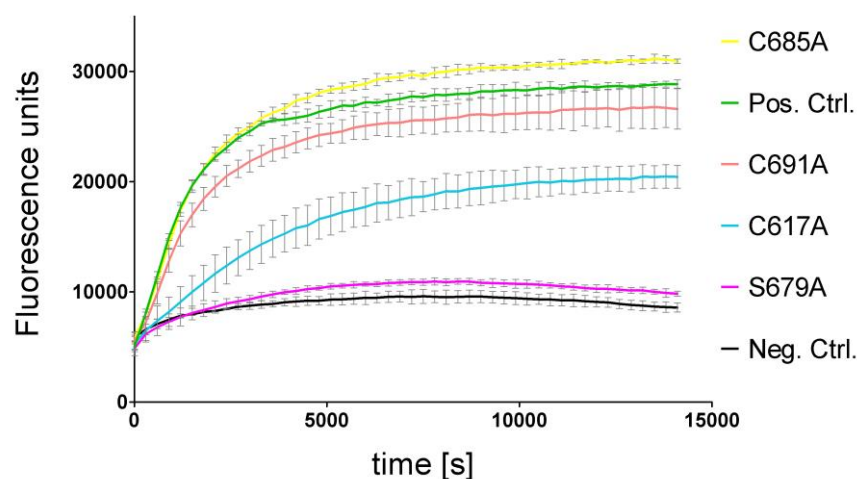


Figure 23 Activity analysis of the Lon mutants with the FRET assay. Neg. Ctrl.: Negative control without *E. coli* Lon. Pos. Ctrl.: Positive control with wild type Lon).

We next labeled the mutants as well as the wild type *E. coli* Lon with **98**. All the samples including the preinhibited wild type enzyme were labeled with similar intensities (**Figure 24**). In contrast with the previous labeling, the active site of the wild type enzyme was preblocked with **61**, which was confirmed for complete inactivation. However, neither preinhibition nor the inactive S679A mutant showed decreased labeling. Only C617A displayed weaker band intensity. These led to the conclusion that the binding of the probes do not occur at the active site serine residue, but probably at the cysteine residues C617A since it is close to the active site and maybe at C685A as well.

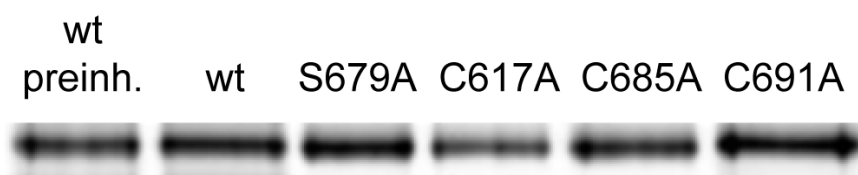


Figure 24 Labeling of *E. coli* Lon wild type and mutants with **98** (20 μ M). wt: *E. coli* Lon wild type. wt preinh.: Lon preinhibited with **61** (1 μ M).

Mass spectrometry analyses to identify the binding site of the probe were unsuccessful. In case of ESI-MS measurements, the intact protein was probably too large to fly and give good signals. When a tryptic digest was performed, even though the sequence coverage was not too low (35%, data not shown), the active site peptide was not covered. The use of a Matrix-assisted laser desorption/ionization (MALDI) MS gave a similar result for a tryptic digest (69% peptide coverage, data not shown) without coverage of the active site peptide. Better signals were obtained with the MALDI-MS measurements of the intact protein as it was possible to detect the single, double and triple charged ions. Unfortunately, the resolution of the peaks was too low to see a mass shift of 200-300 Daltons upon the binding of the probe to the enzyme. We then tried to increase the mass difference by coupling a larger group on the alkyne group of the probe via click chemistry. However, no signal was observed probably due to loss of the protein during the removal of the excess click reagents.

At this point, the binding site of the thiiranes on the *E. coli* Lon protease as well as their specificity remains to be elucidated.

4 Conclusions and Outlook

“If we really want science to advance, people should have chips implanted in their skulls that explode when they say something stupid.” Sheldon Cooper

The major goal of this thesis was to develop ABPs for serine proteases. This was tackled in three different projects: 1) rapid synthesis of DPP ABPs and showing the ability to modulate their selectivity via the recognition elements in the peptide chain, 2) synthesis of qABPs to overcome the drawbacks of fluorescent tags for real-time imaging applications and 3) inhibitor screening for an unconventional serine protease and evaluation of the hit compounds for potential use as ABPs.

4.1 On-resin strategies for synthesis of diphenyl phosphonate ABPs

Depending on the application, ABPs with low or high selectivity are desired. Quantification techniques like ICAT, iTRAQ, SILAC and ABPP-MudPIT as well the inhibitor screening method Fluopol-ABPP require the use of nonselective probes (p. 18). For the monitoring of specific protease activities without the need for separation methods, highly selective probes are in demand.

While considerable progress has been made in the applications of ABPs, the limiting factor remains the development of probes with the desired selectivity. In this sense it is beneficial to avoid the time-consuming solution phase synthesis, and apply SPPS. For cysteine proteases there are several selective and nonselective ABPs that are synthesized via solid phase if not a combination of solid and solution phase chemistries (**Figure 25**). The general cysteine protease ABP DCG-04 is based on the natural product E-64,¹⁰⁸ which is a promiscuous irreversible inhibitor of cysteine protease from Clan CA (papain-like proteases). DCG-04 was synthesized via solid phase chemistry with the epoxide building block made in solution and it labels all four of the main rat liver cathepsins (Z, B, H, C).⁴⁵ *O*-acyl hydroxamates were synthesized via a semisolid phase synthesis. They target papain family cysteine proteases and selectively label falcipain 1.¹⁰⁹ Selective vinyl sulfone ABPs targeting cathepsin C were synthesized via SPPS.^{46b} The double-headed epoxysuccinyl probe based on DCG-04 was also synthesized via SPPS and it selectively labels cathepsin B.^{46a} Caspases are selectively labeled by AOMK probes, which were synthesized on solid support.⁴⁸

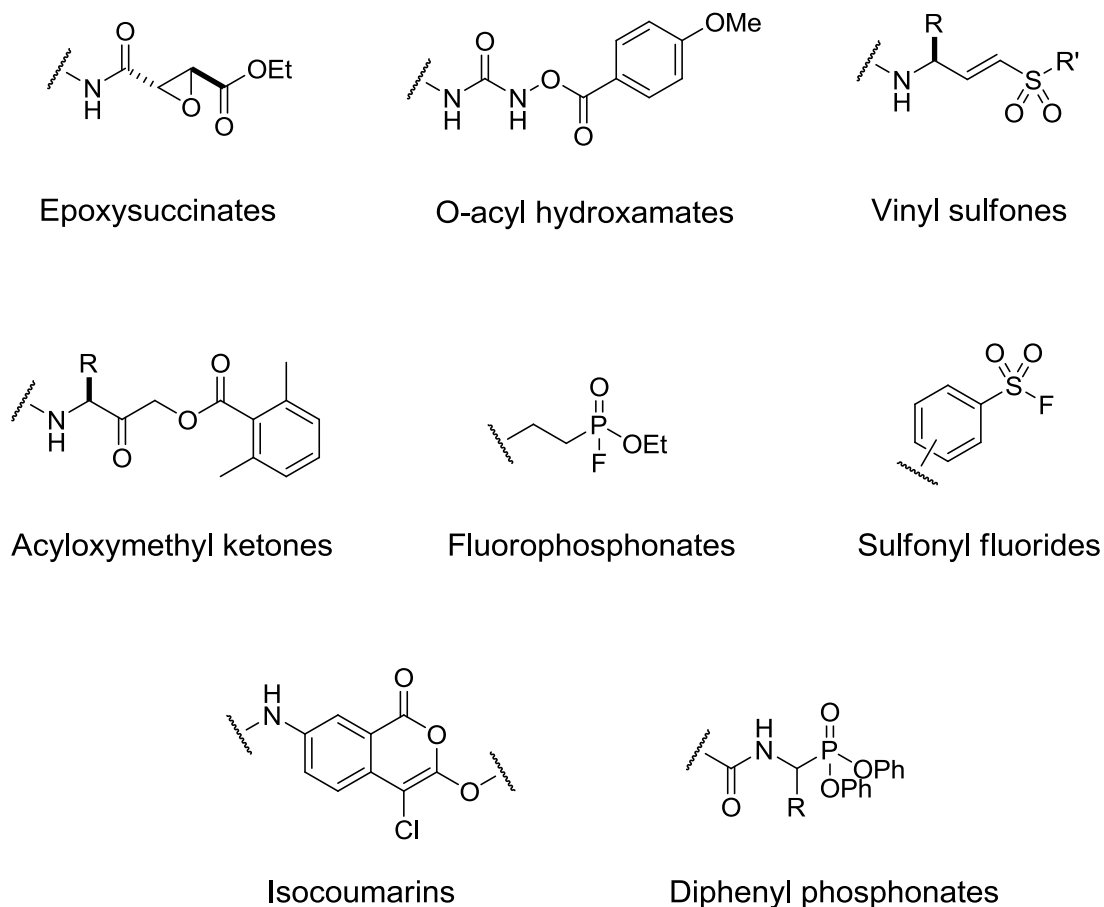


Figure 25 Protease reactive warheads mentioned above. Epoxysuccinates, O-acyl hydroxamates, vinyl sulfones and acyloxymethyl ketones target cysteine proteases. Fluorophosphonates, sulfonyl fluorides, isocoumarins and diphenyl phosphonates target serine proteases.

Also for serine proteases both general and selective ABPs exist (**Figure 25**). The nonselective fluorophosphonate probes targeting serine hydrolases are among the first ABPs reported.⁴⁹ Another broad spectrum probe is the recently described sulfonyl fluoride ABP based on the known irreversible serine protease inhibitor AEBSF.⁵⁰ Peptidic diphenyl phosphonates are more selective and they have been designed to monitor specific serine proteases such as dipeptidyl peptidase IV^{52a} and trypsin-like serine proteases.¹¹⁰ Another class of selective ABPs are isocoumarins.^{51a} However, all these probes have been made by time-consuming solution phase chemistries. Even though peptide aldehyde probes could be synthesized via the more

rapid solid phase synthesis, they target a variety of proteolytic enzymes simultaneously.¹¹¹ There have also been attempts to incorporate SPPS into the construction of peptidic diphenyl phosphonates. The tripeptidyl DPP targeting uPA includes a synthesis of a dipeptide on a resin.¹¹² Synthesis of the selective granzyme A and B diphenyl phosphonate probes was achieved via SPPS synthesis of the peptidic portion, and solution phase synthesis of the phosphonate head and their coupling together again in solution.^{52b}

Diphenyl esters of α -aminophosphonates are phosphonic analogues of naturally occurring amino acids. They selectively, covalently and irreversibly bind to the active site serine residue of serine proteases. These features qualify them as attractive warheads for ABPs. The selectivity of DPPs can be modulated via the adjustment of the group at the P1 position and the non-primed site residues. While synthetic strategies to generate DPPs in solution have been reported, an easy and rapid way to synthesize DPP ABPs remains a challenge.

We chose DPP as the reactive warhead and incorporated a peptide chain to accommodate recognition elements for increased selectivity. The rapid synthesis of the peptide moiety was achieved by SPPS, while the building blocks that carry the P1 recognition element and the warhead were prepared by solution phase synthesis. On-resin click reaction was then employed to attach the P1 building blocks to the peptides. Using this approach we synthesized eight different DPP ABPs, and labeled serine proteases of different specificities. The probes display activity-dependent labeling of proteases in purified forms as well as within complex proteomes. We demonstrated that it is possible to tune the activity and selectivity of the DPP ABPs by varying the extended recognition elements. Molecular modeling suggests that the probes interact with the non-primed sites, which explains their higher potency and capacity to influence the selectivity towards the protease targets. We envision that this strategy will allow for future probe optimization when selective serine protease ABPs are required.

Since our probes carry an alkyne handle we are flexible in the choice of a detection tag. The DPP ABPs synthesized here could further be equipped with a biotin tag to enable enrichment and purification for target identification by MS analysis. Further

improvement in the development of peptidyl phosphonate ABPs should include their complete synthesis via solid phase chemistry to allow for very rapid and easy synthesis. The difficulty, however, lies in the lability of the phosphonate warhead under basic conditions used for the removal of Fmoc protection in standard SPPS. Therefore this reactive group either needs optimized SPPS chemistry or – as described here – needs to be incorporated in the last synthetic step. A very recent addition to such strategies has been reported by Sienczyk where peptide amides were synthesized on solid support, followed by a single step solution phase formation of phosphonates via a modified Oleksyszyn procedure.¹¹³ Furthermore, even though we clearly can steer the probes towards our desired target protease via the P1-P4 residues, incorporation of the nonprimed site recognition elements as well as unnatural amino acids could provide truly selective probes. This could be done by changing the reactive group to include one leaving group and one functionalized alkoxy group, which adds extra recognition (see also 4.2) or by utilizing a phosphinate group. Phosphinate analogues have been proven to be superior to its diphenylphosphonate counterpart in inactivating its target protease.⁸⁷ The difficulty of the latter strategy is that an efficient way to introduce a leaving group to the phosphinate structure has yet to be developed.

4.2 Quenched phosphonate ABPs for imaging protease activity

To gain functional understanding of proteases it is not only required to determine which proteases are active in a certain sample, but also where these proteases are located within a cell or tissue. The major drawback of fluorescent probes in imaging applications is high back ground due to the intrinsic fluorescence in unbound state when free in solution. In a study by Craik lab in 2011 cell surface proteases have been labeled by a phosphonate ABP.¹¹⁴ The probe carries a biotin tag, which was visualized with a streptavidin-conjugated dye after it has reacted with its target. Live cells from two different epithelial cancer cell lines were treated with the ABP and analyzed by fluorescence microscopy and flow cytometry. Even though not commented on by the authors in the article, high background is seen in microscopy images even after three washing steps after incubation with the probe and the dye.

Especially the quantification of the fluorescence intensity with flow cytometry for one of the cell lines shows a signal intensity that is only slightly over the noise level.

The problem of the intrinsic fluorescence of fluorophore-carrying ABPs was overcome by the design of quenched ABPs that fluoresce only after covalent binding to its target enzyme. In 2005 dynamic imaging of cysteine protease activity with qABPs in live human cells have been reported for the first time.⁹⁵ In a follow-up study when quenched and nonquenched AOMK ABPs were compared in optical imaging of tumors in live mice, despite their efficiency fluorescent probes suffered from high background, requiring extended clearance times.⁴⁰ Quantification of the overall signal-to-background ratios from whole-body images resulted in similar values for both types of ABPs. However, qAPB reached its maximum more rapidly than its nonquenched version while showing virtually no background. To date there are no reports on such “smart” probes for serine proteases.

For the development of qABPs for serine proteases we modified the DPP structure to have only one leaving group. Therefore, diethyl phosphonates with the P1 recognition element were synthesized. One of the ethyl groups was selectively dealkylated and a leaving group was introduced. Subsequently an alkyne handle was attached to enable introduction of a fluorophore via click chemistry and the quencher was coupled to the leaving group, forming the qABP. In this form the probes are “silent”, and become fluorescent only upon covalent modification of the target enzyme. These phosphonate probes represent the first qABPs for serine proteases. Compared to cysteine protease qABPs, the molecules described here are more challenging in their synthesis as the phosphonate warhead is not compatible with standard solid phase synthesis, and therefore needed to be made in solution.

We synthesized two qABPs targeting tryptic enzymes and neutrophil elastase. When labeling purified serine proteases the probes displayed a high quenching efficiency as well as activity-dependent reaction according to the expected substrate specificities. Unfortunately our attempts to monitor matriptase-2¹¹⁵ activity in transfected HEK293 cells with our qABPs failed. Most likely because the matriptase is 1) bound to an endogenous inhibitor, 2) not trafficked to the cell surface¹¹⁶ or 3) detaching from the membrane and floating away in the medium. We therefore moved

to a different system of atherosclerosis tissue sections and of neutrophil elastase secreted from primary neutrophils. Imaging experiments with the phosphonate qABPs are currently under way. Furthermore, probes with a higher degree of potency and selectivity may be constructed by incorporation of an extended peptide element between the phosphonate warhead and the alkyne group. This may be achieved by several synthetic strategies: 1) by coupling a diethyl building block to a peptide, 2) by a modified Oleksyszyn reaction with a peptide-amide as described for DPPs. Both these strategies requires that the final diethyl phosphonate peptide can be selectively transformed into a mono-ethyl phosphonate), 3) by on-resin click chemistry, as described in the previous part of this thesis.

Application of quenched probes into imaging comes with advantages, but is not without drawbacks. The major advantage of these molecules is their covalent binding to their target enzyme, which at the same time is the main disadvantage. In case of imaging applications substrate probes fail to report on the localization of active proteases as they diffuse away from the reaction site. The irreversible binding of ABPs circumvents this problem and allows direct analysis of the probe-enzyme complex. However, this binding also inactivates the enzyme. Each ABP molecule binds to a single protease molecule, making signal amplification through multiple processing events impossible. As discussed in a comparative study,³⁹ other features of ABPs still make them preferable for imaging applications. These features include the small size of ABPs enabling rapid uptake and clearance of these molecules, and the ability to design highly selective probes via the warhead and extended recognition elements.

An alternative probe design for real-time imaging of proteases has recently been reported by Schultz lab.¹¹⁷ The probe structure was based on a FRET peptide substrate, which was lipidated to allow for local activity information of the membrane-bound neutrophil elastase. The lipid anchors solve the problem of diffusion that is faced with substrate probes while the FRET pair eliminates the background. To prevent unspecific cleavage of the substrate by proteases other than the target enzyme P4-P4' peptide recognition sequence was incorporated. This design also overcomes the enzyme inactivation that occurs via irreversible binding of ABPs to their targets. This approach might be promising for future applications

especially when considering the high concentrations of endogenous protease inhibitors.

4.3 FRET-based assay for inhibitor screening of Lon protease

The ATP-dependent serine protease Lon is essential for cellular homeostasis. It mediates protein quality control by degrading abnormal and damaged proteins, as well as short-lived regulatory proteins. In addition to the proteolytic function, Lon also has a chaperone-like function and promotes the assembly of protein complexes. However, the mechanism by which the ATP-dependent Lon protease functions is yet not well understood. Its involvement in bacterial pathogenicity has led to the emergence of Lon as a therapeutic target as well.

In order to improve our understanding of the mechanisms of Lon's functions, it is crucial to possess the right chemical tools. Inhibitors as well as ABPs are important chemical tools to assess more information. The main challenge in Lon research is the lack of specific inhibitors. However, some proteasome inhibitors (**Figure 26**) such as the peptide aldehyde MG132 have been shown to diffuse into the mitochondria and inhibit the degradation of steroidogenic acute regulatory protein (StAR), a physiological substrate of mammalian Lon.¹¹⁸ This mechanistic similarity of Lon and proteasome was strengthened when the screening of commercially available peptide-based proteasome inhibitors led to the identification of the peptidyl boronate MG262 as a potent inhibitor of *S. typhimurium* Lon protease.²⁵ In this screen a FRET-peptide substrate was employed. This substrate mimic differs from the peptide that was described by Lee *et al.*²⁷ by one amino acid. Still, both the peptide aldehyde and the boronate are about 2000-fold more potent against the 20S proteasome. In a search for nonpeptidic inhibitors, a FITC-casein assay yielded in the discovery of coumarinic derivatives as inhibitors of the human Lon protease but not the yeast 20S proteasome.²⁶ The FRET-peptide substrate, FRETN 89-98 by Lee, was derived from the λ N protein. It contains the residues 89-98 of the λ N protein with a fluorophore and quencher pair. The sequence of this peptide is as follows: YRGITCSRQ – the cleavage site being between C and S. After the discovery of boronates as Lon

inhibitors DBN93 was designed from a product of FRETN 89-98 peptide hydrolysis by Lon (YRGIT-Abu) with a boronic acid moiety at the carboxy terminus.²⁸ DBN93 inhibits the Lon substrate StAR in isolated mitochondria. It does not inhibit human ClpXP.

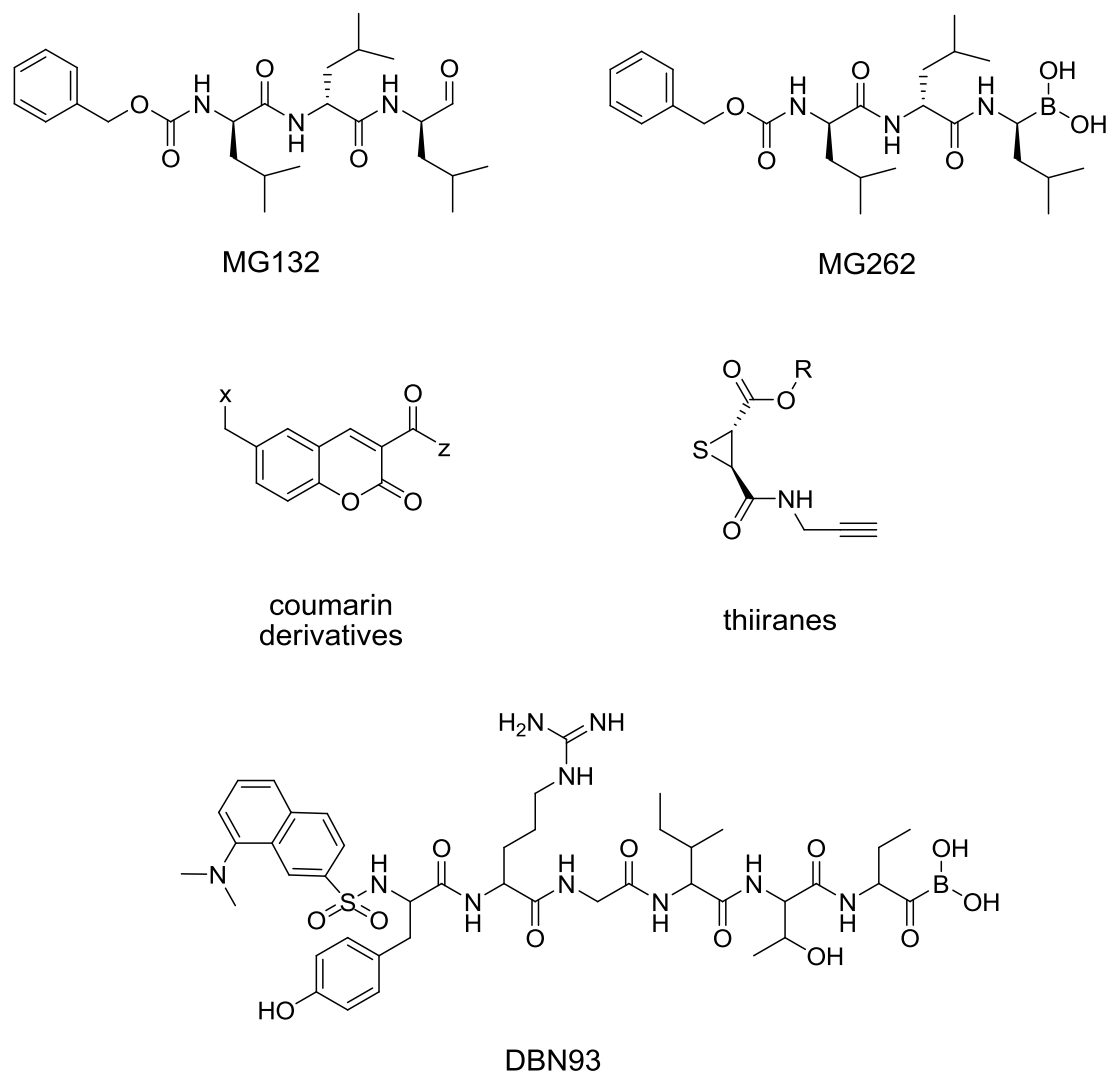


Figure 26 Structures of known Lon protease inhibitors and the newly identified thiiranes.

We aimed to enrich the chemical toolbox for the *E. coli* Lon protease with specific inhibitors and study their potential for use as ABPs. Therefore, we established an

assay to screen a focused library of small molecules for inhibitors of the *E. coli* Lon protease. For this purpose, we used the FRETN 89-98 with a different fluorophore and quencher pair than the reported one. We observed the increase in fluorescence intensity generated from the cleavage of this substrate by Lon and used this as a direct measure of enzymatic activity, thus evaluating the inhibitory effects of each library compound.

After further evaluation of the hit structures we identified four compounds as final hits of the screen. Two of these compounds are thiiranes and represent a new class of irreversible inhibitors of the Lon protease (**Figure 26**). To our surprise, our attempt to use thiiranes as ABPs in labeling experiments led to the discovery that the binding does not take place at the active site serine residue of the enzyme but at the cysteine residues. Unfortunately, mutations of the three cysteines in the catalytic domain did not provide conclusive information about at which specific cysteine residue the binding occurs.

Further research will include the investigation of binding site and mechanism of the thiiranes to the *E. coli* Lon protease. We anticipate that double and triple cysteine mutants as well as MS measurements with these mutants might provide the necessary information. Moreover, the selectivity of thiiranes will also be tested. The potency of these compounds against other ATP-dependent proteases, especially the proteasome, will also be subject to further research. We foresee that this new structure will contribute to the design of more potent and selective inhibitors of Lon to implement a better understanding of its mechanism.

5 Experimental

Organic chemistry

General

All starting materials were obtained from Sigma-Aldrich and used without further purification. Thin layer chromatography (TLC) was performed on ALUGRAM sil G/UV254 TLC plates (Carl Roth). Solvents used for SPPS and purification via column chromatography were purchased from Applichem. Compounds were separated over silica gel with a grain distribution of 0.04-0.063 mm and a pore size of 60 Å (Carl Roth). Creosalus was the supplier for Fmoc-protected L-amino acids, Rink resin and coupling reagents for SPPS. LC-MS spectra were recorded by an Agilent 1100 Series LC system coupled to an Agilent 6210 ESI TOF mass spectrometer, with elution by solvents A (5% ACN/H₂O + 0.1% FA) and B (95% ACN/H₂O + 0.1% FA). A Zorbax SB C18 5 µm (0.5 x 150 mm) column was used to separate samples at r.t. with a flow rate of 20 µl/min and with a gradient of 2.57% ACN/min starting from A for 35 min. HPLC purifications were carried out on Waters Xbridge C18, 5 µm (4.6 x 150 mm) and a Waters Xbridge BEH130 Prep C18 5 µm (19 x 150 mm) columns. ¹H and ¹³C NMR spectra were measured on a Bruker 400MHz DRX (400; 100 MHz). Chemical shifts (δ) are given in parts per million (ppm) relative to tetramethylsilane as an internal standard.

TLC stains

Name	Composition	Application
Cerium ammonium molybdate - CAM	1 g Ce(SO ₄) ₂	universal
	5 g (NH ₄) ₆ Mo ₇ O ₂₄ ·4H ₂ O	
	90 mL H ₂ O	
	10 mL H ₂ SO ₄	
Ninhydrin	1,5 g ninhydrin	amines
	100 mL n-BtOH	
	3 mL AcOH	

Potassium permanganate (KMnO ₄)	1.5 g KMnO ₄ 10 g K ₂ CO ₃ 1.25 mL 10% NaOH 200 mL H ₂ O	olefins, oxidizable groups
2,4-Dinitrophenyl-hydrazine	12 g 2,4-DNPH 60 mL H ₂ SO ₄ conc. 80 mL H ₂ O 200 mL EtOH	aldehydes/ ketones

Cbz deprotection

Cbz protected compound was treated with 33% HBr/AcOH solution until all the starting material was consumed as followed by TLC with ninhydrin stain. The solvent was removed and the oily residue was dissolved in a minimal amount of MeOH; excess diethyl ether was added and o/n storage at -20 °C led to crystallization. The crystals were filtered, washed with cold Et₂O and dried. The purity of the compounds was sufficient for further reactions.

General SPPS procedures

Kaiser test solutions

Solution	Composition
A	2% KCN (0.01 M in H ₂ O) / Pyridine (v/v)
B	5% Ninhydrin/Ethanol (w/v)
C	4:1 Phenol/Ethanol (w/v)

Amino acid coupling and Fmoc deprotection

Fmoc groups were deprotected by 20% piperidine/DMF (v/v) for 20 min. For amino acid couplings Fmoc-aa-OH (3 eq., 0.25 M in DMF), DIC (3 eq.) and HOBt (3 eq.) were added to the resin and shaken at room temperature for 1-3 h. Completion of the reactions was checked by Kaiser test.

Biochemistry

General procedure for labeling of purified enzymes

Each enzyme was treated for 30 min at rt with either a suitable inhibitor (**Table 1**) or DMSO. Pretreatment was followed by labeling with ABPs for 30 min at rt. In case of alkynylated probes, TAMRA azide (25 μ M) was subsequently clicked onto the ABPs in presence of CuSO₄ (1 mM), TBTA (50 μ M) and sodium ascorbate (0.5 mM) for 30 min at rt in the dark. All reactions were stopped with 4x sample buffer. The samples were boiled at 95 °C for 3 min. Protein samples were resolved on a 12% acrylamide SDS gel and gels were visualized by a Typhoon Trio+ scanner (GE Healthcare, Glattbrugg, Switzerland).

Table 1 Active-site directed inhibitors for listed serine proteases and corresponding concentrations.

Enzyme	Inhibitor	Concentration
Chymotrypsin	DAP22c	0.1 mM
Cathepsin G	PMSF	1 mM
<i>E. coli</i> Lon	PMSF	5 mM
Trypsin	TLCK	1 mM
Urokinase-type plasminogen activator	DFP	1 mM
Neutrophil elastase	DFP	1 mM

Preparation of competent *E. coli* cells

For the preparation of electrocompetent *E. coli* cells a volume of 400 mL of LB medium was inoculated with a fresh overnight culture. If necessary an adequate volume of the corresponding antibiotic was added. The cells were grown in a shaker at 37 °C and 300 rpm to an OD₆₀₀ of 0.6. The cells were then chilled on ice for at least 15 min. For all following steps it was crucial, that the cells were always cooled down to 4 °C. The cells were transferred to an ice cold centrifuge bottle and spun down at 4000 g for 15 min at 4 °C. Afterwards the supernatant was discarded and the cells were resuspended in 100 mL of ice cold 10% (w/v) glycerol. The resuspended cells were centrifuged at 4000 g for 10 min at 4°C. The supernatant was discarded again and the cells were resuspended in 50 mL of ice cold 10% glycerol. The centrifugation step was repeated as described above and the supernatant was discarded. The cells were resuspended in 20 mL of ice cold 10% glycerol and they were spun down as described. Once again the supernatant was discarded and the *E. coli* cells were resuspended in a final volume of 3-5 mL of ice cold 10% glycerol. From the final volume 100 µL aliquots were prepared and immediately frozen in liquid nitrogen. The cells were stored at -80 °C.

Buffers and solutions

Name	Compostion
PBS pH 7.4	137 mM NaCl
	2.7 mM KCl
	10 mM Na ₂ HPO ₄
	1.8 mM of KH ₂ PO ₄
PBST pH 7.4	PBS
	0.1% Tween (v/v)
HEPES pH 7.4	50 mM HEPES
	100 mM NaCl

SDS-PAGE sample buffer (4x)	500 mM Tris-HCl, pH 6.8 12% SDS (w/v) 20% 2-Mercaptoethanol 40% Glycerol (v/v) 0.04% Bromophenol blue (w/v)
SDS-PAGE running buffer (5x)	0.62 M Tris-HCl, pH 8.3 4.8 M Glycine 0.5% SDS
SDS-PAGE running buffer (3x wide gels)	20 mM Tris-HCl, pH 8.3 192 mM Glycine 0.1% SDS (w/v)
Separating gel buffer	1.5 M Tris-HCl, pH 8.8
Stacking gel buffer	0.5 M Tris-HCl, pH 6.8 2% (w/v) Bromophenol Blue

5.1 On-resin strategies for synthesis of diphenyl phosphonate ABPs

5.1.1 Synthesis

5.1.1.1 General methods for the synthesis of propynoylated diphenyl α -aminoalkylphosphonate building blocks

5.1.1.1.1 Birum-Oleksyszyn reaction

Benzyl carbamate (1 eq.) was combined with triphenylphosphite (1 eq.), the corresponding aldehyde (1.5 eq.) and AcOH (0.1-0.2 mL per mmol aldehyde) and heated to 82 °C for 2 h. The reaction was monitored by TLC until benzyl carbamate was consumed. Volatile components were removed and methanol was added to allow crystallization at -20 °C o/n. Crystals were collected by filtration, washed with cold methanol and dried. The resulting solids were sufficiently pure for the following reactions.

Compounds **2b-g** were made according to this general procedure. Compound **2a** was made via a slightly different procedure as described below.

Diphenyl α -N-(benzyloxycarbonyl)amino-methylphosphonate (**2a**)

A mixture of benzyl carbamate (1 eq.), acetic anhydride (1.25 eq.), and paraformaldehyde (1 eq.) in AcOH (100 μ L/mmol) was heated at 65 °C for 3 h. The resulting solution was treated with triphenyl phosphite (1 eq.) and heated at 115 °C for 2 h. The mixture was concentrated under high vacuum, and a small volume of diethyl ether was added to allow crystallization at -20 °C o/n. The precipitate was then collected by filtration. The resulting solid was sufficiently pure for the following

reactions. The title compound was isolated as a white solid in 26% yield. ESI-MS: $[M+H]^+$ m/z 398.1194 (found), 398.1151 (calculated).

Diphenyl α -N-(benzyloxycarbonyl)amino-2-methylpropylphosphonate (**2b**)⁸⁵

The title compound was isolated as white crystals in 52% yield. ESI-MS: $[M+H]^+$ m/z 440.1577 (found), 440.1621 (calculated).

Diphenyl α -N-(benzyloxycarbonyl)amino-3-methylbutylphosphonate (**2c**)⁸⁵

The title compound was isolated as white crystals in 69% yield. ESI-MS: $[M+H]^+$ m/z 454.1737 (found), 454.1777 (calculated).

Diphenyl α -N-(benzyloxycarbonyl)amino-2-phenylethylphosphonate (**2d**)⁸⁵

The title compound was isolated as a white solid in 40% yield. ESI-MS: $[M+H]^+$ m/z 488.1566 (found), 488.1621 (calculated).

Diphenyl α -N-(benzyloxycarbonyl)amino-(4-nitro-phenyl)methanephosphonate (**2e**)⁵⁹

The title compound was isolated as white crystals in 86% yield. ESI-MS: $[M+H]^+$ m/z 519.1321 (found), 519.1315 (calculated).

Diphenyl α -*N*-(benzyloxycarbonyl)amino-(4-amino-phenyl)methanephosphonate (**2f**)⁵⁹

The title compound was isolated as an orange solid in 90% yield. ESI-MS: [M+H]⁺ *m/z* 489.1622 (found), 489.1573 (calculated).

Diphenyl α -*N*-(benzyloxycarbonyl)amino-(4-*N,N*-diBoc-guanidinium-phenyl)methanephosphonate (**2g**)⁵⁹

The title compound was isolated as a white solid in 57% yield. ESI-MS: [M+H]⁺ *m/z* 731.2890 (found), 731.2840 (calculated).

5.1.1.1.2 Transformation of the NO₂ group to a Boc-protected guanidine

AcOH (4 mL/mmol) was added to a mixture of the nitro compound (1 eq.) and Fe powder (9 eq.). The reaction mixture was heated to 70 °C and stirred under N₂ for 2 h. Afterwards, the acid was removed and the crude residue was dissolved in EtOAc. Fe₂O₃ was centrifuged down and the supernatant was concentrated to form the crude product.

The aniline (1 eq.) was mixed with 1,3-bis-(*tert*-butoxycarbonyl)-2-methyl-2-thiopseudourea (1.1 eq.) and mercury(II)chloride (1.2 eq.). Subsequently, DCM and Et₃N (3 eq.) were added resulting in a yellowish suspension, which was stirred *o/n*. DCM was evaporated and the residue was redissolved in EtOAc. The remaining solid was centrifuged down; the supernatant decanted and washed with 1 M KHSO₄, saturated NaHCO₃ solution and brine. The organic phase was dried over MgSO₄ and the solvent was removed. Further purification was carried out via silica column chromatography.

5.1.1.1.3 Coupling of propiolic acid

Propiolic acid (2.6 eq.) was preactivated with DIC (1.3 eq.) in THF (0.3 mL/mmol propiolic acid) for 1 h at 0 °C. The DPP hydrobromide (1 eq.) was dissolved in DMF (0.75 mL/mmol), treated with DIEA (2 eq.) and then added to the preactivated propiolic acid solution and stirred o/n at rt. Base was neutralized with AcOH and the volatile components were removed. The residue was dissolved in EtOAc and washed 2x with 1 M HCl, 2x with H₂O, 2x with saturated NaHCO₃ solution, and brine. The organic phase was dried over MgSO₄ and concentrated at reduced pressure. If necessary, compounds were further purified via silica column chromatography.

Diphenyl α -*N*-(propiolamido)-methylphosphonate (**3a**)

ESI-MS: [M+H]⁺ *m/z* 316.0735 (found), 316.0732 (calculated). ¹H-NMR (400 MHz, CDCl₃): δ = 7.40 – 7.32 (m, 4 H), 7.26 – 7.16 (m, 6 H), 6.66 (s, 1 H), 4.11 (dd, *J* = 12.0 Hz, *J* = 6.0 Hz, 2 H), 2.88 (s, 1 H).

Diphenyl α -*N*-(propiolamido)-2-methylpropylphosphonate (**3b**)

The title compound was isolated as yellowish oil in 45% yield. ESI-MS: [M+H]⁺ *m/z* 358.1237 (found), 358.1202 (calculated). ¹H-NMR (400 MHz, CDCl₃): δ = 7.40 – 7.28 (m, 4 H), 7.26 – 7.09 (m, 6 H), 6.46 (d, *J* = 10.4 Hz, 1 H), 4.83 (ddd, *J* = 19.2 Hz, *J* = 10.4 Hz, *J* = 4.3 Hz, 1 H), 2.90 (s, 1 H), 2.57 – 2.37 (m, 2 H), 1.19 – 1.08 (m, 6 H).

Diphenyl α -*N*-(propiolamido)-3-methylbutylphosphonate (**3c**)

The title compound was isolated as yellowish oil in 29% yield. ESI-MS: $[M+H]^+$ m/z 372.1350 (found), 372.1358 (calculated). $^1\text{H-NMR}$ (400 MHz, CDCl_3): δ = 7.39 – 7.29 (m, 4 H), 7.26 – 7.08 (m, 6 H), 6.64 (d, J = 10.2 Hz, 1 H), 5.06 – 4.87 (m, 1 H), 2.84 (s, 1 H), 1.91 – 1.71 (m, 3 H), 1.06 – 0.90 (m, 6 H).

Diphenyl α -*N*-(propiolamido)-2-phenylethylphosphonate (**3d**)

The title compound was isolated as a white solid in 52% yield. ESI-MS: $[M+H]^+$ m/z 406.1255 (found), 406.1202 (calculated). $^1\text{H-NMR}$ (400 MHz, CDCl_3): δ = 7.49 – 6.94 (m, 15 H), 5.38 – 5.01 (m, 1 H), 3.59 – 3.27 (m, 1 H), 3.15 – 2.97 (m, 1 H), 2.74 (s, 1 H).

Diphenyl α -*N*-(propiolamido)-(4-nitro-phenyl)methanephosphonate (**3e**)

The title compound was isolated as an orange solid in 48% yield. ESI-MS: $[M+H]^+$ m/z 437.10 (found), 437.08 (calculated). $^1\text{H-NMR}$ (400 MHz, CDCl_3): δ = 8.19 (d, J = 8.0 Hz, 2 H), 7.71 (dd, J = 8.0 Hz, J = 2.0 Hz, 2 H), 7.41 – 7.33 (m, 2 H), 7.28 – 7.21 (m, 3 H), 7.20 – 7.12 (m, 3 H), 6.94 – 6.89 (m, 2 H), 6.03 (dd, J = 24.0 Hz, J = 8.0 Hz, 1 H), 2.83 (s, 1 H).

Diphenyl α -*N*-(propiolamido)-(4-amino-phenyl)methanephosphonate (**3f**)

The title compound was isolated in 75% yield. ESI-MS: $[M+H]^+$ m/z 407.13 (found), 407.11 (calculated). $^1\text{H-NMR}$ (400 MHz, DMSO-d_6): δ = 10.14 (d, J = 9.7 Hz, 1 H), 7.41 – 7.30 (m, 6 H), 7.24 – 7.15 (m, 2 H), 7.07 (d, J = 7.5 Hz, 2 H), 6.94 (d, J = 7.5

Hz, 2 H), 6.74 (d, $J = 7.5$ Hz, 2 H), 5.77 (dd, $J = 21.3$ Hz, $J = 9.7$ Hz, 1 H), 4.34 (s, 1 H).

Diphenyl α -*N*-(propiolamido)-(4-guanidinium-phenyl)methanephosphonate (**3g**)

ESI-MS: $[M+H]^+$ m/z 449.1413 (found), 449.1372 (calculated). $^1\text{H-NMR}$ (400 MHz, DMSO- d_6): $\delta = 10.35$ (d, $J = 10.0$ Hz, 1 H), 9.71 (s, 1 H), 7.71 (dd, $J = 8.4$ Hz, 2.0 Hz, 2 H), 7.46 (s, 3 H), 7.42 - 7.32 (m, 4 H), 7.29 (d, $J = 8.4$ Hz, 2 H), 7.26 - 7.19 (m, 2 H), 7.09 (d, $J = 8.4$ Hz, 2 H), 7.02 (d, $J = 8.4$ Hz, 2 H), 6.00 (dd, $J = 22.6$ Hz, $J = 10.0$ Hz, 1 H), 4.41 (s, 1 H).

5.1.1.2 General methods for solid phase peptide synthesis of peptide diphenyl α -aminoalkylphosphonates

5.1.1.2.1 Diazotransfer

Triflyl azide (TfN_3) was freshly prepared from sodium azide (NaN_3) (5 eq.) and triflic anhydride (Tf_2O) (1 eq.). NaN_3 was dissolved in H_2O (0.16 mL/mmol). At 0 °C DCM (0.27 mL/mmol) was added to the clear solution under heavy stirring. Tf_2O was added dropwise and the reaction mixture was stirred at 0 °C for 2 h. The water phase was extracted 2x with DCM. The combined organic phases were washed once with saturated NaHCO_3 solution. The maximal volume of the organic phase was 2.70 mL/mmol TfN_3 . For the diazotransfer, the Fmoc deprotected tripeptide on the resin (1 eq.) was treated with TfN_3 (0.37 M, 16.7 eq.) in DCM and CuSO_4 (12.6 mM, 0.1 eq.) in MeOH for 24 h while shaking. Before a Kaiser test was performed, the resin was washed with NMP (3x 2 min), 0.5% DIEA/NMP (3x 2 min), 0.05 M sodium diethyldithiocarbamate in NMP (3x 10 min), NMP (5x 5 min) and DCM (3x 3 min) and Et_2O .

5.1.1.2.2 On-resin click reaction

The resin-tripeptide azide conjugate (1 eq.) was resuspended in DMF and the building block (3 eq.) was added as a solution in DMF (0.45 M), followed by the click reagents TBTA (0.2 eq.), CuSO₄ (0.1 eq.) and sodium ascorbate (3 eq.) in DMF/H₂O (10/1, v/v). The reaction was shaken at rt for about 24 h, followed by three washing steps each with DCM, DMF, 0.02 M sodium diethyldithiocarbamate in DMF, DMF, MeOH, DMF, DCM and Et₂O.

5.1.1.2.3 Resin Cleavage

The resin was treated with 95% TFA, 2.5% H₂O and 2.5% TIS for 1 h. Supernatant was collected and compounds were precipitated by addition of excess Et₂O. The precipitates were dried under a N₂ stream and purified by HPLC.

PraAlaGlu(triazole)Val^P(OPh)₂ (**5**)

The title compound was isolated as a white solid in 3% yield after HPLC purification. ESI-MS: [M+H]⁺ *m/z* 696.2496 (found), 696.2541 (calculated).

PraAlaAla(triazole)Leu^P(OPh)₂ (**6**)

The title compound was isolated as a white solid in 40% yield after HPLC purification. ESI-MS: [M+H]⁺ *m/z* 652.2603 (found), 652.2642 (calculated).

PraAlaAla(triazole)Phe^P(OPh)₂ (**7**)

The title compound was isolated as a white solid in 7% yield after HPLC purification. ESI-MS: [M+H]⁺ *m/z* 686.2456 (found), 686.2486 (calculated).

PraMetPhe(triazole)Phe^P(OPh)₂ (**8**)

The title compound was isolated as a white solid in 4% yield after HPLC purification. ESI-MS: [M+H]⁺ *m/z* 822.2804 (found), 822.2833 (calculated).

PraAlaAla(triazole)Gua^P(OPh)₂ (**9**)

The title compound was isolated as a white solid in 8% yield after HPLC purification. ESI-MS: [M+H]⁺ *m/z* 729.2622 (found), 729.2656 (calculated).

PraAlaSer(triazole)Gua^P(OPh)₂ (**10**)

The title compound was isolated as a white solid in 9% yield after HPLC purification. ESI-MS: [M+H]⁺ *m/z* 745.2548 (found), 745.2605 (calculated).

PraNleThr(triazole)Gua^P(OPh)₂ (**11**)

The title compound was isolated as a white solid in 8% yield after HPLC purification. ESI-MS: [M+H]⁺ *m/z* 801.3216 (found), 801.3231 (calculated).

PraLeuPhe(triazole)Gua^P(OPh)₂ (**12**)

The title compound was isolated as a white solid in 7% yield after HPLC purification. ESI-MS: [M+H]⁺ *m/z* 847.3404 (found), 847.3439 (calculated).

5.1.2 Docking experiments

The phosphonate **10** (with the same chirality at the P1 position as a natural substrate) was geometry optimized with a MMFF94 force field and defined as an extension of the side chain of the bovine trypsin S195 (PDB-coordinates: 1MAX, from which the original covalent phosphonate inhibitor structure was deleted). Docking of the inhibitor as a flexible side chain of S195 was performed with AutoDock Vina. A non-covalent inhibitor bound to bovine trypsin was taken as a comparison (PDB coordinates: 2ZFT). Pictures were generated using VMD 1.9.

5.1.3 Labeling experiments

5.1.3.1 Labeling of purified enzymes

Each enzyme in PBS was labeled in a final volume of 50 μ L as described earlier. Probe concentration: 5 μ M for DPP ABPs, 1 μ M for FP-R. Protein/lane: 100 ng.

5.1.3.2 Labeling of purified proteases in a proteome background

Each protease was diluted in a lysate of an HT-29 cell line (1 mg/mL) as 1% of total protein. Afterwards the protocol for labeling of purified enzymes was followed. Protein loading: 10 μ g/lane.

5.1.3.3 Labeling in enterokinase-activated rat pancreas lysate

Rat pancreas lysate in PBS (concentration of total protein: 3.5 mg/mL) was activated with enterokinase (1 U/mg protein) for 2 h on ice. Labeling with ABPs was carried out at a protein concentration of 3 mg/mL following the protocol for labeling of purified enzymes. Protein samples were resolved on a 15% acrylamide SDS gel. Protein loading: 15 µg/lane.

5.2 Quenched phosphonate ABPs for imaging protease activity

5.2.1 Synthesis

5.2.1.1 General procedure for dealkylation with LiBr

Compound to be dealkylated (1 eq.) and LiBr (1.2 eq.) were stirred in butanone (0.5 mL/mmol) and refluxed at 70 °C for 24 h. The precipitate was filtered and washed with diethyl ether and redissolved in 1 M HCl. The water phase was extracted 4x with EtOAc. The collected organic layers were subsequently washed with brine and dried over MgSO₄. The purity of the compounds was sufficient for further reactions.

5.2.1.2 General procedure for coupling of 5-hexynoic acid

5-hexynoic acid (2 eq.) was mixed with HATU (1.9 eq.) and DIEA (4 eq.) in DMF (4 mL) for 20 min at rt. To this, Cbz deprotected phosphonate (1 eq., 1 mmol) and DIEA (1.6 eq.) in DMF (3 mL) were added and stirred o/n at rt. The solvent was removed, and the oily product was redissolved in EtOAc and washed 2x with 1 M HCl, 2x with saturated NaHCO₃, and brine. The organic layer was subsequently dried over MgSO₄. For further purification a silica column was performed.

5.2.1.3 General procedure for coupling of QSY-7

TAMRA phosphonate (1 eq.), QSY-7 succinimidylester (1.1 eq.) and DIEA (1.8 eq.) were mixed in DMSO (25 μL/μmol phosphonate) at rt for 3 h.

Diethyl α -(*N*-benzyloxycarbonylamino)-(4-nitro-phenyl)methanephosphonate (14)

Benzyl carbamate (1 eq., 10 mmol) was mixed with diethyl phosphite (1 eq.) in AcOH (8 mL) and SOCl₂ (3 mL). 4-nitrobenzaldehyde (1.04 eq.) was then added and the mixture was stirred for 20 min at rt and subsequently refluxed at 65 °C for 4-5 h. The solvent was coevaporated with toluene and the oily product was redissolved in a small amount of EtOH, and cold H₂O was added. The crystallization took place o/n in the fridge. The crystallization was repeated and the white crystals were filtered resulting in pure product in 93% yield. ESI-MS: [M+H]⁺ *m/z* 423.1293 (found), 423.1315 (calculated). ¹H NMR (500 MHz, DMSO-d₆): δ = 8.64 (d, *J* = 9.2 Hz, 1H), 8.23 (d, *J* = 8.6 Hz, 2H), 7.77 (d, *J* = 7.0 Hz, 2H), 7.41 – 7.28 (m, 5H), 5.34 (dd, *J* = 23.1, 9.9 Hz, 1H), 5.15 – 5.00 (m, 2H), 4.03 – 3.87 (m, 4H), 1.16 (t, *J* = 7.1 Hz, 3H), 1.12 (t, *J* = 7.0 Hz, 3H).

Diethyl α -(*N*-hex-5-ynamido)-(4-nitro-phenyl)methanephosphonate (15)

Cbz was deprotected as described earlier. However, no crystals were formed. The Et₂O layer was discarded and the solvent was removed, giving the product as bright orange solid with a yield of 64%.

5-hexynoic acid was coupled as described above. A silica column with first 60% EtOAc/PE, then 80% EtOAc/PE was performed, leading to the product in 74% yield as yellowish crystals. ESI-MS: [M+H]⁺ *m/z* 383.1385 (found), 383.1366 (calculated). ¹H NMR (500 MHz, DMSO-d₆): δ = 9.09 (d, *J* = 9.6 Hz, 1H), 8.26 – 8.22 (m, 2H), 7.74 (d, *J* = 6.8 Hz, 2H), 5.63 (dd, *J* = 22.5, 9.6 Hz, 1H), 4.08 – 3.84 (m, 4H), 2.78 (t, *J* = 2.6 Hz, 1H), 2.43 – 2.28 (m, 2H), 2.16 (tt, *J* = 7.1, 2.6 Hz, 2H), 1.71 – 1.64 (m, 2H), 1.20 (t, *J* = 7.0 Hz, 3H), 1.12 (t, *J* = 7.0 Hz, 3H).

Ethyl-(*N*-Boc)-Tyramine- α -(*N*-hex-5-ynamido)-(4-nitrophenyl)methanephosphonate (**16**)

15 (1 eq., 2.4 mmol) was dealkylated as described above, leading to the ethylhydroxyl-phosphonate as a white powder in 65% yield. ESI-MS: $[M+H]^+$ m/z 355.1071 (found), 355.1054 (calculated).

The monohydroxyl phosphonate (1 eq., 141 μ mol), DMAP (0.1 eq.), *N*-Boc-Tyramine (1.1 eq.) and DIC (8 eq.) were mixed in DMF (1.5 mL). The reaction was set under N_2 and refluxed at 70 °C for 2 h. The solvent was removed and the oily product was redissolved in EtOAc. The organic layer was then washed 1x with saturated $NaHCO_3$, 1x with 1 M HCl and brine, and subsequently dried over $MgSO_4$. The relatively pure product obtained in 90% yield as a white powder was directly used for the next reaction. ESI-MS: $[M+H]^+$ m/z 574.2348 (found), 574.2313 (calculated).

Ethyl-(*N*-Boc)-Tyramine- α -(*N*-hex-5-ynamido)-(4-*N,N*-diBoc-guanidiniumphenyl)methanephosphonate (**17**)

16 (1 eq., 565 μ mol) and $SnCl_2$ (5 eq.) were mixed in EtOH (2 mL) and refluxed at 70 °C for 1 h. The solvent was removed and the oily product was redissolved in saturated $NaHCO_3$. The water phase was then extracted 3x with EtOAc, and the collected organic phases were washed with brine and dried over $MgSO_4$. The product was directly used for the next reaction without further purification. ESI-MS: $[M+H]^+$ m/z 544.2681 (found), 544.2571 (calculated).

The aniline (1 eq., 471 μ mol), 1,3-di-Boc-2-(trifluoromethylsulfonyl)guanidine (1.6 eq.) and TEA (2 eq.) were mixed in DCM (5 mL) and refluxed o/n at 40 °C. The reaction was diluted with DCM and the organic phase was washed with 2x 40% $KHSO_4$, 1x with saturated $NaHCO_3$ and brine and subsequently dried over $MgSO_4$. The crude product was purified via silica column with a 50% EtOAc/PE solvent system. The target compound was isolated as white crystals in 19% yield (over

2 steps). ESI-MS: $[M+H]^+$ m/z 786.4017 (found), 786.3838 (calculated). 1H NMR (500 MHz, DMSO- d_6): δ = 11.44 (d, J = 34.5 Hz, 1H), 10.02 (s, 1H), 9.03 (dd, J = 9.9, 2.2 Hz, 1H), 7.55 (d, J = 6.6 Hz, 2H), 7.48 (d, J = 7.1 Hz, 2H), 7.17 (d, J = 8.5 Hz, 2H), 7.02 (d, J = 8.2 Hz, 2H), 6.85 (t, J = 5.7 Hz, 1H), 5.65 (dd, J = 21.5, 9.8 Hz, 1H), (4.06 – 3.99 (m, 2H)/ 3.98 – 3.91 (m, 2H)), 3.11 (dt, J = 8.0, 6.3 Hz, 2H), 2.77 (t, J = 2.6 Hz, 1H), 2.66 (dd, J = 8.4, 6.5 Hz, 2H), 2.29 (td, J = 7.3, 4.4 Hz, 2H), 2.14 (t, J = 6.4 Hz, 2H), 1.68 – 1.61 (m, 2H), 1.48 (d, J = 22.4 Hz, 9H), 1.41 (d, J = 7.4 Hz, 9H), 1.37 (s, 9H), (1.18 (t, J = 7.1 Hz, 3H)/ 1.10 (t, J = 7.0 Hz, 3H)).

Ethyl-((N-QSY-7)-Tyramine)- α -(4-[1-(3-aminopropyl)triazol-4-yl]butanamido)-(4-guanidinium-phenyl)methanephosphonate (**PB2**)

17 (1 eq., 100 μ mol) and TIS (1 eq.) were mixed in 0.5 mL TFA/DCM (50%) for 30 min at rt. The solvent was removed, and the oily product was purified by HPLC, leading to the desired compound as a white powder in 37% yield. ESI-MS: $[M+H]^+$ m/z 486.2244 (found), 486.2265 (calculated).

The Boc deprotected compound (1 eq., 2.1 μ mol), 5(6)-TAMRA *N*-succinimidyl ester (1.1 eq.), DIEA (2 eq.), 1 mM CuSO₄, 1 mM Na ascorbate, 0.6 mM TBTA and 0.5 mM CuBr are mixed in 50 μ L ACN/H₂O (50%). The reaction took place o/n at rt. The product was purified by HPLC, leading to the desired compound as a pink powder in 16% yield.

QSY-7 was coupled to the TAMRA phosphonate as described above. Subsequently the reaction was diluted with 50% ACN/H₂O + 0.1% TFA and purified via HPLC, leading to the final quenched product as a purple powder in 18% yield. ESI-MS: $[M+H]^+$ m/z 1638.6636 (found), 1638.6707 (calculated).

Diethyl α -(*N*-benzyloxycarbonyl)amino-(2-methylpropyl) methanephosphonate (**19**)

Benzyl carbamate (1 eq., 20 mmol) was mixed with diethyl phosphite (1 eq.) in acetyl chloride (15 mL) and stirred at -5 °C in an ice/salt bath. Isobutyraldehyde (1.25 eq.) was added dropwise within 10 min. The mixture was first stirred for 1 h at 0 °C and subsequently o/n at rt. The solvent was removed and the oily product was redissolved in DCM and washed 1x with H₂O, 2x with 40% NaHSO₃, 3x with saturated NaHCO₃, 1x with 1 M HCl, 2x with H₂O and dried over MgSO₄. For further purification a silica column with first 50% EtOAc/PE, then 80% EtOAc/PE was performed leading to the product in 78% yield as colorless viscous oil. ESI-MS: [M+H]⁺ *m/z* 344.1904 (found), 344.1622 (calculated).

Ethyl-(*N*-Boc)-Tyraminyl- α -(*N*-benzyloxycarbonyl)amino-(2-methylpropyl) methanephosphonate (**20**)

19 (1 mmol) was dealkylated as described earlier. ESI-MS: [M+H]⁺ *m/z* 316.1307 (found), 316.1309 (calculated).

The monohydroxyl phosphonate (1 eq.), DMAP (0.5 eq.), *N*-Boc-Tyramine (1.1 eq.) and DIC (8 eq.) were mixed in toluene (9 mL). The reaction was set under N₂ and refluxed at 70 °C o/n. The solvent was removed and the oily product was redissolved in EtOAc. The organic layer was then washed 1x with saturated NaHCO₃, 1x with 1 M HCl and brine, and subsequently dried over MgSO₄. The relatively pure product obtained in 90% yield as a white powder was directly used for the next reaction. ESI-MS: [M+H]⁺ *m/z* 535.2590 (found), 535.2568 (calculated).

Ethyl-(*N*-Boc)-Tyramine- α -(*N*-hex-5-ynamido)-(2-methylpropyl) methanephosphonate (**21**)

20 (1 eq.), AcOH (2.5 eq.) and Pd/C (1 mg/10 mg of **20**) was stirred under hydrogen in EtOH (4 mL). The catalyst was filtered and the solvent was evaporated. ESI-MS: $[M+H]^+$ m/z 401.2218 (found), 401.2199 (calculated).

5-hexynoic acid was coupled to **20** as described earlier. ESI-MS: $[M+H]^+$ m/z 495.2599 (found), 495.2619 (calculated). Yield = 26% (over 4 steps).

Ethyl-((*N*-QSY-7)-Tyramine)- α -(4-[1-(3-aminopropyl)triazol-4-yl]butanamido)-(2-methylpropyl)methanephosphonate (**SEV2**)

21 (1 eq., 2 μ mol) and TAMRA(propyl) N_3 (1.1 eq.) were mixed with CuBr (1 mM), TBTA (2 mM) and sodium ascorbate (10 mM) in *t*BuOH/H₂O (1/1) (50 μ L). The reaction set under N₂ and reacted at 40 °C for 24 h. ESI-MS: $[M+2H]^{2+}$ m/z 504.2381 (found), 504.2432 (calculated).

Boc protection of the tyramine was removed with TFA/DCM (1/1) + 2.5% H₂O (50 μ L) for 1 h at rt. ESI-MS: $[M+2H]^{2+}$ m/z 454.2139 (found), 454.2169 (calculated).

QSY-7 was coupled to the TAMRA phosphonate as described earlier. Subsequently the reaction was diluted with 50% ACN/H₂O + 0.1% TFA and purified via HPLC, leading to the final quenched product as a purple powder in 16% yield over 3 steps. ESI-MS: $[M+3H]^{3+}$ m/z 516.2116 (found), 516.5559 (calculated).

5.2.2 Unquenching of **PB2**

A black 96 well plate is used. Well 1 contains 100 μ L PBS as negative control, well 2 contains 99 μ L PBS and 1 μ L TAMRA- N_3 (2 μ M), well 3 contains 98 μ L PBS and

2 μL **PB2** (2 μM) and well 4 contains 93 μL PBS, 2 μL PB2 (2 μM) and 5 μL Trypsin (2 μM). The samples are measured for 20 min with a fluorimeter.

5.2.3 Labeling experiments

5.2.3.1 Labeling of purified enzymes

Each enzyme (375 ng) in PBS was labeled in a final volume of 50 μL as described earlier. Probe concentration: 5 μM for **SEV2**, 2 μM for **PB2**. Protein/lane: 114 ng.

5.3 FRET-based assay for inhibitor screening of Lon protease

5.3.1 Synthesis

Boc-Lys(DABCYL)-COOH (**24**)

4-(dimethylaminoazo)benzene-4-carboxylic acid (DABCYL-COOH) (1 eq., 0.25 mmol) was dissolved in DMF by heating-up to 80 °C for 10 min. NHS (1.2 eq.), DIC (1.1 eq.) and DMF were added and the reaction took place at rt o/n. Product formation (**23**) was also confirmed by LC-MS $[M+H]^+$ m/z 367.15 (found), 367.15 (calculated). Subsequently, Boc-Lys-COOH (1.1 eq.) and DIEA (3 eq.) were added and left o/n at rt to react. All reaction steps were monitored with TLC. DMF was evaporated under vacuum. The concentrated reaction products were dissolved in EtOAc and washed twice with 1 M HCl. The organic phase was then dried by $MgSO_4$, filtered, and concentrated. Further purification was carried out via silica column chromatography with a gradient from 20% EtOAc/80% Toluene to 100% EtOAc. The title compound was isolated in 36% yield. ESI-MS: $[M+H]^+$ m/z 498.28 (found), 498.26 (calculated).

K(DABCYL)RGITCSGRK(FITC) (**27**)

The peptide synthesis was done by general Fmoc solid phase synthesis procedures as described earlier, except for Ile (0.25 M in NMP), which was coupled using HATU (2.9 eq.) and DIEA (5 eq.) at rt for 2 h.

The coupling of FITC to the lysine side chain was performed directly after the coupling of the lysine to the resin. The Mtt protection of the ϵ -amino group was removed by treatment with 6x 1% TFA in DCM at rt for 5 min. Subsequently, fluorescein isothiocyanate (1.5 eq., 0.125 M in DMF) and DIEA (3 eq.) were added.

The reaction took place at rt for 2 h. After this step all following reactions were performed in the dark.

Boc-Lys(DABCYL)-COOH (**24**) (1.5 eq., 0.125 M in DMF/DCM 1:1) was preactivated with HBTU (1.5 eq.) and DIEA (3 eq.) at rt for 10 min. This reaction mixture was then added to the resin and coupled at rt o/n. Final cleavage from the resin was done by 88% TFA, 5% DTT, 5% H₂O and 2% TIS at rt for 2 h. The cleaved peptide was precipitated in cold diethylether and the precipitate was dried with a stream of nitrogen. The HPLC purification gave the desired product with a final yield of 27%. ESI-MS: [M+5H]⁺ *m/z* 375.56 (found), 375.56 (calculated).

5.3.2 Buffers

Mary buffer

50 mM HEPES-NaOH (pH 8.0), 1 mM DTT, 350 mM NaCl, 10% sucrose. Lysis buffer was a Mary buffer with 25 mM imidazole. Washing and elution buffers for the purification were Mary buffers with imidazole concentrations of 25 mM, 50 mM, 100 mM, 200 mM and 500 mM.

Lon reaction buffer

50 mM HEPES-NaOH (pH 8.0), 1 mM DTT, 100 mM KCl, 10 mM MgCl₂

ATP stock solution

500 mM HEPES-NaOH (pH 8.0), 100 mM Na₂ATP

5.3.3 Protein expression and purification

For the expression of *E. coli* Lon a pCA24N vector from the group of Hirotada Mori, Keio University, Japan was used. This vector is a high copy number plasmid, carrying a chloramphenicol resistance gene. Attached to the N-terminus of the Lon is a histidine tag for purification, separated from the protein by seven spacer amino acids. The expression is controlled by an IPTG inducible promoter, which is repressed by the lacIq repressor gene product.

The plasmid DNA was transformed into competent BL21 (DE3) cells by adding 1 μ L of DNA (440 ng/ μ L) into 50 μ L of competent cells. The cells were then transferred into an ice cold electroporation cuvette, and a voltage pulse was performed. Immediately afterwards 600 μ L of LB media without antibiotics were added and incubated for 1 h at 37 °C. The cells were plated on agar containing chloramphenicol (30 μ g/mL). The agar plates were incubated o/n at 37 °C.

One colony was picked and incubated in 5 mL LB media with chloramphenicol (30 μ g/mL) to grow a day culture at 37 °C. The o/n culture was prepared by adding 100 μ L of the day culture into 5 mL fresh LB media with chloramphenicol (30 μ g/mL) and incubated at 37 °C. 2.5 mL of the o/n culture were used to inoculate 250 mL sterile LB media containing chloramphenicol (30 μ g/mL) to an OD₆₀₀ of 0.4 - 0.6. Cells were then induced with IPTG (0.4 mM) and grown for 2 h at 37 °C for. Afterwards the cells were harvested by centrifugation at 7000 g for 25 min at 4 °C and the pellet was resuspended in 5 mL Mary buffer. The cells were then lysed with a French Press (Aminco French Press, G. Heinemann, Schwäbisch Gmünd, Germany), followed by centrifugation at 7000 g for 10 min at 4 °C to remove insoluble cell debris.

The supernatant was incubated with 1 mL Ni²⁺-NTA agarose beads at 4 °C o/n. The mixture was then filled into a cartridge and the flow-through was collected. The beads were washed with 4 mL of Mary buffer with 25 mM, 50 mM and 2 mL of Mary buffer with 100 mM imidazole. The target protein was eluted with 500 μ L Mary buffer with 200 mM imidazole and 500 μ L Mary buffer with 500 mM

imidazole. Afterwards the elution fractions were dialyzed three times for 2 h against 200 mL reaction buffer in a dialysis membrane (Spectra Por MWCO 1000, Spectrum labs, Rancho Dominguez, USA). Protein concentrations were determined colorimetrically by DC Protein Assay (Bio-Rad, Hercules, USA). Aliquots of the enzyme were snap frozen in liquid nitrogen and stored at -80 °C.

50 µL samples for analysis were taken before induction, after induction and at the end of expression, of the supernatant after spinning down the lysed cells, of the flow through after incubation with Ni²⁺-NTA beads and after each washing step. 2 µL samples were taken from the elution fractions. All samples were analyzed on a 15% polyacrylamide gel, at 150 V, 2 h, and stained with Coomassie Biosafe (Bio-Rad, Hercules, USA).

5.3.4 Gel-based activity assay of Lon

The activity of the enzyme was checked by casein digestion. The assay was performed with 5 µM β-casein, 1.5 µM Lon, 10 mM ATP and 5 mM PMSF in 150 µL reaction buffer. β-casein in reaction buffer was used as negative control. The digestion of casein with Lon was done both with and without ATP. Preinhibition with PMSF was done in presence of ATP. Lon was preincubated with PMSF for 30 min at 37 °C. Prior to the addition of ATP the samples were preincubated with β-casein for 2 min at 37 °C. 50 µL samples were taken after 1 h, 2 h and o/n. Afterwards 16 µL 4x sample buffer were added and the samples were boiled for 2 min. 12 µL of each sample were analyzed on a 15% polyacrylamide gel, at 150 V, 2 h (Protein loading: 1.1 µg/lane β-casein, 1.2 µg/lane Lon).

5.3.5 FRET assay

The FRET assay was performed with 0.275 µM Lon, 5.5 mM ATP, 3 µM β-casein and 100 µM inhibitor or DMSO in reaction buffer in a final volume of 100 µL. After incubation for 30 min at 37 °C the mixture was transferred into a prewarmed, black

96-well plate, containing 80 μM FRET peptide in 10 μL reaction buffer. The blank contained only reaction buffer and the negative control an additional volume of reaction buffer instead of Lon. The assay was performed at 37 $^{\circ}\text{C}$ and the fluorescence was measured with a plate reader (FLUOstar Optima, BMG Labtech, Ortenberg, Germany) for 3 h. The gain of the plate reader was set to 800, the excitation filter to 485 nm and the emission filter to 520 nm. All samples were prepared and measured in duplicates. The fluorescence data were processed with Graph Pad Prism software. The fluorescence intensity was plotted as a function of time. The enzymatic activity was calculated by determining the slope of the linear part of this function. The slope of the sample treated with DMSO was set to 100% and the slope of the negative control (without Lon) to 0%. The slopes of all other samples were normalized according to these two values.

5.3.6 Reversibility check

The reversibility of the hit compounds was also determined with the FRET assay. Same conditions as above were used. *E. coli* Lon was preincubated with 200 μM **98** or **99**, or with 500 μM **95** or **96** for 30 min at 37 $^{\circ}\text{C}$. The columns for gel filtration (Zeba Spin Desalting column 7K MWCO, 0.5 mL, Thermo Scientific, Waltham, USA) were three times equilibrated with reaction buffer and the gel filtration was performed according to manufacturer's instructions. The flow-through was then immediately transferred to a warmed, black 96-well plate, containing 80 μM FRET peptide in 10 μL reaction buffer. The fluorescence was measured as described earlier.

5.3.7 Labeling of *E. coli* Lon

To label Lon with an ABP, six different samples of 463 ng Lon were prepared in a final volume of 25 μL reaction buffer. One sample was preheated for 25 min at 72 $^{\circ}\text{C}$. Four other samples were incubated for 30 min at 37 $^{\circ}\text{C}$ with 5 mM PMSF or DMSO with and without 3.8 mM ATP. As a control, free cysteine residues were

alkylated by incubating with 100 mM iodoacetamide for 1 h at 37 °C. The labeling was then done as described earlier with 20 μM probe concentration. Protein/lane: 150 ng

5.3.8 Site-directed mutagenesis

The mutagenesis was performed according to the manual of the QuikChange II Site-directed Mutagenesis Kit (Stratagene). The primer sequences were generated with the online tool recommended by Stratagene (<https://www.stratagene.com/qcprimerdesign>) (**Table 2**). The new plasmids were isolated using the Plasmid Mini Kit I (Omega Bio-Tec, Norcross, USA) and verified by DNA sequencing.

Table 2 Primer sequences for the site-directed mutagenesis. The mutated base pairs are highlighted in yellow.

Name	Sequence 5' → 3'
S679A sense	GCCGAAAGATGGTCCG GCT GCCGGTATTGCTATG
S679A antisense	CATAGCAATACCGGCAG GC CGGACCATCTTTCGGC
C617A sense	ACTTGCTGACCATTGAAACCGCA GCT TGTTCCGGGTAAAG
C617A antisense	CTTTACCCGGAACAG GCT TGCGGTTTCAATGGTCAGCAAGT
C685A sense	CCGAGTGCCGGTATTGCTATG GCT ACCGCGCTGGTTT
C685A antisense	AAACCAGCGCGGT AGCC CATAGCAATACCGGCACTCGG
C691A sense	CACCGCGCTGGTTTCT GCT CTGACCGGTAACCCGG
C691A antisense	CCGGGTTACCGGTCAG AGC AGAAACCAGCGCGGTG



List of Abbreviations

ABP	Activity-based probe
ABPP	Activity-based protein profiling
AcOH	Acetic acid
ACN	Acetonitrile
AEBSF	4-(2-Aminoethyl)benzenesulfonyl fluoride hydrochloride
Ala (A)	Alanine
APS	Ammonium persulfate
Asp	Aspartic acid
ATP	Adenosine-5'-triphosphate
Boc	<i>t</i> -Butyloxycarbonyl
BSA	Bovine Serum Albumin
Cat G	Cathepsin G
Cbz	Benzyl carbamate
Chy	Chymotrypsin
Cys (C)	Cysteine
DABCYL	4-(dimethylaminoazo)benzene-4-carboxylic acid
DAP22c	Biotin-Ala-Ala-Phe-diphenylphosphonate
DCI	3,4-Dichloroisocoumarin
DCM	Dichloromethane
DFP	Diisopropylfluorophosphate
DIC	Diisopropylcarbodiimide
DIEA	Diisopropylethylamine
DMAP	Dimethylaminopyridine
DMF	Dimethylformamide
DMSO	Dimethyl sulfoxide

DPP	Diphenylphosphonate
DTT	Dithiothreitol
<i>E. coli</i>	<i>Escherichia coli</i>
EOAc	Ethylacetate
eq.	Equivalent
ESI-MS	Electrospray ionisation mass spectrometry
EtOH	Ethanol
FA	Formic acid
FITC	Fluorescein isothiocyanate
Fmoc	Fluorenylmethoxycarbonyl
FRET	Fluorescence resonance energy transfer
Glu (E)	Glutamic acid
Gly (G)	Glycine
Gua	<i>p</i> -Guanidiniumphenylglycine
HATU	1-[Bis(dimethylamino)methylene]-1H-1,2,3-triazolo[4,5-b]pyridinium 3-oxid hexafluorophosphate
HBr	Hydrobromic acid
HCl	Hydrochloric acid
HEPES	4-(2-hydroxyethyl)-1-piperazine-ethanesulfonic acid
His	Histidine
HOBt	N-Hydroxybenzotriazole
HPLC	High-pressure liquid chromatography
HT-29	Human colon adenocarcinoma cell line
IAM	Iodoacetamide
ICAT	Isotope-coded affinity tagging
IPTG	Isopropyl β -D-1-thiogalactopyranoside
iTRAQ	Isobaric tags for relative and absolute quantification
KCl	Potassium chloride

kD	Kilo Dalton
LB	Lysogeny broth
Leu (L)	Leucine
Lys (K)	Lysine
MALDI-MS	Matrix-assisted laser desorption/ionization mass spectrometry
MEK	Methyl ethyl ketone
MeOH	Methanol
Met (M)	Methionine
MudPIT	Multidimensional protein identification
MW	Molecular weight
N ₂	Nitrogen
NaOH	Sodium hydroxide
NHS	<i>N</i> -hydroxysuccinimide
nLeu (n)	Norleucine
NMP	<i>N</i> -Methyl-2-pyrrolidone
NMR	Nuclear magnetic resonance
NTA	Nitrilotriacetic acid
OD	Optical density
o/n	Overnight
PAGE	Polyacrylamide gel electrophoresis
PBS	Phosphate buffer saline
PBST	Phosphate buffer saline with Tween
PCC	Pyridinium chlorochromate
PCR	Polymerase chain-reaction
Phe (F)	Phenylalanine
PMSF	Phenylmethanesulfonyl fluoride
Pra	Propargylglycine

qABP	Quenched activity-based probe
rt	Room temperature
Ser (S)	Serine
SDS	Sodium dodecyl sulfate
SILAC	Stable isotope labeling of amino acids in cell culture
SPPS	Solid phase peptide synthesis
TAMRA	Carboxy-tetramethyl-rhodamine
TBTA	Tris[(1-benzyl-1H-1,2,3-triazol-4-yl)methyl]amine
TEMED	Tetramethylethylenediamine
THF	Tetrahydrofuran
THPTA	Tris(3-hydroxypropyltriazolylmethyl)amine
Thr (T)	Threonine
TIS	Triisopropylsilane
TLC	Thin-layer chromatography
TLCK	Tosyl-L-lysine chloromethyl ketone
TFA	Trifluoroacetic acid
TRIS	Tris(hydroxymethyl)-aminomethane
Try	Trypsin
uPA	Urokinase-type plasminogen activator
Val (V)	Valine

List of figures

Figure 1 Activation of pancreatic enzymes.....	8
Figure 2 Nomenclature of protease specificities.....	9
Figure 3 General design of an activity-based probe.....	12
Figure 4 Design of a quenched activity-based probe.....	14
Figure 5 Influencing the selectivity of phosphonate ABPs.....	17
Figure 6 Labeling of purified proteases with FP-rhodamine, P1 and extended DPP probes.....	27
Figure 7 In-gel fluorescence (left) of proteases labeled in the context of a proteome (a cell lysate of the human colon adenocarcinoma cell line HT-29).....	28
Figure 8 Fluorescent labeling of endogenous proteases in enterokinase-activated rat pancreas lysate by DPP ABPs with extended recognition elements and FP-R.....	29
Figure 9 Docking of probe 10 bound to Ser195 in bovine beta-trypsin.....	31
Figure 10 Schematic illustration of a phosphonate qABP, binding to a serine protease.....	33
Figure 11 Labeling of purified serine proteases with qABPs.....	37
Figure 12 Quenching efficiency of PB2	38
Figure 13 FRET peptide with the N-terminal quencher DABCYL and the C-terminal fluorophore FITC.....	40
Figure 14 Purification of <i>E. coli</i> Lon via the His ₆ -tag using Ni-NTA beads.....	43
Figure 15 Lon activity assay.....	44
Figure 16 FRET assay for the inhibitor screening of <i>E. coli</i> Lon.....	45
Figure 17 Inhibitor screening of <i>E. coli</i> Lon.....	47
Figure 18 Inhibition of β -casein digestion by <i>E. coli</i> Lon with potential inhibitors discovered by the FRET assay.....	48
Figure 19 Reversibility check of the hit compounds 95 , 96 , 98 and 99	49
Figure 20 Inhibitors of <i>E. coli</i> Lon identified with the FRET assay library screening.....	50
Figure 21 Titration of the boronates 61 and 63 and the thiiranes 98 and 99 in inhibiting <i>E. coli</i> Lon.....	51
Figure 22 Labeling of <i>E. coli</i> Lon with thiiranes.....	52
Figure 23 Activity analysis of the Lon mutants with the FRET assay.....	53

Figure 24 Labeling of <i>E. coli</i> Lon wild type and mutants with 98 (20 μ M).....	54
Figure 25 Protease reactive warheads mentioned above.....	57
Figure 26 Structures of known Lon protease inhibitors and the newly identified thiiranes.	63

List of schemes

Scheme 1 Ser/His/Asp catalytic triad mechanism.	7
Scheme 2 Mechanism of serine protease inhibition by α -aminophosphonate diphenyl esters.	16
Scheme 3 Mechanism of the Birum-Oleksyszyn reaction.	23
Scheme 4 A) Synthesis of building blocks with hydrophobic side chains. B) Synthesis of building blocks with basic side chains.	25
Scheme 5 Solid phase peptide synthesis of DPP ABPs.	26
Scheme 6 Synthesis of a basic P1 probe.	35
Scheme 7 Synthesis of a P1 Valine probe.	36
Scheme 8 Synthesis of the FRET peptide 27	42

References

1. Sienczyk, M.; Lesner, A.; Wysocka, M.; Legowska, A.; Pietruszewicz, E.; Rolka, K.; Oleksyszyn, J., New potent cathepsin G phosphonate inhibitors. *Bioorg. Med. Chem.* **2008**, *16* (19), 8863-8867.
2. Rawlings, N. D.; Barrett, A. J.; Bateman, A., MEROPS: the peptidase database. *Nucleic Acids Res.* **2010**, *38*, D227-D233.
3. Rawlings, N. D.; Barrett, A. J.; Bateman, A., Asparagine Peptide Lyases: A seventh catalytic type of proteolytic enzymes. *J. Biol. Chem.* **2011**, *286* (44), 38321-38328.
4. Turk, B., Targeting proteases: successes, failures and future prospects. *Nat. Rev. Drug Discov.* **2006**, *5* (9), 785-799.
5. Polgar, L., The catalytic triad of serine peptidases. *Cell. Mol. Life Sci.* **2005**, *62* (19-20), 2161-2172.
6. Gettins, P. G. W., Serpin structure, mechanism, and function. *Chem. Rev.* **2002**, *102* (12), 4751-4803.
7. Zheng, X. L.; Kitamoto, Y.; Sadler, J. E., Enteropeptidase, a type II transmembrane serine protease. *Frontiers in bioscience (Elite edition)* **2009**, *1*, 242-9.
8. Schechte, I.; Berger, A., On size of active site in proteases .I. Papain. *Biochem. Biophys. Res. Commun.* **1967**, *27* (2), 157-&.
9. Venkatesh, S.; Lee, J.; Singh, K.; Lee, I.; Suzuki, C. K., Multitasking in the mitochondrion by the ATP-dependent Lon protease. *Biochimica Et Biophysica Acta-Molecular Cell Research* **2012**, *1823* (1), 56-66.

-
10. Huisman, O.; Dari, R.; Gottesman, S., Cell-division control in Escherichia-coli – Specific induction of the SOS function SfiA protein is sufficient to block septation. *Proceedings of the National Academy of Sciences of the United States of America-Biological Sciences* **1984**, *81* (14), 4490-4494.
 11. Gottesman, S.; Stout, V., Regulation of capsular polysaccharide synthesis in Escherichia-Coli. *Molecular Microbiology* **1991**, *5* (7), 1599-1606.
 12. Gottesman, S.; Gottesman, M.; Shaw, J. E.; Pearson, M. L., Protein-degradation in Escherichia-coli – The lon mutation and bacteriophage-N Lambda-N and CII protein stability. *Cell* **1981**, *24* (1), 225-233.
 13. Takaya, A.; Tomoyasu, T.; Tokumitsu, A.; Morioka, M.; Yamamoto, T., The ATP-dependent Lon protease of Salmonella enterica serovar Typhimurium regulates invasion and expression of genes carried on Salmonella pathogenicity island 1. *Journal of bacteriology* **2002**, *184* (1), 224-232.
 14. Brazas, M. D.; Breidenstein, E. B. A.; Overhage, J.; Hancock, R. E. W., Role of Lon, an ATP-dependent protease homolog, in resistance of Pseudomonas aeruginosa to ciprofloxacin. *Antimicrobial Agents and Chemotherapy* **2007**, *51* (12), 4276-4283.
 15. Van Dyck, L.; Langer, T., ATP-dependent proteases controlling mitochondrial function in the yeast Saccharomyces cerevisiae. *Cell. Mol. Life Sci.* **1999**, *56* (9-10), 825-842.
 16. Hori, O.; Ichinoda, F.; Tamatani, T.; Yamaguchi, A.; Sato, N.; Ozawa, K.; Kitao, Y.; Miyazaki, M.; Harding, H. P.; Ron, D.; Tohyama, M.; Stern, D. M.; Ogawa, S., Transmission of cell stress from endoplasmic reticulum to mitochondria: enhanced expression of Lon protease. *Journal of Cell Biology* **2002**, *157* (7), 1151-1160.

-
17. Bota, D. A.; Ngo, J. K.; Davies, K. J. A., Downregulation of the human Lon protease impairs mitochondrial structure and function and causes cell death. *Free Radical Biology and Medicine* **2005**, *38* (5), 665-677.
18. Ogura, T.; Wilkinson, A. J., AAA(+) superfamily ATPases: common structure-diverse function. *Genes to Cells* **2001**, *6* (7), 575-597.
19. Botos, I.; Melnikov, E. E.; Cherry, S.; Tropea, J. E.; Khalatova, A. G.; Rasulova, F.; Dauter, Z.; Maurizi, M. R.; Rotanova, T. V.; Wlodawer, A.; Gustchina, A., The catalytic domain of Escherichia coli Lon protease has a unique fold and a Ser-Lys dyad in the active site. *J. Biol. Chem.* **2004**, *279* (9), 8140-8148.
20. Licht, S.; Lee, I., Resolving individual steps in the operation of ATP-dependent proteolytic molecular machines: From conformational changes to substrate translocation and processivity. *Biochemistry* **2008**, *47* (12), 3595-3605.
21. Goldberg, A. L.; Waxman, L., The role of ATP hydrolysis in the breakdown of proteins and peptides by protease La from Escherichia-Coli. *J. Biol. Chem.* **1985**, *260* (22), 2029-2034.
22. Waxman, L.; Goldberg, A. L., Protease La from Escherichia-Coli hydrolyzes ATP and proteins in a linked fashion. *Proceedings of the National Academy of Sciences of the United States of America-Biological Sciences* **1982**, *79* (16), 4883-4887.
23. Gur, E.; Sauer, R. T., Recognition of misfolded proteins by Lon, a AAA(+) protease. *Genes & Development* **2008**, *22* (16), 2267-2277.
24. Waxman, L.; Goldberg, A. L., Protease La, the Lon gene-product, cleaves specific fluorogenic peptides in an ATP-dependent reaction. *J. Biol. Chem.* **1985**, *260* (22), 2022-2028.

-
25. Frase, H.; Hudak, J.; Lee, I., Identification of the proteasome inhibitor MG262 as a potent ATP-dependent inhibitor of the *Salmonella enterica* serovar typhimurium lon protease. *Biochemistry* **2006**, *45* (27), 8264-8274.
26. Bayot, A.; Basse, N.; Lee, I.; Gareil, M.; Pirotte, B.; Bulteau, A. L.; Friguet, B.; Reboud-Ravaux, M., Towards the control of intracellular protein turnover: Mitochondrial Lon protease inhibitors versus proteasome inhibitors. *Biochimie* **2008**, *90* (2), 260-269.
27. Lee, I.; Berdis, A. J., Adenosine triphosphate-dependent degradation of a fluorescent lambda N substrate mimic by lon protease. *Anal. Biochem.* **2001**, *291* (1), 74-83.
28. Fishovitz, J.; Li, M.; Frase, H.; Hudak, J.; Craig, S.; Ko, K.; Berdis, A. J.; Suzuki, C. K.; Lee, I., Active-Site-Directed Chemical Tools for Profiling Mitochondrial Lon Protease. *Acs Chemical Biology* **2011**, *6* (8), 781-788.
29. Haedke, U.; Kutter, E. V.; Vosyka, O.; Yang, Y. L.; Verhelst, S. H. L., Tuning probe selectivity for chemical proteomics applications. *Curr. Opin. Chem. Biol.* **2013**, *17* (1), 102-109.
30. Sadaghiani, A. M.; Verhelst, S. H.; Bogyo, M., Tagging and detection strategies for activity-based proteomics. *Curr Opin Chem Biol* **2007**, *11* (1), 20-8.
31. Willems, L. I.; van der Linden, W. A.; Li, N.; Li, K. Y.; Liu, N.; Hoogendoorn, S.; van der Marel, G. A.; Florea, B. I.; Overkleeft, H. S., Bioorthogonal chemistry: applications in activity-based protein profiling. *Acc. Chem. Res.* **2011**, *44* (9), 718-29.
32. Saxon, E.; Bertozzi, C. R., Cell surface engineering by a modified Staudinger reaction. *Science* **2000**, *287* (5460), 2007-2010.

-
33. Speers, A. E.; Adam, G. C.; Cravatt, B. F., Activity-based protein profiling in vivo using a copper(I)-catalyzed azide-alkyne [3+2] cycloaddition. *Journal of the American Chemical Society* **2003**, *125* (16), 4686-4687.
34. Kolb, H. C.; Finn, M. G.; Sharpless, K. B., Click chemistry: Diverse chemical function from a few good reactions. *Angewandte Chemie-International Edition* **2001**, *40* (11), 2004-2021.
35. Jewett, J. C.; Bertozzi, C. R., Cu-free click cycloaddition reactions in chemical biology. *Chem Soc Rev* **2010**, *39* (4), 1272-9.
36. Willems, L. I.; Verdoes, M.; Florea, B. I.; van der Marel, G. A.; Overkleeft, H. S., Two-step labeling of endogenous enzymatic activities by Diels-Alder ligation. *ChemBioChem* **2010**, *11* (12), 1769-81.
37. Puente, X. S.; Sanchez, L. M.; Overall, C. M.; Lopez-Otin, C., Human and mouse proteases: A comparative genomic approach. *Nature Reviews Genetics* **2003**, *4* (7), 544-558.
38. Edgington, L. E.; Verdoes, M.; Bogyo, M., Functional imaging of proteases: recent advances in the design and application of substrate-based and activity-based probes. *Curr Opin Chem Biol* **2011**, *15* (6), 798-805.
39. Blum, G.; Weimer, R. M.; Edgington, L. E.; Adams, W.; Bogyo, M., Comparative Assessment of Substrates and Activity Based Probes as Tools for Non-Invasive Optical Imaging of Cysteine Protease Activity. *PloS one* **2009**, *4* (7).
40. Blum, G.; von Degenfeld, G.; Merchant, M. J.; Blau, H. M.; Bogyo, M., Noninvasive optical imaging of cysteine protease activity using fluorescently quenched activity-based probes. *Nat Chem Biol* **2007**, *3* (10), 668-77.

-
41. Verdoes, M.; Edgington, L. E.; Scheeren, F. A.; Leyva, M.; Blum, G.; Weiskopf, K.; Bachmann, M. H.; Ellman, J. A.; Bogyo, M., A nonpeptidic cathepsin S activity-based probe for noninvasive optical imaging of tumor-associated macrophages. *Chem. Biol.* **2012**, *19* (5), 619-628.
42. Cutter, J. L.; Cohen, N. T.; Wang, J.; Sloan, A. E.; Cohen, A. R.; Panneerselvam, A.; Schluchter, M.; Blum, G.; Bogyo, M.; Basilion, J. P., Topical application of activity-based probes for visualization of brain tumor tissue. *PloS one* **2012**, *7* (3), e33060.
43. Evans, M. J.; Cravatt, B. F., Mechanism-based profiling of enzyme families. *Chem Rev* **2006**, *106* (8), 3279-301.
44. Serim, S.; Haedke, U.; Verhelst, S. H., Activity-based probes for the study of proteases: recent advances and developments. *ChemMedChem* **2012**, *7* (7), 1146-59.
45. Greenbaum, D.; Medzihradzky, K. F.; Burlingame, A.; Bogyo, M., Epoxide electrophiles as activity-dependent cysteine protease profiling and discovery tools. *Chemistry & Biology* **2000**, *7* (8), 569-581.
46. (a) Verhelst, S. H. L.; Bogyo, M., Solid-phase synthesis of double-headed epoxysuccinyl activity-based probes for selective targeting of papain family cysteine proteases. *ChemBioChem* **2005**, *6* (5), 824-827; (b) Yuan, F.; Verhelst, S. H. L.; Blum, G.; Coussens, L. M.; Bogyo, M., A selective activity-based probe for the papain family cysteine protease dipeptidyl peptidase I cathepsin C. *Journal of the American Chemical Society* **2006**, *128* (17), 5616-5617.
47. Kato, D.; Boatright, K. M.; Berger, A. B.; Nazif, T.; Blum, G.; Ryan, C.; Chehade, K. A. H.; Salvesen, G. S.; Bogyo, M., Activity-based probes that target diverse cysteine protease families. *Nat. Chem. Biol.* **2005**, *1* (1), 33-38.

-
48. Berger, A. B.; Witte, M. D.; Denault, J. B.; Sadaghiani, A. M.; Sexton, K. M.; Salvesen, G. S.; Bogyo, M., Identification of early intermediates of caspase activation using selective inhibitors and activity-based probes. *Mol. Cell* **2006**, *23* (4), 509-521.
49. (a) Kidd, D.; Liu, Y. S.; Cravatt, B. F., Profiling serine hydrolase activities in complex proteomes. *Biochemistry* **2001**, *40* (13), 4005-4015; (b) Liu, Y. S.; Patricelli, M. P.; Cravatt, B. F., Activity-based protein profiling: The serine hydrolases. *Proc. Natl. Acad. Sci. U. S. A.* **1999**, *96* (26), 14694-14699.
50. Shannon, D. A.; Gu, C.; McLaughlin, C. J.; Kaiser, M.; van der Hoorn, R. A. L.; Weerapana, E., Sulfonyl Fluoride Analogues as Activity-Based Probes for Serine Proteases. *ChemBioChem* **2012**, *13* (16), 2327-2330.
51. (a) Haedke, U.; Gotz, M.; Baer, P.; Verhelst, S. H. L., Alkyne derivatives of isocoumarins as clickable activity-based probes for serine proteases. *Bioorg Med Chem* **2012**, *20* (2), 633-40; (b) Powers, J. C.; Kam, C. M.; Narasimhan, L.; Oleksyszyn, J.; Hernandez, M. A.; Ueda, T., Mechanism-Based Isocoumarin Inhibitors For Serine Proteases - Use Of Active-Site Structure And Substrate-Specificity In Inhibitor Design. *Journal Of Cellular Biochemistry* **1989**, *39* (1), 33-46.
52. (a) Gilmore, B. F.; Carson, L.; McShane, L. L.; Quinn, D.; Coulter, W. A.; Walker, B., Synthesis, kinetic evaluation, and utilization of a biotinylated dipeptide proline diphenyl phosphonate for the disclosure of dipeptidyl peptidase IV-like serine proteases. *Biochem. Biophys. Res. Commun.* **2006**, *347* (1), 373-379; (b) Mahrus, S.; Craik, C. S., Selective chemical functional probes of granzymes A and B reveal granzyme B is a major effector of natural killer cell-mediated lysis of target cells. *Chem Biol* **2005**, *12* (5), 567-77; (c) Pan, Z.; Jeffery, D. A.; Chohade, K.; Beltman, J.; Clark, J. M.; Grothaus, P.; Bogyo, M.; Baruch, A., Development of activity-based probes for trypsin-family serine proteases. *Bioorg. Med. Chem. Lett.* **2006**, *16* (11), 2882-2885.

-
53. Kafarski, P.; Lejczak, B., Biological-activity of aminophosphonic acids. *Phosphorus Sulfur and Silicon and the Related Elements* **1991**, *63* (1-2), 193-215.
54. Powers, J. C.; Asgian, J. L.; Ekici, O. D.; James, K. E., Irreversible inhibitors of serine, cysteine, and threonine proteases. *Chem. Rev.* **2002**, *102* (12), 4639-4750.
55. Jansen, E. F.; Nutting, M. D. F.; Jang, R.; Balls, A. K., Inhibition of the proteinase and esterase activities of trypsin and chymotrypsin by diisopropyl fluorophosphate – Crystallization of inhibited Cchymotrypsin. *J. Biol. Chem.* **1949**, *179* (1), 189-199.
56. Mazur, A., An enzyme in animal tissues capable of hydrolyzing the phosphorus-fluorine bond of alkyl fluorophosphates. *J. Biol. Chem.* **1946**, *164* (1), 271-289.
57. Kilby, B. A.; Kilby, M., The toxicity of alkyl fluorophosphonates in man and animals. *British Journal of Pharmacology and Chemotherapy* **1947**, *2* (4), 234-240.
58. Oleksyszyn, J.; Powers, J. C., Irreversible Inhibition of Serine Proteases by Peptidyl Derivatives of Alpha-Aminoalkylphosphonate Diphenyl Esters. *Biochem. Biophys. Res. Commun.* **1989**, *161* (1), 143-149.
59. Oleksyszyn, J.; Powers, J. C., Amino-Acid and Peptide Phosphonate Derivatives as Specific Inhibitors of Serine Peptidases. *Methods in Enzymology* **1994**, *244*, 423-441.
60. Grzywa, R.; Sienczyk, M., Phosphonic Esters and their Application of Protease Control. *Current Pharmaceutical Design* **2013**, *19* (6), 1154-1178.
61. Abuelyaman, A. S.; Hudig, D.; Woodard, S. L.; Powers, J. C., Fluorescent Derivatives of Diphenyl [1-(N-Peptidylamino)Alkyl]Phosphonate Esters - Synthesis and Use in the Inhibition and Cellular-Localization of Serine Proteases. *Bioconjugate Chemistry* **1994**, *5* (5), 400-405.

-
62. Jessani, N.; Liu, Y. S.; Humphrey, M.; Cravatt, B. F., Enzyme activity profiles of the secreted and membrane proteome that depict cancer cell invasiveness. *Proc. Natl. Acad. Sci. U. S. A.* **2002**, *99* (16), 10335-10340.
63. Greenbaum, D. C.; Baruch, A.; Grainger, M.; Bozdech, Z.; Medzihradzky, K. F.; Engel, J.; DeRisi, J.; Holder, A. A.; Bogyo, M., A role for the protease falcipain 1 in host cell invasion by the human malaria parasite. *Science* **2002**, *298* (5600), 2002-2006.
64. Wang, J.; Loveland, A. N.; Kattenhorn, L. M.; Ploegh, H. L.; Gibson, W., High-molecular-weight protein (pUL48) of human cytomegalovirus is a competent deubiquitinating protease: mutant viruses altered in its active-site cysteine or histidine are viable. *J Virol* **2006**, *80* (12), 6003-12.
65. Dang, T. H.; de la Riva, L.; Fagan, R. P.; Storck, E. M.; Heal, W. P.; Janoir, C.; Fairweather, N. F.; Tate, E. W., Chemical probes of surface layer biogenesis in *Clostridium difficile*. *ACS Chem Biol* **2010**, *5* (3), 279-85.
66. Bachovchin, D. A.; Ji, T.; Li, W.; Simon, G. M.; Blankman, J. L.; Adibekian, A.; Hoover, H.; Niessen, S.; Cravatt, B. F., Superfamily-wide portrait of serine hydrolase inhibition achieved by library-versus-library screening. *Proc. Natl. Acad. Sci. USA* **2010**, *107* (49), 20941-20946.
67. Yang, Y.; Hahne, H.; Kuster, B.; Verhelst, S. H., A simple and effective cleavable linker for chemical proteomics applications. *Mol Cell Proteomics* **2013**, *12* (1), 237-44.
68. Bachovchin, D. A.; Brown, S. J.; Rosen, H.; Cravatt, B. F., Identification of selective inhibitors of uncharacterized enzymes by high-throughput screening with fluorescent activity-based probes. *Nat. Biotechnol.* **2009**, *27* (4), 387-394.

-
69. Bachovchin, D. A.; Mohr, J. T.; Speers, A. E.; Wang, C.; Berlin, J. M.; Spicer, T. P.; Fernandez-Vega, V.; Chase, P.; Hodder, P. S.; Schurer, S. C.; Nomura, D. K.; Rosen, H.; Fu, G. C.; Cravatt, B. F., Academic cross-fertilization by public screening yields a remarkable class of protein phosphatase methylesterase-1 inhibitors. *Proc. Natl. Acad. Sci. USA* **2011**, *108* (17), 6811-6816.
70. Wolf, E. V.; Zeissler, A.; Vosyka, O.; Zeiler, E.; Sieber, S.; Verhelst, S. H. L., A new class of rhomboid protease inhibitors discovered by activity-based fluorescence polarization. *PloS one* **2013**, *8* (8).
71. Gygi, S. P.; Rist, B.; Gerber, S. A.; Turecek, F.; Gelb, M. H.; Aebersold, R., Quantitative analysis of complex protein mixtures using isotope-coded affinity tags. *Nat. Biotechnol.* **1999**, *17* (10), 994-999.
72. Ross, P. L.; Huang, Y. N.; Marchese, J. N.; Williamson, B.; Parker, K.; Hattan, S.; Khainovski, N.; Pillai, S.; Dey, S.; Daniels, S.; Purkayastha, S.; Juhasz, P.; Martin, S.; Bartlett-Jones, M.; He, F.; Jacobson, A.; Pappin, D. J., Multiplexed protein quantitation in *Saccharomyces cerevisiae* using amine-reactive isobaric tagging reagents. *Mol. Cell. Proteomics* **2004**, *3* (12), 1154-1169.
73. Everley, P. A.; Gartner, C. A.; Haas, W.; Saghatelian, A.; Elias, J. E.; Cravatt, B. F.; Zetter, B. R.; Gygi, S. P., Assessing enzyme activities using stable isotope labeling and mass spectrometry. *Mol. Cell. Proteomics* **2007**, *6* (10), 1771-7.
74. Jessani, N.; Niessen, S.; Wei, B. Q. Q.; Nicolau, M.; Humphrey, M.; Ji, Y. R.; Han, W. S.; Noh, D. Y.; Yates, J. R.; Jeffrey, S. S.; Cravatt, B. F., A streamlined platform for high-content functional proteomics of primary human specimens. *Nature Methods* **2005**, *2* (9), 691-697.
75. Chen, G. Y.; Uttamchandani, M.; Zhu, Q.; Wang, G.; Yao, S. Q., Developing a strategy for activity-based detection of enzymes in a protein microarray. *ChemBioChem* **2003**, *4* (4), 336-9.

-
76. Wu, H.; Ge, J.; Yang, P.-Y.; Wang, J.; Uttamchandani, M.; Yao, S. Q., A Peptide Aldehyde Microarray for High-Throughput Profiling of Cellular Events. *Journal of the American Chemical Society* **2011**, *133* (6), 1946-1954.
77. Uttamchandani, M.; Liu, K.; Panicker, R. C.; Yao, S. Q., Activity-based fingerprinting and inhibitor discovery of cysteine proteases in a microarray. *Chemical Communications* **2007**, (15), 1518-1520.
78. (a) Funeriu, D. P.; Eppinger, J.; Denizot, L.; Miyake, M.; Miyake, J., Enzyme family-specific and activity-based screening of chemical libraries using enzyme microarrays. *Nat Biotechnol* **2005**, *23* (5), 622-7; (b) Eppinger, J.; Funeriu, D. P.; Miyake, M.; Denizot, L.; Miyake, J., Enzyme microarrays: On-chip determination of inhibition constants based on affinity-label detection of enzymatic activity. *Angew Chem Int Ed Engl* **2004**, *43* (29), 3806-10.
79. Yang, J.; Chaurand, P.; Norris, J. L.; Porter, N. A.; Caprioli, R. M., Activity-based probes linked with laser-cleavable mass tags for signal amplification in imaging mass spectrometry: analysis of serine hydrolase enzymes in mammalian tissue. *Anal. Chem.* **2012**, *84* (8), 3689-3695.
80. Serim, S.; Mayer, S. V.; Verhelst, S. H., Tuning activity-based probe selectivity for serine proteases by on-resin 'click' construction of peptide diphenyl phosphonates. *Org Biomol Chem* **2013**, *11* (34), 5714-21.
81. Sienczyk, M.; Oleksyszyn, J., Irreversible Inhibition of Serine Proteases - Design and In Vivo Activity of Diaryl alpha-Aminophosphonate Derivatives. *Curr. Med. Chem.* **2009**, *16* (13), 1673-1687.
82. Rijkers, D. T. S.; van Vugt, H. H. R.; Jacobs, H. J. F.; Liskamp, R. M. J., A convenient synthesis of azido peptides by post-assembly diazo transfer on the solid phase applicable to large peptides. *Tetrahedron Lett.* **2002**, *43* (20), 3657-3660.

-
83. (a) Angelo, N. G.; Arora, P. S., Solution- and solid-phase synthesis of triazole oligomers that display protein-like functionality. *J. Org. Chem.* **2007**, *72* (21), 7963-7967; (b) Aucagne, V.; Leigh, D. A., Chemoselective formation of successive triazole linkages in one pot: "Click-click" chemistry. *Org. Lett.* **2006**, *8* (20), 4505-4507.
84. (a) Angell, Y. L.; Burgess, K., Peptidomimetics via copper-catalyzed azide-alkyne cycloadditions. *Chem. Soc. Rev.* **2007**, *36* (10), 1674-1689; (b) Pedersen, D. S.; Abell, A., 1,2,3-Triazoles in Peptidomimetic Chemistry. *Eur. J. Org. Chem.* **2011**, (13), 2399-2411.
85. Oleksyszyn, J.; Subotkowska, L.; Mastalerz, P., Diphenyl 1-Aminoalkanephosphonates. *Synthesis-Stuttgart* **1979**, (12), 985-986.
86. Birum, G. H., Urylenediphosphonates – General method for synthesis of alpha-ureidophosphonates and related structures. *J. Org. Chem.* **1974**, *39* (2), 209-213.
87. Walker, B.; Wharry, S.; Hamilton, R. J.; Martin, S. L.; Healy, A.; Walker, B. J., Asymmetric preference of serine proteases toward phosphonate and phosphinate esters. *Biochem. Biophys. Res. Commun.* **2000**, *276* (3), 1235-1239.
88. Winiarski, L.; Oleksyszyn, J.; Sienczyk, M., Human Neutrophil Elastase Phosphonic Inhibitors with Improved Potency of Action. *Journal of Medicinal Chemistry* **2012**, *55* (14), 6541-6553.
89. Ordonez, M.; Rojas-Cabrera, H.; Cativiela, C., An overview of stereoselective synthesis of alpha-aminophosphonic acids and derivatives. *Tetrahedron* **2009**, *65* (1), 17-49.
90. Sienczyk, M.; Oleksyszyn, J., A convenient synthesis of new alpha-aminoalkylphosphonates, aromatic analogues of arginine as inhibitors of trypsin-like enzymes. *Tetrahedron Lett.* **2004**, *45* (39), 7251-7254.

-
91. (a) Gosalia, D. N.; Salisbury, C. M.; Maly, D. J.; Ellman, J. A.; Diamond, S. L., Profiling serine protease substrate specificity with solution phase fluorogenic peptide microarrays. *Proteomics* **2005**, *5* (5), 1292-1298; (b) Harris, J. L.; Backes, B. J.; Leonetti, F.; Mahrus, S.; Ellman, J. A.; Craik, C. S., Rapid and general profiling of protease specificity by using combinatorial fluorogenic substrate libraries. *Proc. Natl. Acad. Sci. U. S. A.* **2000**, *97* (14), 7754-7759.
92. Raymond, W. W.; Trivedi, N. N.; Makarova, A.; Ray, M.; Craik, C. S.; Caughey, G. H., How Immune Peptidases Change Specificity: Cathepsin G Gained Tryptic Function but Lost Efficiency during Primate Evolution. *Journal Of Immunology* **2010**, *185* (9), 5360-5368.
93. Patricelli, M. P.; Giang, D. K.; Stamp, L. M.; Burbaum, J. J., Direct visualization of serine hydrolase activities in complex proteomes using fluorescent active site-directed probes. *Proteomics* **2001**, *1* (9), 1067-1071.
94. Sienczyk, M.; Oleksyszyn, J., Inhibition of trypsin and urokinase by Cbz-amino(4-guanidino-phenyl)methanephosphonate aromatic ester derivatives: The influence of the ester group on their biological activity. *Bioorg. Med. Chem. Lett.* **2006**, *16* (11), 2886-2890.
95. Blum, G.; Mullins, S. R.; Keren, K.; Fonovic, M.; Jedeszko, C.; Rice, M. J.; Sloane, B. F.; Bogyo, M., Dynamic imaging of protease activity with fluorescently quenched activity-based probes. *Nature Chemical Biology* **2005**, *1* (4), 203-209.
96. Edgington, L. E.; Verdoes, M.; Ortega, A.; Withana, N. P.; Lee, J.; Syed, S.; Bachmann, M. H.; Blum, G.; Bogyo, M., Functional Imaging of Legumain in Cancer Using a New Quenched Activity-Based Probe. *Journal of the American Chemical Society* **2013**, *135* (1), 174-182.
97. Frase, H.; Lee, I., Peptidyl boronates inhibit *Salmonella enterica* serovar typhimurium lon protease by a competitive ATP-dependent mechanism. *Biochemistry* **2007**, *46* (22), 6647-6657.

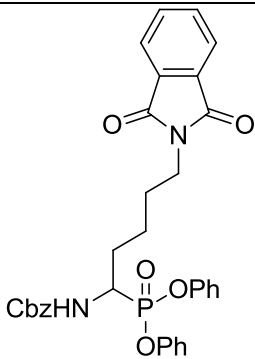
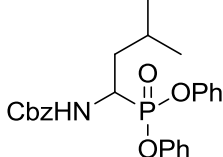
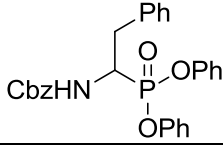
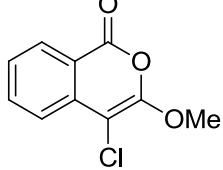
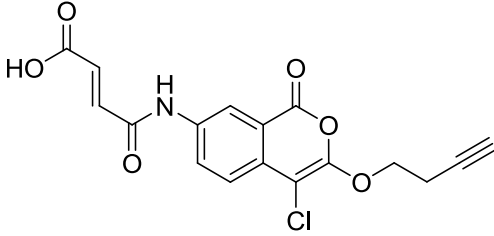
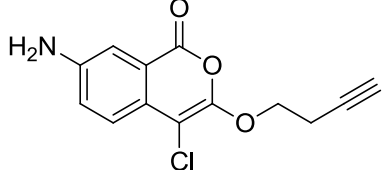
-
98. Maurizi, M. R., Degradation in vitro of bacteriophage-lambda N-protein by Lon protease from Escherichia-Coli. *J. Biol. Chem.* **1987**, *262* (6), 2696-2703.
99. Madler, S.; Bich, C.; Touboul, D.; Zenobi, R., Chemical cross-linking with NHS esters: a systematic study on amino acid reactivities. *J. Mass Spectrom.* **2009**, *44* (5), 694-706.
100. Cuatrecasas, P.; Parikh, I., Adsorbents for affinity chromatography – Use of N-hydroxysuccinimide esters of agarose. *Biochemistry* **1972**, *11* (12), 2291-&.
101. Goldberg, A. L.; Moerschell, R. P.; Chung, C. H.; Maurizi, M. R., ATP-dependent protease La (Lon) from Escherichia-Coli. *Methods Enzymol.* **1994**, *244*, 350-375.
102. Kettner, C. A.; Shenvi, A. B., Inhibition of the serine proteases leukocyte elastase, pancreatic elastase, cathepsin-G, and chymotrypsin by peptide boronic acids. *J. Biol. Chem.* **1984**, *259* (24), 5106-5114.
103. Matthews, D. A.; Alden, R. A.; Birktoft, J. J.; Freer, S. T.; Kraut, J., X-ray crystallographic study of boronic acid adducts with subtilisin BPN' (novo) – Model for catalytic transition-state. *J. Biol. Chem.* **1975**, *250* (18), 7120-7126.
104. Verdoes, M.; Florea, B. I.; van der Linden, W. A.; Renou, D.; van den Nieuwendijk, A.; van der Marel, G. A.; Overkleeft, H. S., Mixing of peptides and electrophilic traps gives rise to potent, broad-spectrum proteasome inhibitors. *Org. Biomol. Chem.* **2007**, *5* (9), 1416-1426.
105. Adams, J.; Behnke, M.; Chen, S. W.; Cruickshank, A. A.; Dick, L. R.; Grenier, L.; Klunder, J. M.; Ma, Y. T.; Plamondon, L.; Stein, R. L., Potent and selective inhibitors of the proteasome: Dipeptidyl boronic acids. *Bioorg. Med. Chem. Lett.* **1998**, *8* (4), 333-338.
106. Chew, W.; Harpp, D. N., Recent aspects of thiirane chemistry. *Sulfur reports* **1993**, *15* (1), 1-39.

-
107. Pitscheider, M.; Mausbacher, N.; Sieber, S. A., Antibiotic activity and target discovery of three-membered natural product-derived heterocycles in pathogenic bacteria. *Chemical Science* **2012**, *3* (6), 2035-2041.
108. Barrett, A. J.; Kembhavi, A. A.; Brown, M. A.; Kirschke, H.; Knight, C. G.; Tamai, M.; Hanada, K., L-Trans-epoxysuccinyl-leucylamido(4-guanidino)butane (E-64) and its analogs as inhibitors of cysteine proteinases including cathepsins B, H and L. *Biochemical Journal* **1982**, *201* (1), 189-198.
109. Verhelst, S. H. L.; Witte, M. D.; Arastu-Kapur, S.; Fonovic, M.; Bogyo, M., Novel aza peptide inhibitors and active-site probes of papain-family cysteine proteases. *ChemBioChem* **2006**, *7* (6), 943-950.
110. Pan, Z. Y.; Jeffery, D. A.; Chehade, K.; Beltman, J.; Clark, J. M.; Grothaus, P.; Bogyo, M.; Baruch, A., Development of activity-based probes for trypsin-family serine proteases. *Bioorg. Med. Chem. Lett.* **2006**, *16* (11), 2882-2885.
111. Sabido, E.; Tarrago, T.; Giralt, E., Using peptidyl aldehydes in activity-based proteomics. *Bioorg. Med. Chem. Lett.* **2009**, *19* (14), 3752-3755.
112. Joossens, J.; Van der Veken, P.; Surpateanu, G.; Lambeir, A. M.; El-Sayed, I.; Ali, O. M.; Augustyns, K.; Haemers, A., Diphenyl phosphonate inhibitors for the urokinase-type plasminogen activator: Optimization of the P4 position. *Journal of Medicinal Chemistry* **2006**, *49* (19), 5785-5793.
113. Skorenski, M.; Oleksyszyn, J.; Sienczyk, M., A convenient method for the one-step synthesis of phosphonic peptides. *Tetrahedron Lett.* **2013**, *54* (36), 4975-4977.
114. Brown, C. M.; Ray, M.; Eroy-Reveles, A. A.; Egea, P.; Tajon, C.; Craik, C. S., Peptide Length and Leaving-Group Sterics Influence Potency of Peptide Phosphonate Protease Inhibitors. *Chemistry & Biology* **2011**, *18* (1), 48-57.

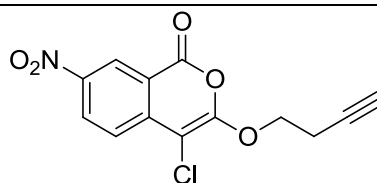
-
115. Velasco, G.; Cal, S.; Quesada, V.; Sanchez, L. M.; Lopez-Otin, C., Matriptase-2, a membrane-bound mosaic serine proteinase predominantly expressed in human liver and showing degrading activity against extracellular matrix proteins. *J. Biol. Chem.* **2002**, *277* (40), 37637-37646.
116. Stirnberg, M.; Maurer, E.; Horstmeyer, A.; Kolp, S.; Frank, S.; Bald, T.; Arenz, K.; Janzer, A.; Prager, K.; Wunderlich, P.; Walter, J.; Gutschow, M., Proteolytic processing of the serine protease matriptase-2: identification of the cleavage sites required for its autocatalytic release from the cell surface. *Biochemical Journal* **2010**, *430*, 87-95.
117. Gehrig, S.; Mall, M. A.; Schultz, C., Spatially Resolved Monitoring of Neutrophil Elastase Activity with Ratiometric Fluorescent Reporters. *Angewandte Chemie-International Edition* **2012**, *51* (25), 6258-6261.
118. Granot, Z.; Geiss-Friedlander, R.; Melamed-Book, N.; Eimerl, S.; Timberg, R.; Weiss, A. M.; Hales, K. H.; Hales, D. B.; Stocco, D. M.; Orly, J., Proteolysis of normal and mutated steroidogenic acute regulatory proteins in the mitochondria: the fate of unwanted proteins. *Molecular Endocrinology* **2003**, *17* (12), 2461-2476.

Supplementary

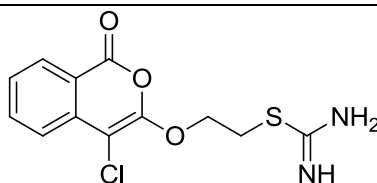
Table 3 List of compounds used in the *E. coli* Lon inhibitor screen.

Cmp	Structure
1	
2	
3	
4	
5	
6	

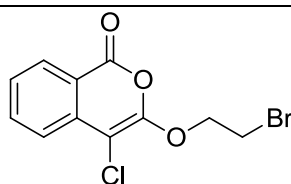
7



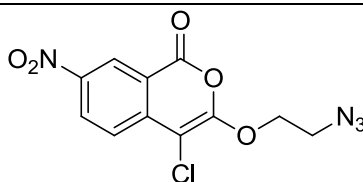
8



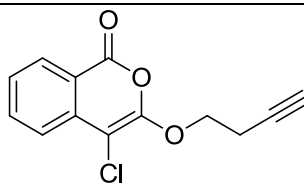
9



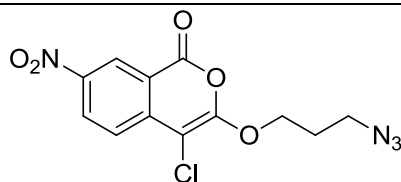
10



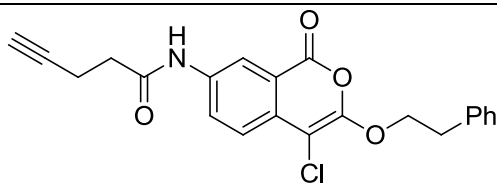
11



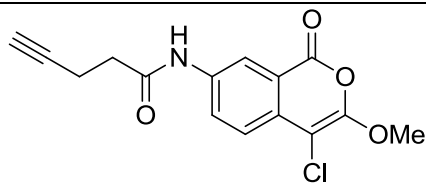
12

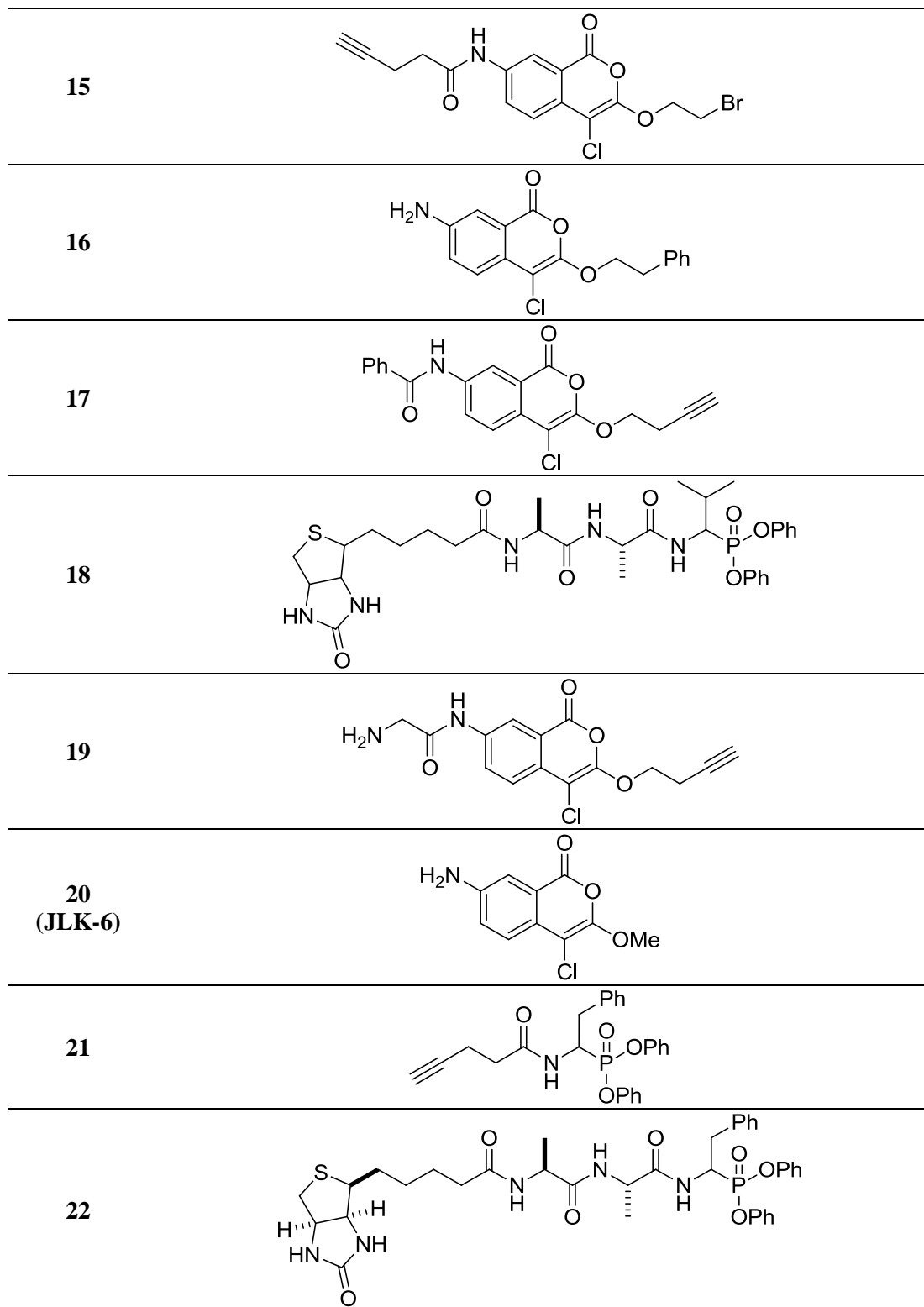


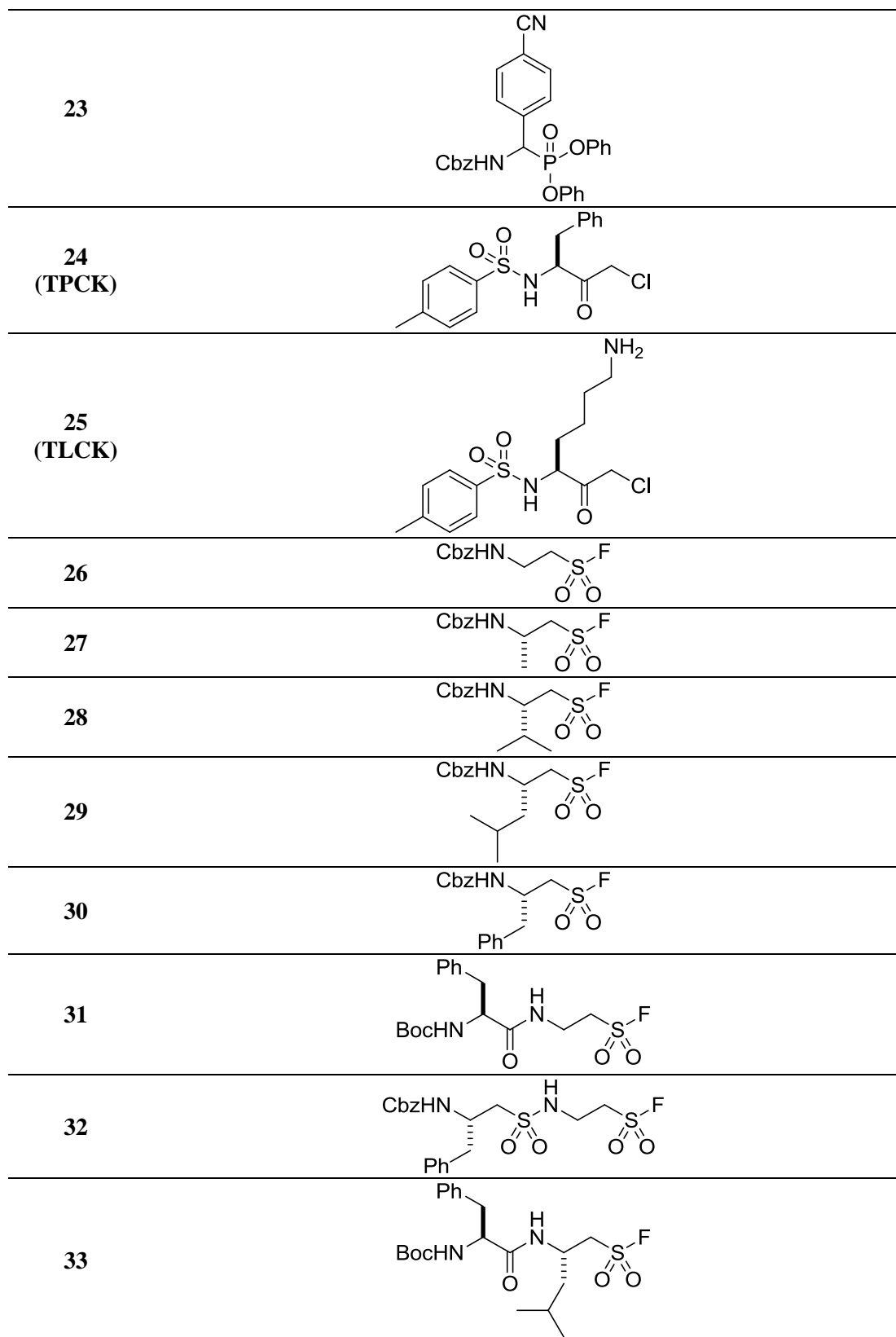
13



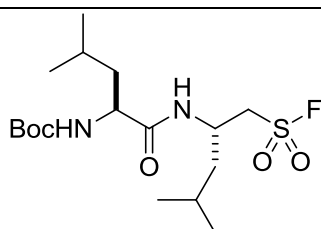
14



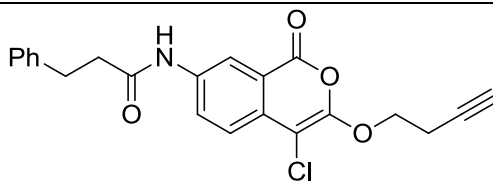




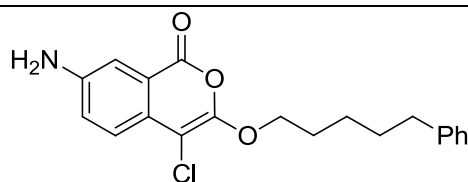
34



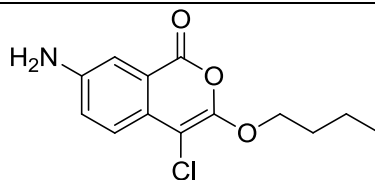
35



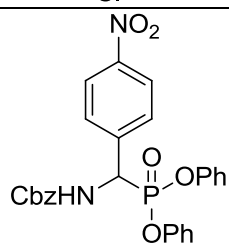
36



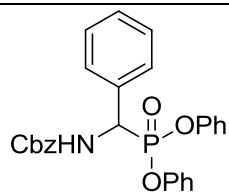
37



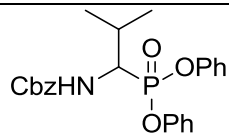
38



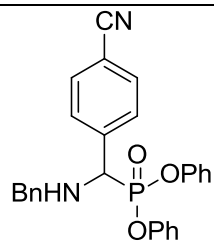
39

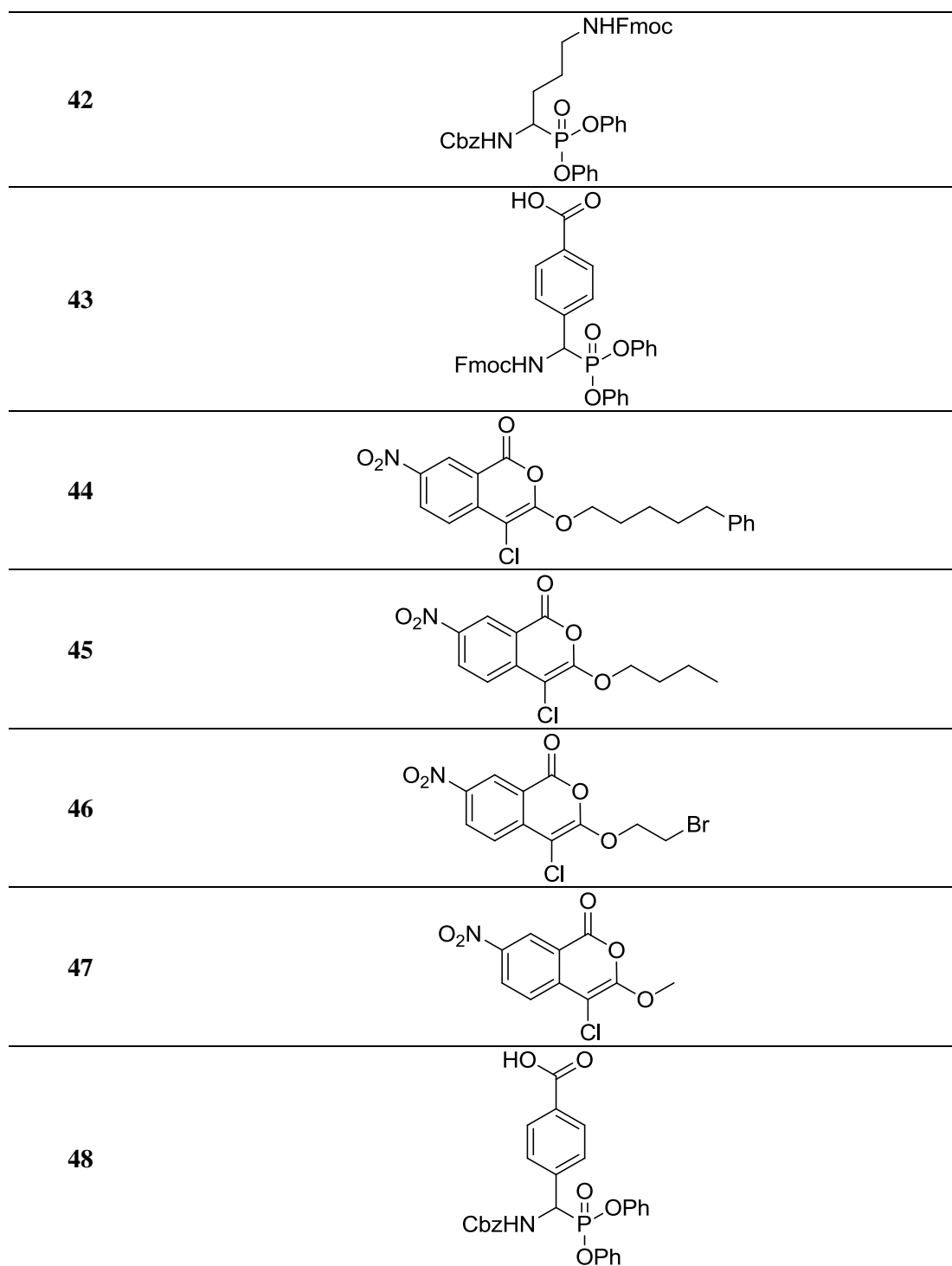


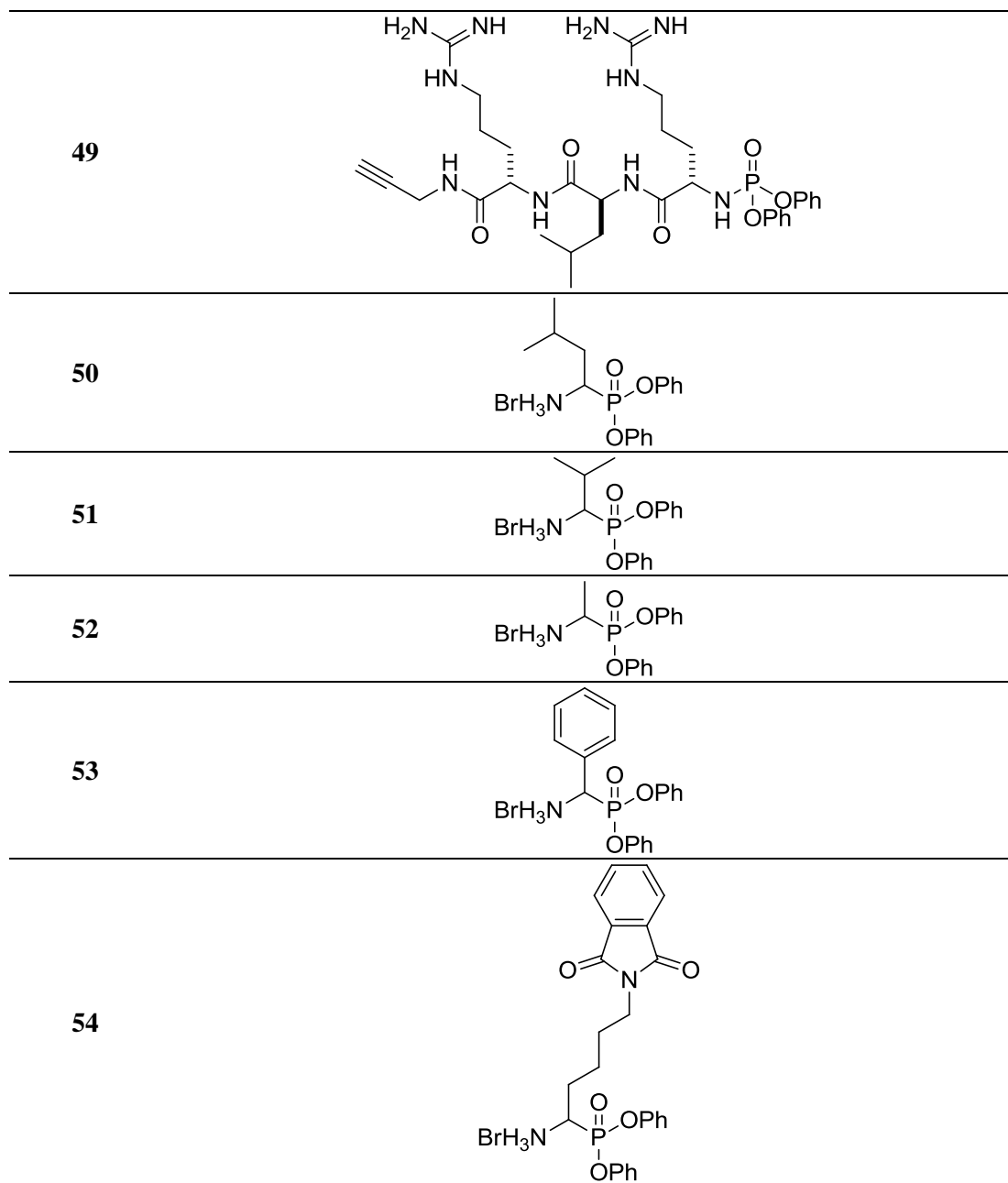
40



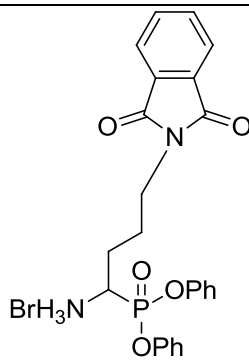
41



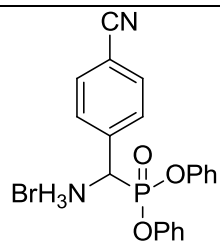




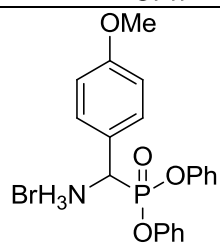
55



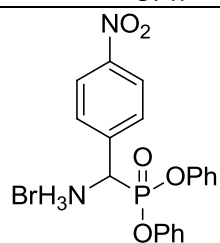
56



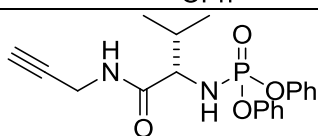
57



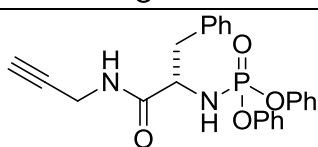
58



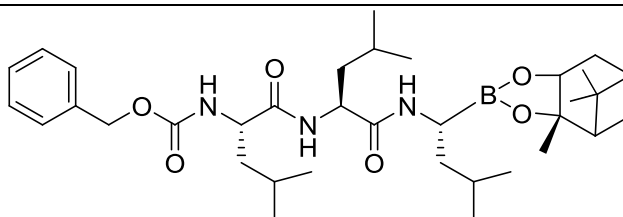
59



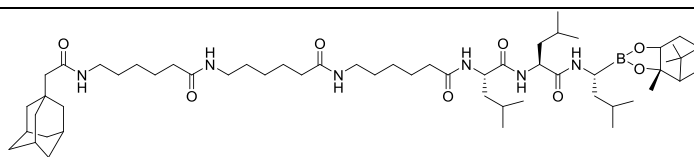
60



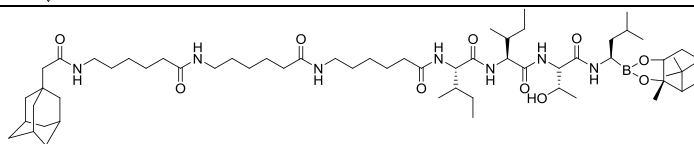
61



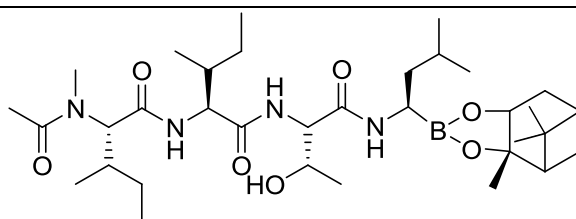
62



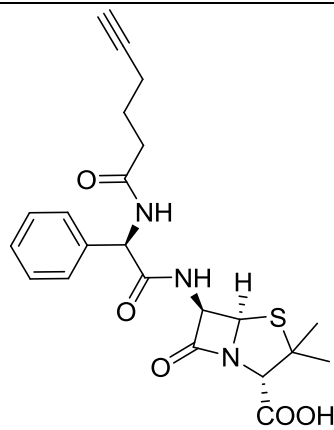
63



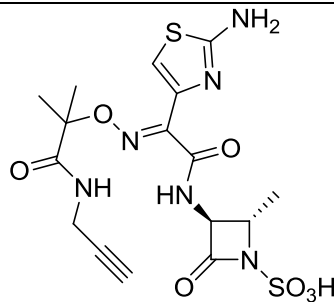
64



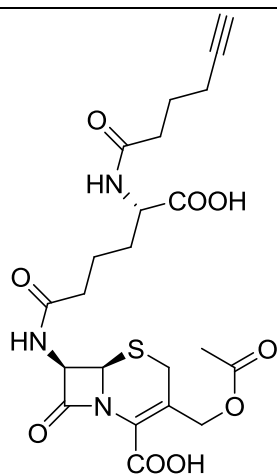
65



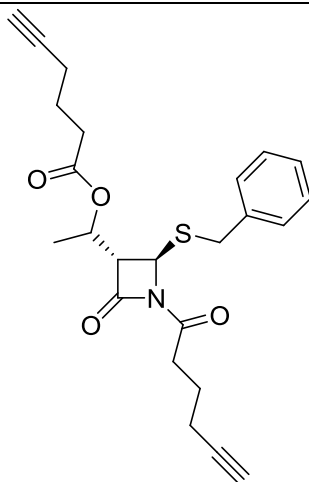
66



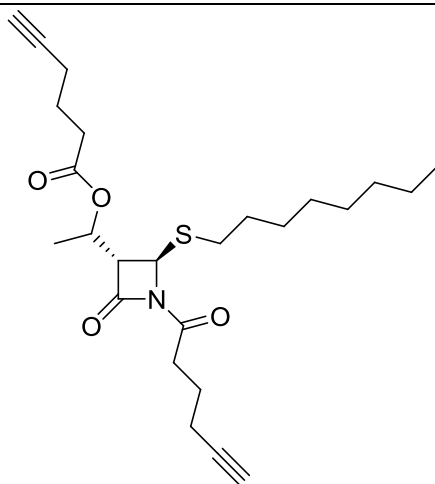
67



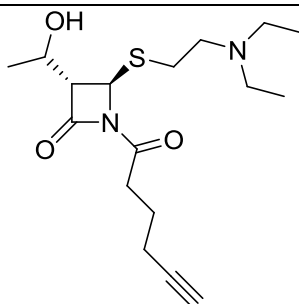
68



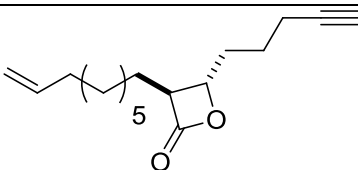
69



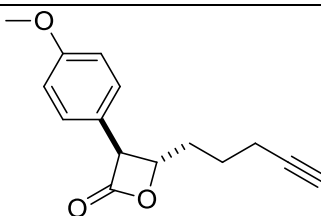
70



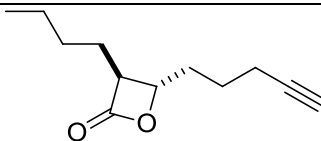
71



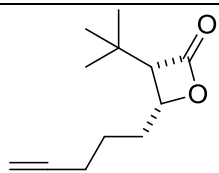
72



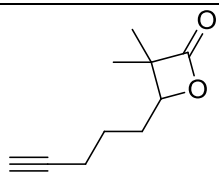
73



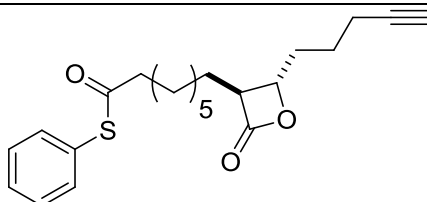
74



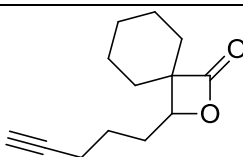
75



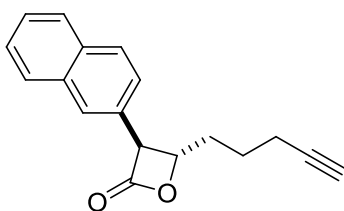
76



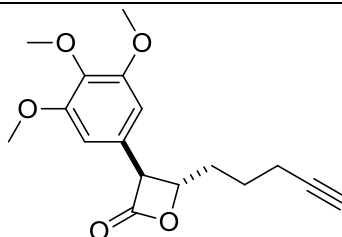
77



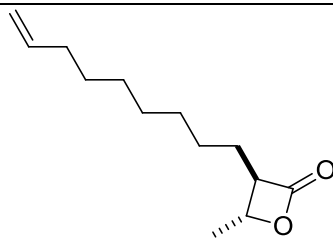
78



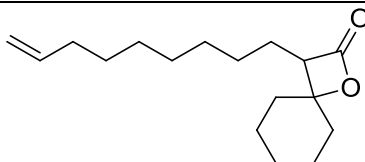
79



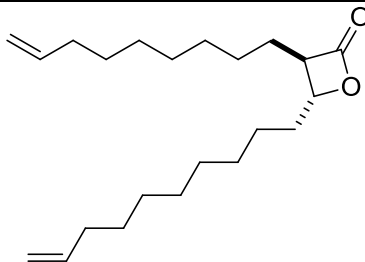
80



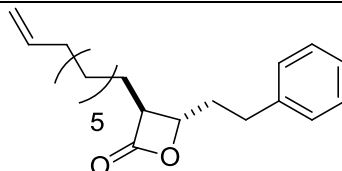
81



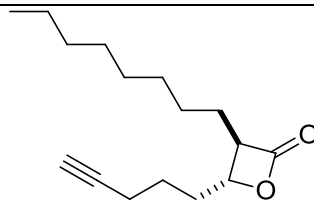
82



83

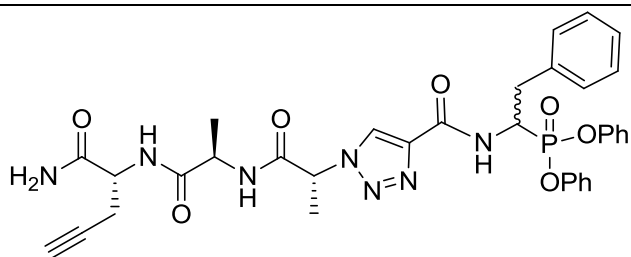


84

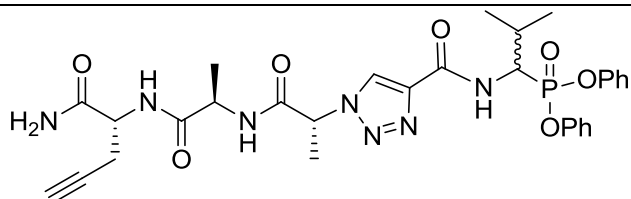


85	<chem>CC(C)C(C#CC(=O)N)COP(=O)(O)OPh</chem>
86	<chem>CC(C)C(C#CC(=O)N)COP(=O)(O)OPh</chem>
87	<chem>Cc1ccc(cc1)CC(C#CC(=O)N)COP(=O)(O)OPh</chem>
88	<chem>C#CC(=O)N[C@@H](COP(=O)(O)OPh)C(=N)N</chem>
89	<chem>C#CC(=O)N[C@@H](COP(=O)(O)OPh)C</chem>
90	<chem>C#CC(=O)N[C@@H](COP(=O)(O)OPh)c1ccc(cc1)[N+](=O)[O-]</chem>
91	<chem>C#CC(=O)N[C@@H](COP(=O)(O)OPh)c1ccc(cc1)N</chem>

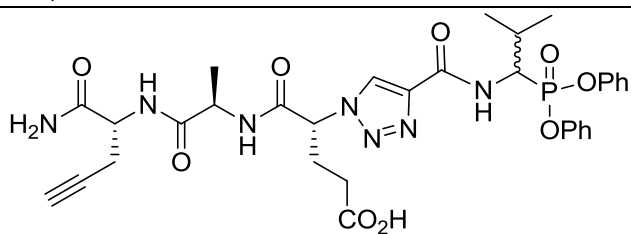
92



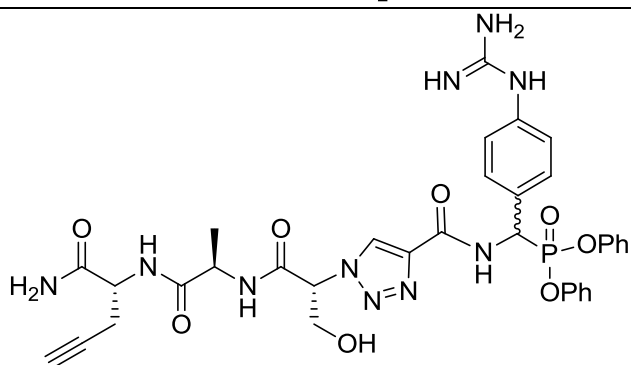
93



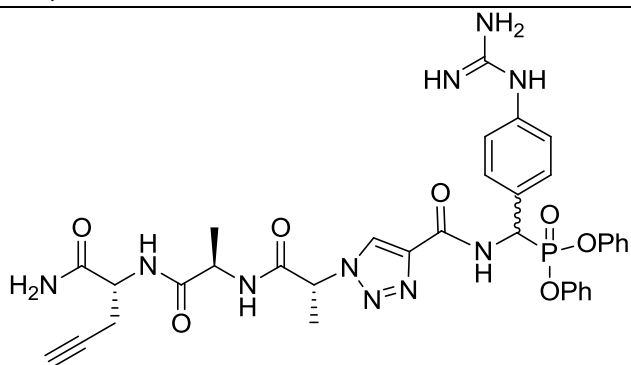
94



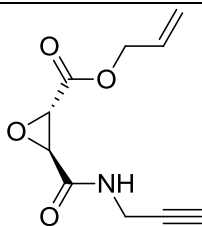
95



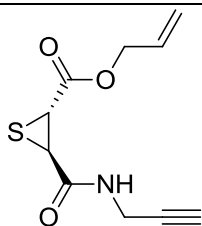
96



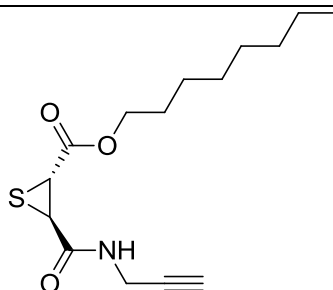
97



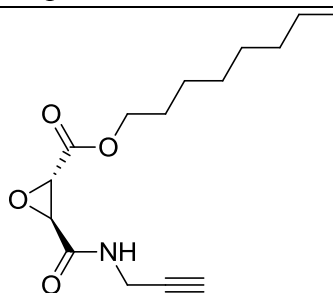
98



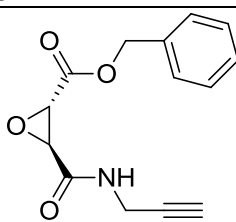
99



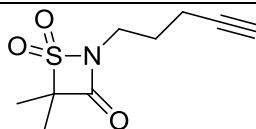
100



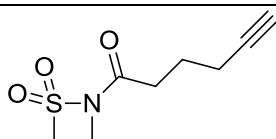
101



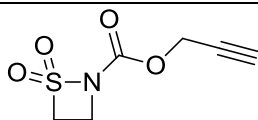
102



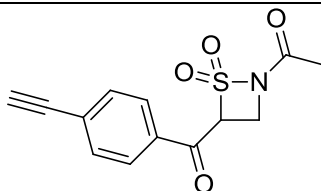
103



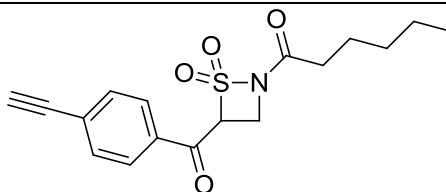
104



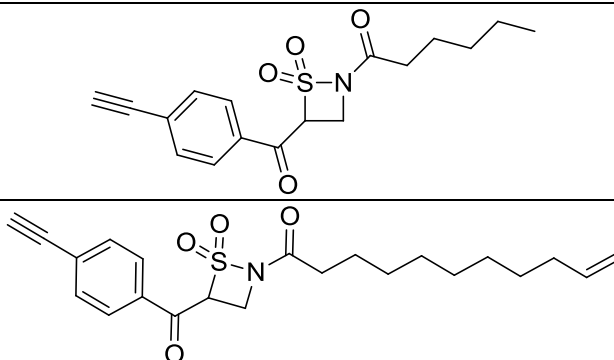
105



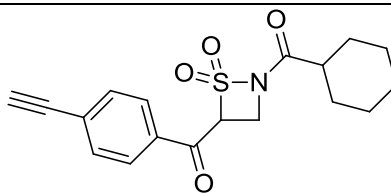
106



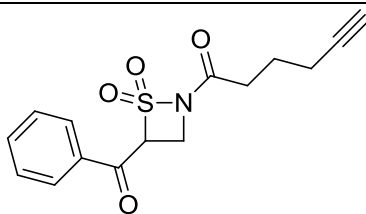
107



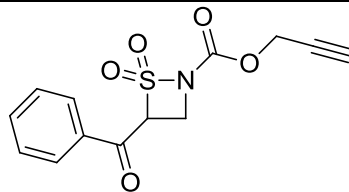
108



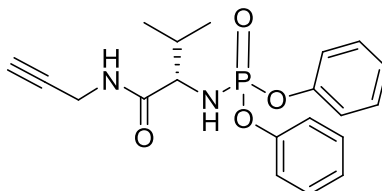
109



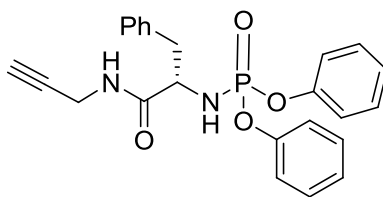
110



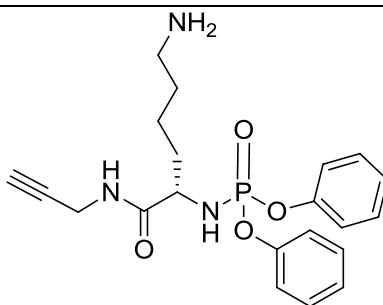
111



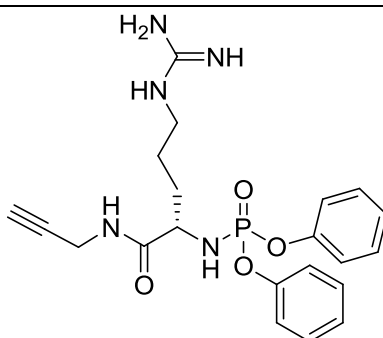
112



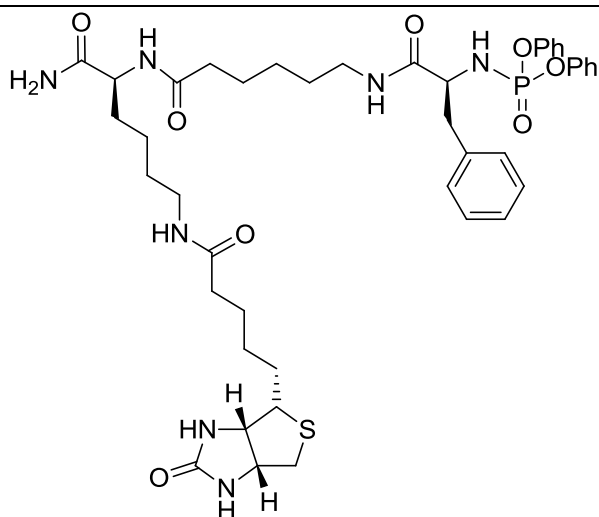
113



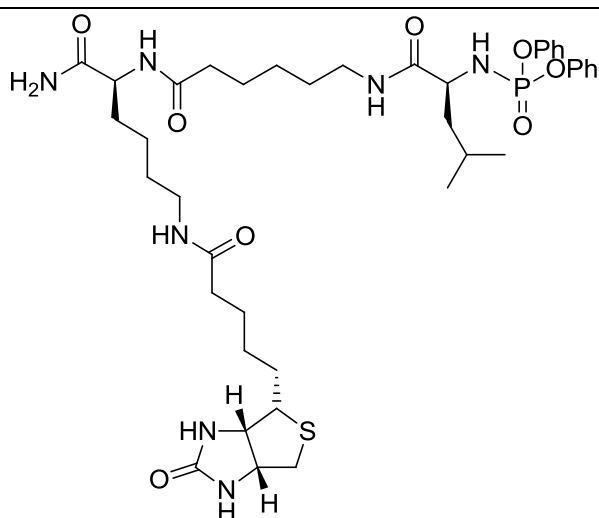
114



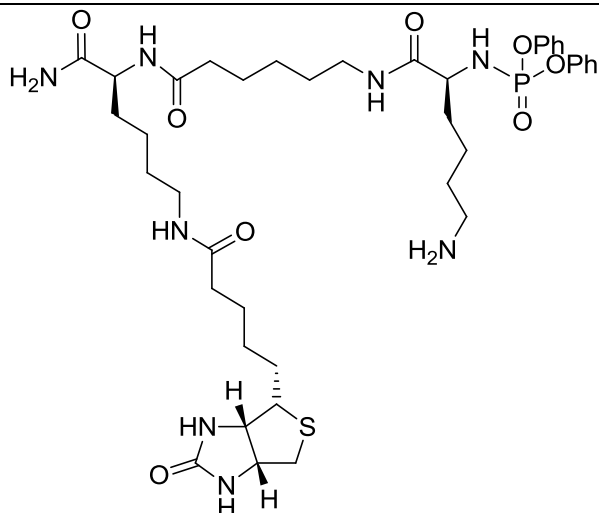
115



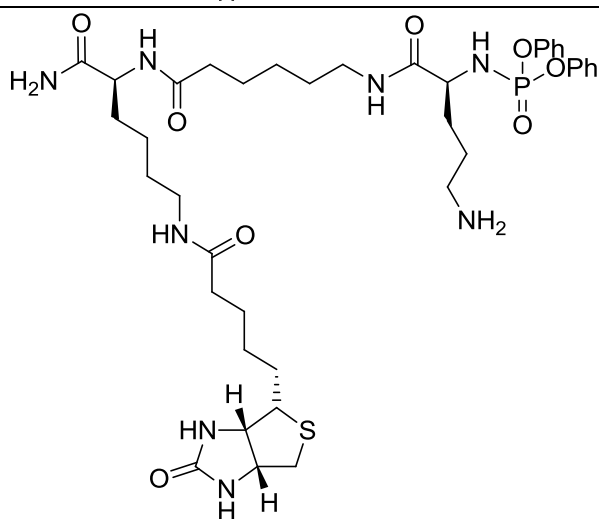
116



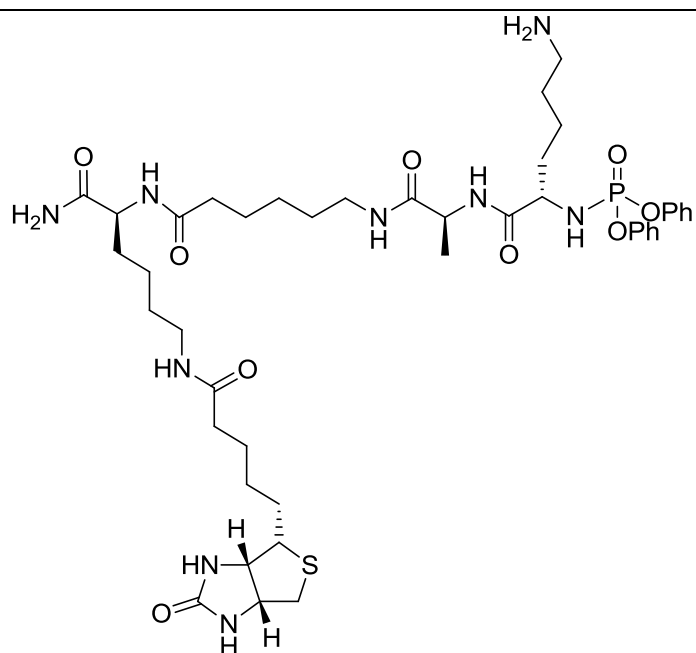
117



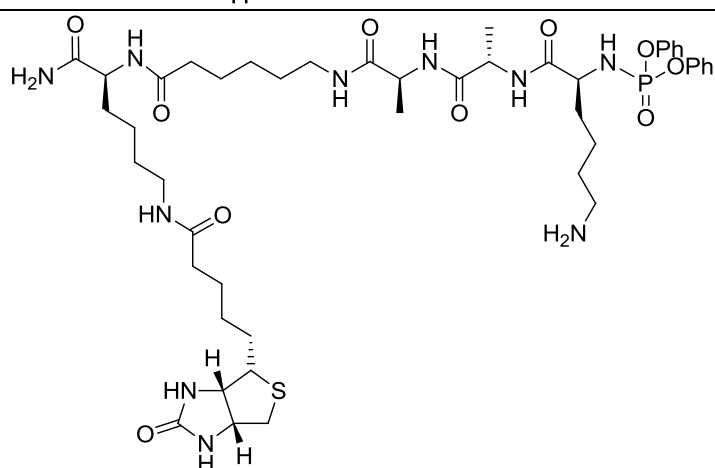
118



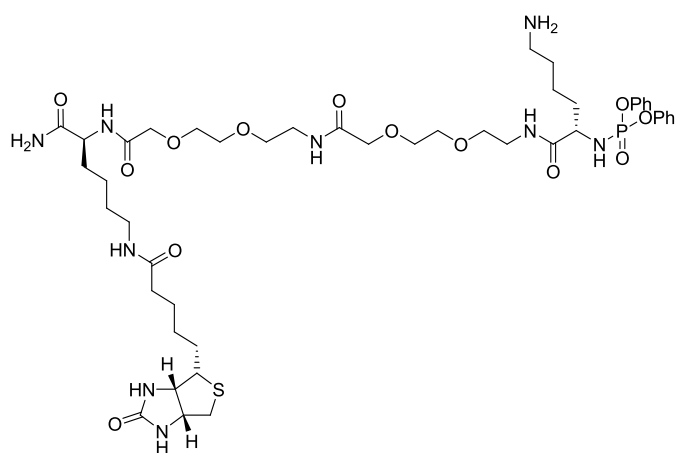
119



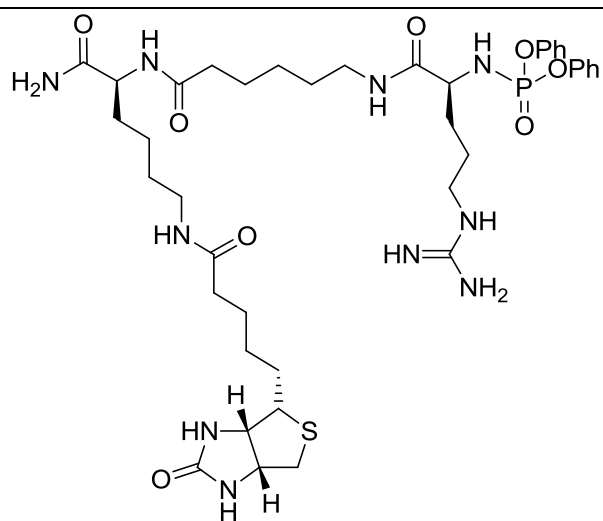
120



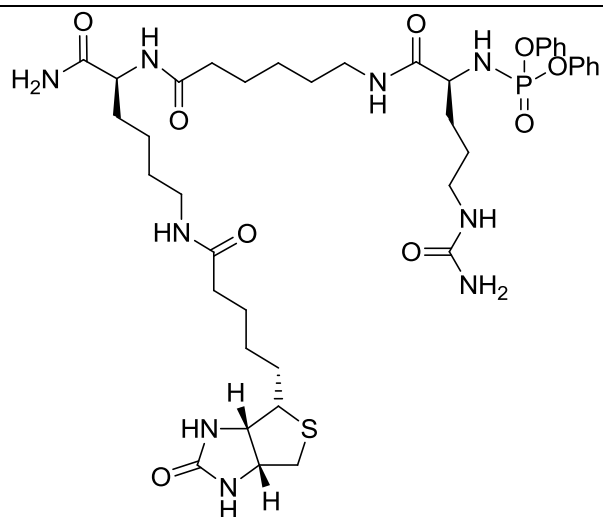
121



122



123



Publications

Part of this thesis have been or will be published in international, peer-reviewed journals:

Activity-based probes for the study of proteases: recent advances and developments.

Serim S, Haedke U, Verhelst SH.

ChemMedChem. **2012** Jul;7(7):1146-59

Tuning activity-based probe selectivity for serine proteases by on-resin 'click' construction of peptide diphenyl phosphonates.

Serim S, Mayer SV, Verhelst SH.

Org Biomol Chem **2013**, *11* (34), 5714-21

Synthesis and biological evaluation of fluorescently quenched activity-based probes for serine proteases. (*Manuscript in preparation*)

Serim S, Baer P, Verhelst SH.

Identification of thiiranes as a new class of inhibitors of *E. coli* Lon. (*Manuscript in preparation*)

Serim S, Graf P, Honz M, Prieler B, Verhelst SH.

Curriculum Vitae

Personal data

Name	Sevnur Serim
Address	Jagdstr. 11 85356 Freising
Email	s.serim@tum.de
Place of birth	Mersin, Turkey
Date of birth	06.09.1982

University

Since Jan 2009	PhD thesis at Technische Universität München, Germany <i>The development of activity-based probes for serine proteases</i>
Oct 2005 – Sep 2008	Master studies at Technische Universität Braunschweig, Germany <i>Synthesis and biological evaluation of cell surface glycoconjugates</i>
Oct 2000 – Jan 2005	Chemistry Bachelor studies at Istanbul Technical University, Turkey

High school

Sep 1993 – June 2000	Icel Anadolu Lisesi, Mersin, Turkey
Sep 1989 – June 1993	3 Ocak Ilkokulu, Mersin, Turkey

| You've crossed the finish line. Won the race but lost your mind. Was it worth it after all?